Break, Flare, Repair:
Rho Flares Locally Reinforce the Tight Junction Barrier

by

Rachel Elizabeth Stephenson

A dissertation submitted in partial fulfillment
of the requirements for the degree of
Doctor of Philosophy
(Molecular, Cellular, and Developmental Biology)
in The University of Michigan
2018

Doctoral Committee:

Associate Professor Ann L. Miller, Chair
Professor David Antonetti
Professor Matthew Chapman
Associate Professor Allen Liu
Associate Professor Erik Nielsen

Rachel E. Stephenson

restep@umich.edu

ORCID ID: 0000-0001-8319-6448

Acknowledgements

I am honored to have had the opportunity to complete my dissertation in Ann Miller's lab. Ann has always inspired me to be better simply by being herself. She is the perfect blend of smart, dedicated, compassionate, and fun, and joining her lab was the best decision I've ever made. A quality of Ann's I particularly admire is that she takes research, mentoring, and teaching seriously without taking herself too seriously. Ann, thank you for accepting me into your lab, for providing me with the resources I need to be successful, for always listening to my ideas, and for making the lab a safe, stimulating, and fun environment.

I would like to thank all the members of the Miller lab for making my graduate school experience special. Tomohito Higashi was a second mentor to me, and he gave me the courage and enthusiasm to pursue this project full force and contributed immensely to the work in Chapter 2. I aspire to be like Tomo: full of knowledge, creativity, and drive, all while being patient and good natured. Torey Arnold, Sara Varadarajan, Jen Landino, Shahana Chumki, and Lotte van den Goor have been wonderful colleagues and friends, and seeing them in lab always brightens my day. I would especially like to thank Sara and Shahana for choosing to work on Rho flares—I'm so excited to see where this project goes. I would also like to thank lab alumni Megan Murt, Ciara Reyes, and Elaina Breznau, who set the tone for the lab in the early days and helped to start a lot of fun traditions. Finally, I would like to thank all the Miller lab undergrads for bringing a lot of energy, enthusiasm, and unique personality to the lab. Thanks especially to Brandon Coy for the hard work he dedicated to his project for four years and for his contributions to Chapter 4.

Torey Arnold has been my baymate, travel buddy, prank partner, and best friend for the last six years. Thank you for challenging me in the lab and out. I can always count on you for your honest feedback and your ability to make me laugh. Additionally, I am grateful to have always been able to depend on Jordann Smak and Julian Bahr for support, commiseration, celebration, and fun. Anna Cotter is my childhood best friend and the reason I ended up in Ann Arbor. Although she left Ann Arbor shortly after I started grad school, I'm grateful I've always been able to count on her support no matter the distance.

Before I started graduate school, I was a technician in the Boles lab at U of M. I would like to thank Blaise for giving me my first full time science job and for helping me realize how much I love doing research. I would also like to give a shout out to all the Boles and Chapman lab members that made being a technician so much fun, inspired me to go to grad school, and gave me a sneak peak into how the PhD sausage gets made. In particular Adnan Syed, Will DePas, David Hufnagel, and Maggie Evans were role models for various aspects of grad school life.

I would also like to thank my thesis committee members, who were always encouraging and supportive, pushed me to focus on what I thought were the most interesting questions, and gave me lots of new things to think about at every meeting. Andrew Goryachev, Ivan Erofeev, and Marcin Leda are collaborators who generously provided their expertise in data analysis and support in the publishing process. Additionally, I would like to thank MCDB and PIBS for providing financial and administrative support. Thanks especially to Mary Carr, Diane Durfy, and Gregg Sobocinski for always being so friendly and helpful.

My family has been a tremendous support throughout grad school. I am especially fortunate to have parents who value science and education and understand the complexities of academia. Shouts out to my dad for teaching me to clone and exposing me to science from a young age, my mom for her practical wisdom and compassion, my sister for still pretending not to know whether I live in Michigan or Minnesota and for giving me plenty of excuses to leave the state, and my grandparents who have always been supportive and proud of me.

Finally, I would like to acknowledge everyone and everything else that helped keep me sane over the past six years, including (but not limited to): podcasts, improv, video games, crocheting, baking, therapy, and my cat, Rex.

Table of Contents

List of Figures

Abstract

Epithelial tissues serve essential functions, such as preventing infection and water loss, regulating absorption and secretion, and creating specialized compartments within complex multicellular organisms. Epithelia are sheets of cells connected by specialized apical cell-cell junctions. Adherens junctions adhere cells to one another and mechanically integrate cells in the tissue, while tight junctions regulate both how much and what kind of materials can cross through the paracellular space (the space between cells). Both tight junctions and adherens junctions are dynamically regulated by filamentous actin and myosin II (actomyosin), which forms a contractile array near the apical cell-cell junctions. The forces generated by the apical actomyosin array can be transmitted to neighboring cells through adherens junctions to drive cell- and tissue-scale changes. Cellular events, such as epithelial cytokinesis, cell extrusion, and wound healing, alter tension on adherens junctions and the dynamics of the apical actomyosin array. However, very little is known about how these changes in cell shape and actomyosin dynamics influence tight junctions and epithelial barrier function.

To better understand how dynamic cell shape change influences epithelial barrier function, we developed a tight junction barrier assay compatible with live imaging. This approach, the Zinc-based Ultrasensitive Microscopic Barrier Assay, or ZnUMBA, allows for the detection of localized, transient leaks. Using this approach in the epithelium of *Xenopus laevis* gastrula-staged embryos, we discovered that leaks that result from cell shape change are rapidly repaired by transient accumulation of the active conformation of the small GTPase RhoA, or Rho flares. Then, using fluorescently-tagged tight junction proteins, I found that occludin and ZO-1 show localized decline prior to Rho

flares and are reinforced afterwards. Using molecular inhibitors of the targets of Rho activity, I concluded that both actin polymerization and Rho Kinase-mediated junction contraction reinforce ZO-1 and occludin, promoting efficient restoration of epithelial barrier function. We hypothesize that Rho flares serve as a rapid repair mechanism to quickly restore barrier function and that this allows epithelial cells to dynamically change shape without prolonged breaches in barrier function.

Rho flares are accompanied by an apical protrusion of the plasma membrane. However, both the cause of the membrane protrusion and its purpose are unclear. I examine three potential causes of membrane protrusion and assess each one by reviewing the temporal and spatial accumulation of F-actin and myosin II, as well as several candidate actin nucleators. Based on the data presented, I propose that a bleb-like protrusion mechanism is likely, and I hypothesize that the protrusion acts to temporarily seal the paracellular space while the tight junction is reinforced.

The work presented in this dissertation advances tight junction biology in several ways. ZnUMBA is a widely adaptable technique that will allow other researchers to examine changes in barrier function with greater temporal and spatial precision. We hope that this will usher in a better understanding about what causes tight junction leaks and how they are repaired. Finally, I describe a previously unknown mechanism for rapid repair of local breaches in epithelial barrier function by active Rho, adding nuance to our understanding of the many roles this small GTPase plays in epithelial tissues.

Chapter 1

Introduction

The importance of barriers in multicellular life

The evolution of multicellular life was one of the first steps in creating the complex organisms that live on earth today. A key step in the evolution of multicellularity is the specialization of cells within a group such that they become interdependent on one another and can no longer survive as individuals (Libby et al., 2016). Another critical aspect in the evolution of multicellularity is the ability of cells to adhere to one another (Harris and Tepass, 2010). When groups of cells evolve the ability to act as barriers, they can generate an internal environment distinct from the outside world, allowing them to preserve and share secreted products (Marchiando et al., 2010). Further compartmentalization within organisms allows for the formation of organs that carry out specialized tasks like digestion, reproduction, and sensory processing, leading to the complex forms of multicellular life that we know today.

With an estimated 37 trillion cells (Bianconi et al., 2013) and roughly 80 organs, the human body requires a high degree of organization. Epithelia aid in organizing the body by creating tissue barriers, sheets of connected cells with the ability to regulate the quantity and type of materials that cross the tissue. In addition to acting as barriers, epithelial tissues are involved in specialized functions like absorption, secretion,

transportation, and signaling. Nearly every organ in our body is covered with or lined by an epithelial tissue that is suited specifically for that organ's task (Figure 1.1a).

Figure 1.1

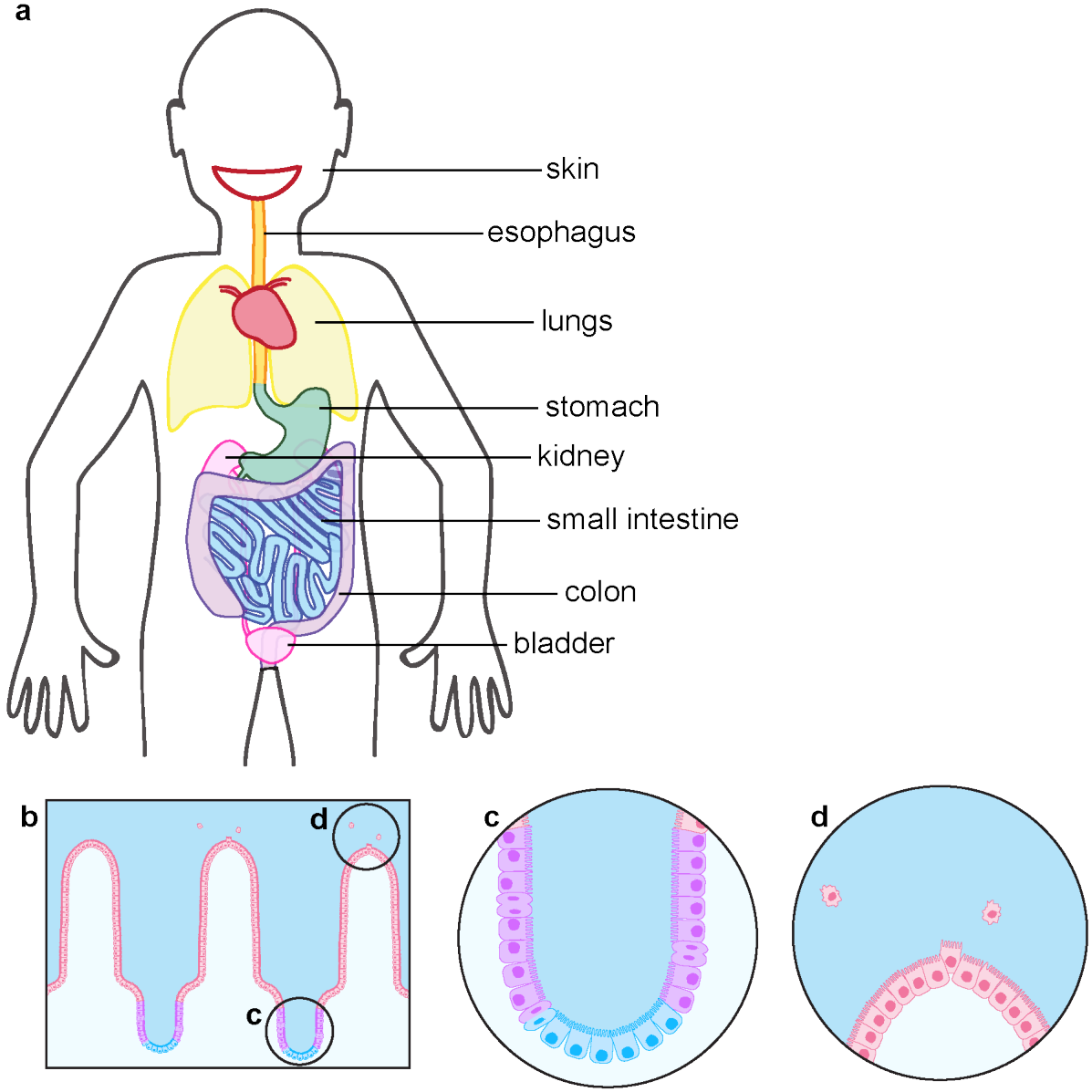

Figure 1.1: Epithelial tissues are diverse, dynamic environments. (a) Most organs of the human body, including all the organs depicted here, are lined with or covered by epithelial tissues. Epithelial tissues undergo changes in morphology due to organ function, such as peristalsis (esophagus, small intestine, large intestine), rhythmic expansion and contraction (heart, lungs), and expansion due to filling (stomach, bladder). **(b)** Epithelial tissues cover the villi of the small intestine, which undergoes rapid cell turnover. **(c)** Stem cells in the crypts of the small intestine (blue) divide to produce new epithelial cells, which further proliferate (purple) and migrate towards the tip of the villus. **(d)** At the tip of the villus, older epithelial cells are shed from the epithelium by extrusion.

During development, epithelial tissues are one of the main drivers of morphogenesis, where changes in cell shape and cell rearrangements drive the stretching, bending, and folding of tissues (Harris and Tepass, 2010). In addition to genetic programming, these tissue movements result in the formation of multiple germ layers and facilitate the genesis of complex organs from a simple ball of cells (Solnica-Krezel and Sepich, 2012). During development, cells proliferate rapidly to contribute to the growth of the organism. In adult tissues, however, many terminally differentiated cell types become quiescent and stop proliferating. In contrast, cell division is common in epithelial tissues, with rates of cell turnover varying by tissue type (Spalding et al., 2005). The relatively high rate of epithelial cell turnover is often attributed to the harsh mechanical and chemical environments these cells face, which may cause higher rates of cell damage (Macara et al., 2014).

An example of a tissue subject to frequent mechanical strain is the transitional epithelium that lines the bladder, the urothelium, which is among the most leak-proof epithelial tissues in the body (Khandelwal et al., 2009; Turner et al., 2014). Umbrella cells that line the lumen of the bladder regularly undergo remarkable shape changes, transitioning from cuboidal in shape when the bladder is empty, to a flattened, stretched morphology as the bladder fills to many times its empty volume (Carattino et al., 2013; Khandelwal et al., 2009). Exocytosis can account for the increase in membrane surface area that is required for this expansion (Truschel et al., 2002), but little is known about how the tight junctions, which are responsible maintaining the leak-proof seal, adapt to the large changes in surface area during the filling and emptying of the bladder (Carattino et al., 2013; Khandelwal et al., 2009).

Figure 1.2

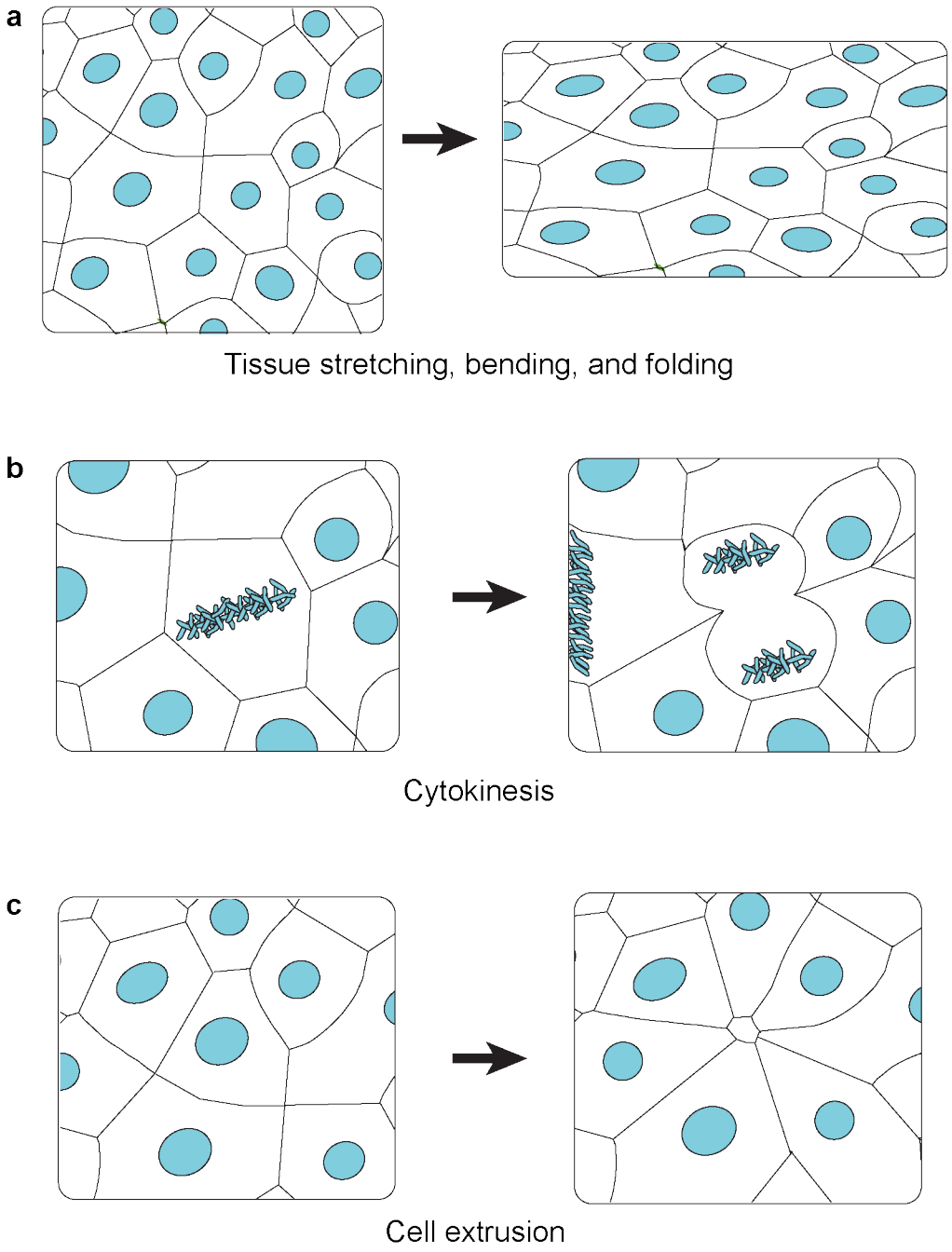

Figure 1.2: Cells change shape as a result of cell- and tissue-scale events. (a) During development and normal organ function, epithelial tissue stretching, bending, and folding results in dramatic cell shape changes. **(b)** During cell division in epithelial tissues, not only does the dividing cell change shape, but the neighboring cells change shape as well. **(c)** Cell extrusion is a process where dying or crowded cells are pushed out of the monolayer by neighboring cells, which change shape to take the place of the extruded cell.

The intestinal epithelium is specialized for nutrient absorption; during digestion, it becomes more permeable to water, ions, and glucose to facilitate nutrient absorption, while remaining impermeable to pathogenic bacteria, viruses, and other antigens, a feature that is critical for maintaining the sterility of the interstitium and other body cavities (Turner et al., 2014). Furthermore, intestinal epithelium must be robust enough to withstand the mechanical strain of peristalsis, a process where waves of smooth muscle contraction move material through the digestive tract. Presenting even more of a challenge to integrity of this tissue is that epithelial cells in the small intestine turn over rapidly (Hooper, 1956; Macara et al., 2014). To accomplish this, a population of stem cells in the crypts of the small intestine divide, giving rise to cells that further proliferate and migrate towards the tips of the villi, where apoptotic cells are shed by extrusion and cleared by phagocytosis (Figure 1.1b-d) (Duszyc et al., 2017; Williams et al., 2015). These processes involve cell shape changes, requiring that cell-cell boundaries expand and contract, posing a potential challenge to the structures that adhere them to one another and support barrier function (Figure 1.2).

It is incredible that tissues so dynamic act as stable barriers. Because proper regulation of barrier function is essential for optimal organ function (Marchiando et al., 2010), we can speculate that cells possess robust mechanisms for maintaining barrier function while remaining plastic enough to adapt to a changing environment. When the intestinal barrier is not maintained, gut bacteria can cross the epithelium where they are greeted by a host of immune cells (Marchiando et al., 2010). Activation of these immune cells can result in an inflammatory response and the release of cytokines, which further increases the permeability of the epithelium (Capaldo and Nusrat, 2009; López-

Posadas et al., 2017). In the intestinal epithelium, increased permeability to macromolecules is associated with Inflammatory Bowel Diseases (IBD) like Crohn's disease and Ulcerative Colitis (Capaldo and Nusrat, 2009; López-Posadas et al., 2017; Odenwald and Turner, 2013). These chronic diseases affect approximately 1.2 million people in the United States, causing an estimated economic burden of at least $14 billion in 2014 (Mehta, 2016). Thus, in addition to being a marvelous feat of evolutionary engineering, understanding how epithelial barriers adapt to the physical challenges they face will impact health care and quality of life in the modern world.

Epithelial cells have polarized cell-cell junctions

Barrier function in vertebrates depends on two types of specialized protein complexes that form between neighboring cells, tight junctions and adherens junctions (Figure 1.3a). Adherens junctions act to stick cells together through a multitude of weak interactions analogous to "hook and loop" interactions in Velcro (Yap et al., 2015). Cadherins are the transmembrane proteins that form these weak interactions by binding their counterparts on neighboring cells (Figure 1.3b). In addition to adhering cells to one another, they mechanically integrate the cells through linkage to the actin cytoskeleton (Charras and Yap, 2018; Vasquez and Martin, 2016). This linkage occurs through catenins, namely β-catenin, which is constitutively bound to the cytoplasmic tail of E-cadherin, and α-catenin, which binds β-catenin and can bind to filamentous- (F-) actin under tension (Buckley et al., 2014). Under high tension, α-catenin adopts an unfolded conformation, revealing a binding site for vinculin (Yao et al., 2014; Yonemura et al., 2010). Vinculin recruitment reinforces the connection to the cytoskeleton by binding α-

catenin and F-actin (Arnold et al., 2017). In this way, adherens junctions can sense and respond to mechanical force, a feature that can drive processes like morphogenesis and wound healing, as well as preserve epithelial integrity (Takeichi, 2014). Recent work suggests that there are tension-sensitive molecules in tight junctions as well (Scott et al., 2016; Spadaro et al., 2017), although little is known about the consequences of mechanosensitivity at tight junctions.

Apical to adherens junctions are tight junctions, which are responsible for creating a tight seal between cells. Tight junctions achieve this seal through a family of transmembrane proteins called claudins, which oligomerize into strands and interlock with their counterparts on neighboring cells to create a Ziploc-like seal (Figure 1.2b). In addition to acting as barriers, different claudins form size- and charge-specific pores (Günzel and Yu, 2013; Rosenthal et al., 2017). In this way, claudins can restrict the flow of some materials while allowing specific ions or water to diffuse across the tissue. This means that tissues can maintain concentration gradients of some ions while allowing others to passively diffuse across the tissue.

Claudins are connected to the actin cytoskeleton through direct and indirect interactions with other tight junction proteins, including occludin, ZO family proteins, and cingulin (Van Itallie and Anderson, 2014). ZO family proteins, including ZO-1, -2, and -3, are cytosolic scaffold proteins that bind to a multitude of proteins found at tight junctions, including claudins, occludin, junction adhesion molecules (JAMs), and other ZO proteins (Fanning et al., 1998; 2007; Itoh et al., 1999; Utepbergenov et al., 2006). Additionally, ZO proteins can bind directly to F-actin and actin binding proteins, serving dual roles of regulating the cytoskeleton and transmitting forces from the cytoskeleton to

the core transmembrane proteins of tight junctions (Fanning and Anderson, 2009; Zihni et al., 2016).

Figure 1.3: Epithelial cells have polarized cell-cell junctions linked to actomyosin. (a) A 3D representation of two epithelial cells. The cell on the left shows the actomyosin array that encircles the apical perimeter of epithelial cells. The cell on the right shows two types of apical junctions: tight junctions are the more apical and are critical for barrier function, while adherens junctions are more basal and function primarily in cell-cell adhesion and force transmission. **(b)** A simplified representation of the molecular components of the tight junction as viewed from above. Claudins and occludin are core transmembrane proteins that make contact with their counterparts on neighboring cells. Scaffolding proteins, like ZO-1 and cingulin, provide a link to the cytoskeleton. **(c)** A simplified representation of the molecular components of the adherens junction as viewed from above. Cadherins are the core transmembrane proteins of AJs that bind to the cytoplasmic catenins. α-catenin binds to F-actin under tension, revealing a vinculin binding site.

Figure 1.3

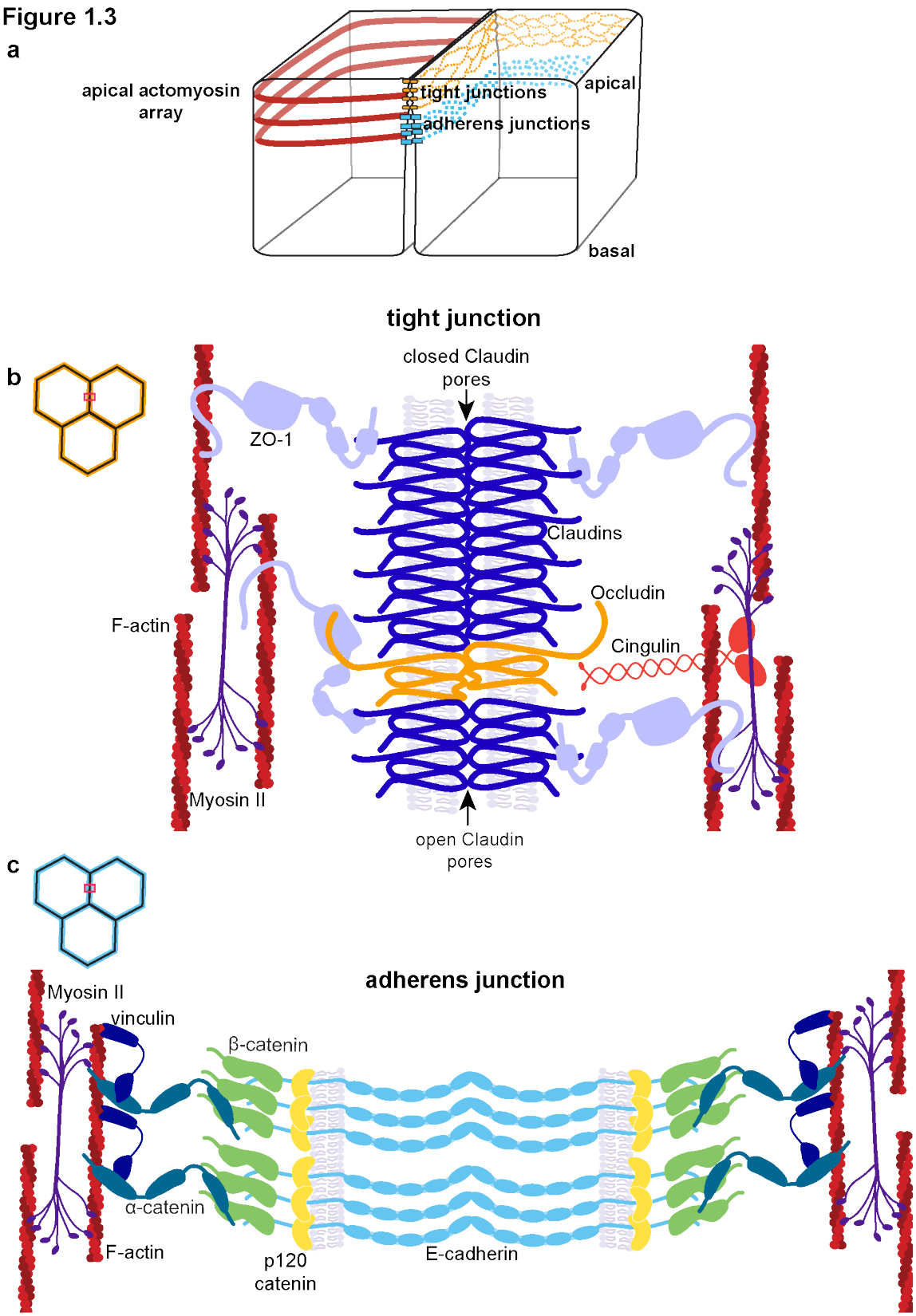
a
apical actomyosin array
tight junctions
adherens junctions
apical
basal
tight junction
b
closed Claudin pores
ZO-1
Claudins
Occludin
Cingulin
F-actin
Myosin II
open Claudin pores
c
adherens junction
Myosin II
vinculin
β-catenin
α-catenin
F-actin
p120 catenin
E-cadherin

Tight junction regulation of paracellular permeability

An early electron microscopy study of epithelial tissues stated “it is apparent that the tight junction is actually a region in which the membranes of adjoining cells come together and fuse, with resultant obliteration of the intercellular space” (Farquhar and Palade, 1963). Tracer studies showed that macromolecules diffused up to the tight junctions and then stopped, indicating that they are responsible for forming the paracellular barrier in epithelial cells. Freeze fracture electron microscopy, which fractures cells and tissues along hydrophobic planes (Severs, 2007), allowed researchers to observe the topology of tight junctions along the plane of the membrane (Claude and Goodenough, 1973). This revealed interwoven strands that encircled the apical surface of cell-cell contacts, visible on the cytoplasmic face as grooves that appeared to stitch the neighboring membranes together. Comparison of epithelial tissues from different organs lead to the hypothesis that strand number was correlated with the “tightness” of the epithelium (Claude and Goodenough, 1973). Discovery of the protein components of tight junctions caused many researchers to abandon the model that membrane fusion is responsible for creating the paracellular barrier; however, some data has caused others to reconsider the membrane fusion model as part of the mechanism of tight junction-mediated barrier function (Lingaraju et al., 2015; Zihni et al., 2016).

The pore pathway

The discovery of claudins in the 1990’s further contributed to our understanding of the molecular basis of epithelial barrier function, particularly the pore pathway (Furuse et al., 1998a). The pore pathway refers to a high-capacity, size- and charge-

selective route for ions and small molecules such as water to cross the tight junction by traveling through claudin pores. In humans, there are 26 claudins with tissue-specific expression patterns (Günzel and Yu, 2013; Rosenthal et al., 2017). Different family members are able to form a variety of size- and charge-selective pores that allow for passive diffusion of these molecules through the paracellular space (Günzel and Yu, 2013). These pores are hypothesized to be gated through a still unknown mechanism (Weber, 2012; Weber et al., 2015; Zihni and Terry, 2015) (Figure 1.4), although a multiprotein complex of claudin-1, claudin-2, ZO-1, and occludin can change cation permeability, indicating that gating may involve intermolecular interactions with cytoplasmic plaque proteins or altered dynamics of the cytoskeleton (Raleigh et al., 2011). Additionally, some claudin family members are thought to act solely as barrier-forming claudins, forming no pores and acting exclusively to seal the paracellular space (Günzel and Yu, 2013; Rosenthal et al., 2017).

Figure 1.4

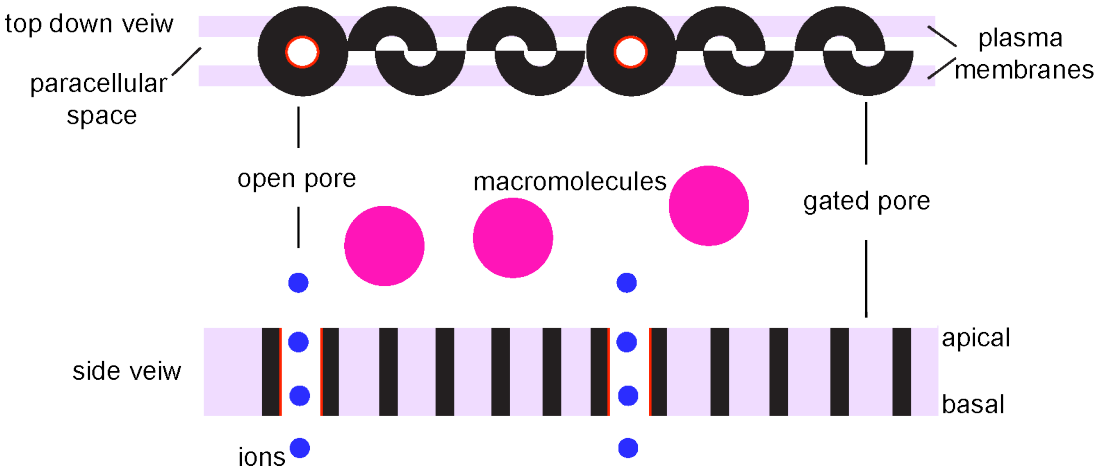

Figure 1.4: Claudin strands are composed of gated claudin pores. Claudin tetramers are hypothesized to form size- and charge-specific gated pores that are impermeable to macromolecules (see also Figure 1.3). These pores can be dynamically gated, although the molecular mechanism of gating remains unknown. Expression of different claudin family members allows tight junctions to become permeable to different ions and small molecules. This is referred to as the pore pathway.

Transepithelial electrical resistance (TER) is a popular method for measuring the magnitude of ion flux through the pore pathway of an epithelial tissue (Anderson and Van Itallie, 2009; Turner et al., 2014). To measure TER, an electric current is generated across the epithelium; the resistance formed by a confluent epithelial monolayer depends on how well ions can conduct the current through the paracellular space. Thus, TER is dictated by the proportion of pore-forming vs. barrier-forming claudins and the open or closed state of the claudin pores.

Tight junction dynamics

Experiments in fibroblasts, which do not normally make tight junctions, led to the conclusion that claudins are the basis for strands seen in freeze fracture EM (Figure 1.5a,b). Expression of single claudins, but not occludin, in fibroblasts led to the formation of strands that were morphologically similar to the strands seen in freeze fracture EM (Furuse et al., 1998b). Fluorescence recovery after photobleaching (FRAP) of the single strands revealed no diffusion of claudin-1 or -2 within the strands (Sasaki et al., 2003; Van Itallie et al., 2017). Later, FRAP studies in epithelial cells confirmed the relative stability of claudin within the membrane while revealing that ZO-1, occludin, and F-actin were surprisingly dynamic and had different modes of exchange within the junction (Higashi et al., 2016; Raleigh et al., 2011; Shen et al., 2008; Yu et al., 2010). Changes in tight junction protein FRAP dynamics are linked to changes in global barrier function (Raleigh et al., 2011; Yu et al., 2010); however, the complexity of tight junctions has made it hard to determine precisely how FRAP dynamics and the formation of multiprotein complexes link to barrier function.

Fibroblast studies have demonstrated that while claudins do not diffuse within the strands, the strands themselves can be very dynamic. Claudin strands can form end-on interactions, breaking apart from one another and resealing with nearby strands, as well as side-to-side interactions (Sasaki et al., 2003; Van Itallie et al., 2017). In fibroblasts, occludin tends to cluster at strand branch points (Figure 1.5b), while co-expression of ZO-1 with claudins reduces strand dynamics and aligns strands with the actin network (Van Itallie et al., 2017). Freeze fracture EM has revealed that some perturbations, such as mechanical stretch and osmotic stress (Hull and Staehelin, 1976; Wade and Karnovsky, 1974), can induce breaks in the strand network (Figure 1.5d,e), indicating the single strand breaks and joins observed in fibroblasts may be biologically relevant.

Figure 1.5: Tight junctions are composed of a dynamic network of claudin strands. (a) 3D depiction of epithelial cells. The red boxed region indicates the strand network that is visible by freeze fracture electron microscopy. Because tight junction strands are closely packed and perpendicular to the plane of the microscope, visualizing strand dynamics in epithelial cells has not yet been possible. **(b)** Dynamic claudin strands have been observed at regions of cell overlap when claudins are expressed in fibroblasts, which do not normally make tight junctions. Because these regions of overlap are parallel to the plane of imaging, they can be more easily visualized. It has been determined that while claudins within the strand are stable (they do not exchange in and out of the strands), the strands move within the membrane, break, and fuse with other strands, making a dynamic network. Occludin localizes to strand ends and fusion points. **(c)** The leak pathway is hypothesized to occur through the dynamic breaking and resealing of claudin strands (blue dotted lines), which would allow small amounts of macromolecules (pink circles) to cross the tight junction in a non-selective manner. **(d,e)** Freeze fracture studies in the large intestine of *Xenopus laevis* tadpoles revealed that strands can break in response to stretch. Author's illustration of freeze fracture electron micrographs originally published in (Hull and Staehelin, 1976). **(d)** In a control intestine, a network of interconnected claudin strands prevents macromolecules from crossing the tight junction. **(e)** When the large intestine is stretched, the strand network becomes disconnected, creating a path for macromolecules to cross the tight junction (pink dotted line).

Figure 1.5

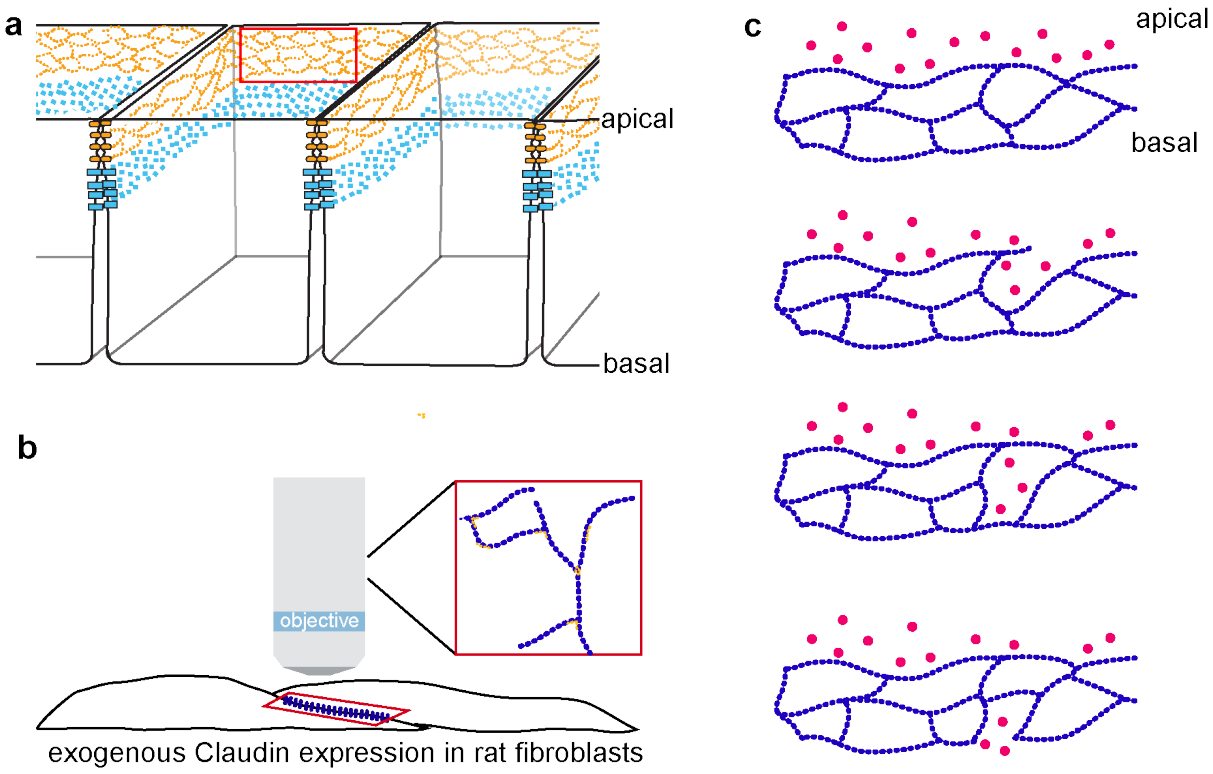
a
apical
basal
b
objective
exogenous Claudin expression in rat fibroblasts
c
apical
basal
d
apical
250 nm
basal
large intestine, stage 58
e
axis of stretch
stretched large intestine, stage 58

The leak pathway

The leak pathway is a low-capacity, non-selective route that permits small volumes of macromolecules to cross the tight junction barrier (Anderson and Van Itallie, 2009; Shen et al., 2011). A popular hypothesis is that claudin strand dynamics form the basis of the leak pathway. That is, progressive breaking and annealing of claudin strands creates small chambers that fill with macromolecules which are eventually permitted to cross the epithelium (Figure 1.5c) (Zihni et al., 2016). The leak pathway can be monitored by adding traceable macromolecules, such as fluorescent dextrans, to the apical surface of an epithelium and monitoring their penetration to the basal side.

By comparing tracer studies with TER, it has become apparent that the leak and pore pathways are regulated by distinct mechanisms. Perturbations that completely disrupt tight junctions decrease TER as well as increase penetration of tracers. However, there are some perturbations that cause an increase in macromolecular flux while decreasing ion flux or leaving it unaffected, and vice versa (Balda et al., 1996; Buschmann et al., 2013; Fanning et al., 2012; Raleigh et al., 2011; Van Itallie et al., 2009). These studies indicated that ZO-1, occludin, and actin dynamics are key regulators of the leak pathway. That macromolecular flux can increase while having little effect on TER speaks to the high capacity of the pore pathway relative to the leak pathway; even when leaks are more frequent, there are still few sites for macromolecules to cross the tight junction relative to ion-conductive pores.

How exactly actin polymerization affects barrier function remains unclear. However, in epithelial tissues, the junctional actin cytoskeleton is also important for epithelial integrity, tissue stiffness, tissue morphogenesis, cytokinesis, wound healing,

and cell extrusion. Because of this, the properties of the actin cytoskeleton in epithelial tissues have been intensively studied (Arnold et al., 2017). In the next section, I will review how Rho family GTPases regulate the actin cytoskeleton in epithelial cells.

Rho GTPases and actomyosin in apical junction regulation

In the initial stages of junction formation in cultured cells, polymerization of branched actin drives cell migration until multiple migrating cells come into contact with one another (Verma et al., 2004). Then, the GTPase Rac1 promotes further actin branching to extend the interface between these two cells, promoting cadherin ligation (Yamazaki et al., 2007). As the junctions mature, these branched actin networks are converted into a contractile array composed of linear actin filaments and non-muscle myosin II mini-filaments (Michael et al., 2016). This F-actin array is linked to the transmembrane components of both tight junctions and adherens junctions through a wide array of actin binding proteins (tight junctions: ZO proteins, cingulin, paracingluin; adherens junctions: α-catenin, vinculin, afadin) (Figure 1.3) (Arnold et al., 2017).

The dynamics of junctional actin is governed by a wide array of proteins, including nucleation and elongation factors (formins, Arp2/3 complex, Ena/Vasp), crosslinking proteins (α-actinin, filamin, anillin), severing proteins (cofilin), and myosin motors (Arnold et al., 2017). Rho family GTPases are master regulators of cytoskeletal dynamics in a wide variety of cell contexts. As GTPases, they cycle between an active, GTP-bound state and an inactive, GDP-bound state under the control of Guanine nucleotide Exchange Factors (GEFs) and GTPase Activating Proteins (GAPs) (Figure 1.6). When in the GTP-bound conformation, GTPases can activate effector proteins,

Figure 1.6

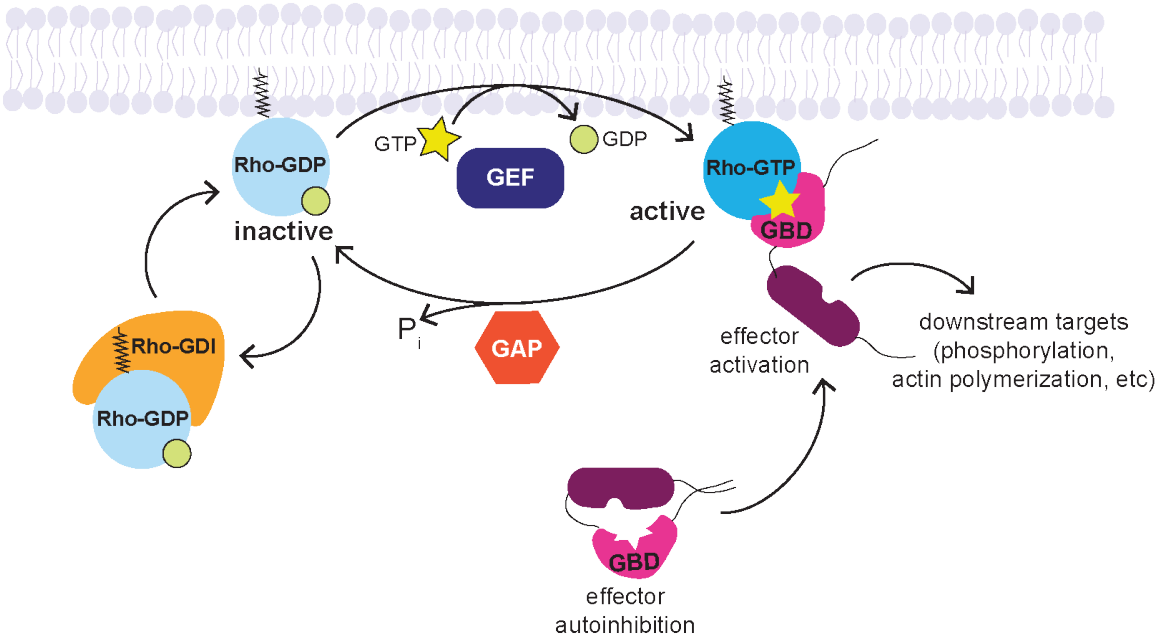

Figure 1.6: Rho GTPases cycle between an active and inactive conformation. Canonical Rho family GTPases are active when bound to GTP. In this state, they can bind to and activate effector proteins, which act on downstream targets. Active GTPases are converted to their inactive, GDP-bound conformation by GAPs (GTPase activating proteins), which stimulate the intrinsic GTP hydrolysis activity of the GTPase. Once inactive, Rho GTPases can be removed from the membrane by Rho GDI (Guanine nucleotide Dissociation Inhibitor), which sequesters them in the cytoplasm and prevents their activation. GEFs (Guanine nucleotide Exchange Factors) convert inactive GTPases to the active conformation by exchanging GDP for GTP. Figure originally published in Stephenson and Miller, 2017.

typically through relief of autoinhibition, and these effector proteins perform their functions on the cytoskeleton or other targets. Effectors typically carry out localized effects in close proximity to the site of activation. Thus, the spatial activation of GTPases and local availability of effectors is critical for GTPase output.

The importance of Rho GTPases in regulating epithelial cell-cell junctions has been evident from the mid-1990s, when constitutively active and dominant negative Rho GTPases were used to test their effects on cell-cell junction architecture and junctional actin assembly (reviewed in Citi et al., 2014; Quiros and Nusrat, 2014). In the decades since, biochemical and immunostaining methods have been applied to learn more about

regulation of junctional Rho GTPases and their downstream consequences (Figure 1.7). Only more recently has GTPase activity been directly observed at cell-cell junctions (Ratheesh et al., 2012; Terry et al., 2011).

Methods for studying Rho GTPase activation

Approaches to study GTPase activity must go beyond simply fluorescently tagging GTPases, as this does not indicate their nucleotide binding state (and does not faithfully reflect the localization when compared with fixed imaging) (Stephenson and Miller, 2017). Instead, approaches to evaluate GTPase activation typically use the GTPase Binding Domains (GBDs) of effector proteins, which preferentially bind the GTP-bound state. GST-GBD pulldowns can detect bulk changes in GTPase activation across an entire tissue; however, this approach lacks spatial information about where the changes in GTPases activation occur (Figure 1.7a). A popular approach to circumvent this issue is to visualize GTPase activation using FRET (Förster resonance energy transfer) biosensors, in which the GTPase and GBD are tagged with donor and acceptor fluorophores, respectively. GTPase activation results in the binding of these components and energy transfer between the two fluorophores (Figure 1.7c). A more straightforward approach is to simply observe the localization of the tagged GBD, which will report relative activation of GTPases when compared to background signal (Figure 1.7b). This has the advantage of being compatible with more fluorescent probes (FRET requires two channels, whereas translocation probes require only one) and simpler analysis.

Figure 1.7

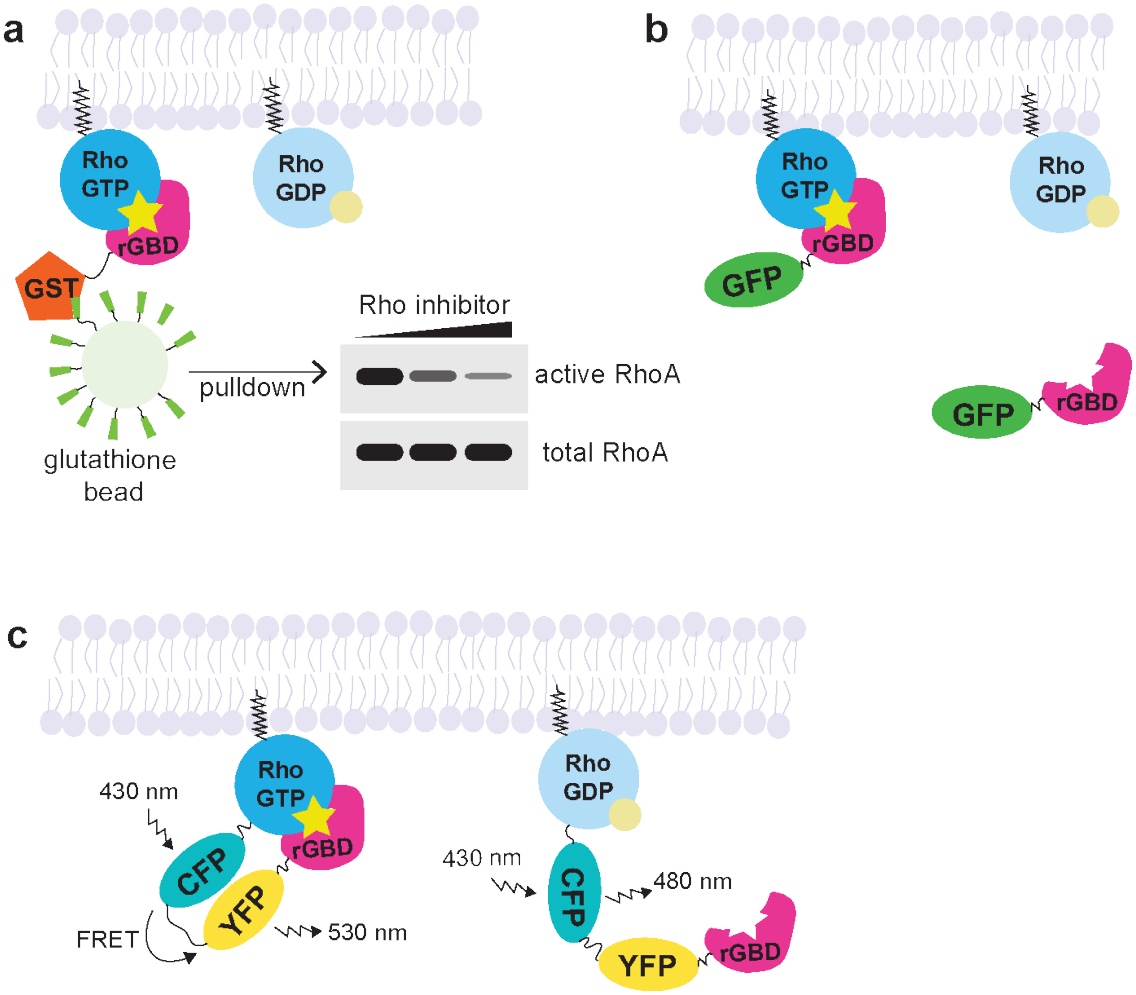

Figure 1.7: Approaches for studying GTPase activation that use GTPase Binding Domains (GBDs) (a) Biochemical approaches to studying GTPases use GBDs fused to tags that can be used for pulldowns, like GST/glutathione. Biochemical approaches allow samples to be processed in bulk, but don't reveal where in the cell the GTPase is active. **(b)** Translocation probes simply fuse the GDB to a fluorescent protein, and measure changes in fluorescence intensity. **(c)** FRET biosensors fuse both GBD and GTPase with fluorophores and measure the energy transfer between fluorophores. This example given is of a unimolecular FRET probe, where all proteins are encoded by one transcript. Figure originally published in (Stephenson and Miller, 2017).

Early studies with FRET biosensors at junctions reported snapshots in time (Ratheesh et al., 2012; Terry et al., 2011), in part because Rho activity was assumed to be uniformly and stably activated at junctions, rather than dynamic across short temporal and spatial scales. Indeed, later work confirmed a "strikingly stable active

zone" of Rho using the C-terminus of anillin as Rho probe (Priya et al., 2015). However, this work was also conducted in mature, cultured epithelial cells. In contrast, our lab found that, in addition to stable baseline activity, active Rho and F-actin accumulate in transient, dynamic "flares" at cell-cell junctions in the epithelium of *Xenopus laevis* embryos (Breznau et al., 2015; Reyes et al., 2014).

Overview of the dissertation

In this dissertation, I investigate the events leading up to Rho flares as well as how Rho flares affect cell-cell junctions. In preliminary experiments, I found that tight junction proteins were locally reduced prior to flares and reinforced following flares. This, in combination with evidence from the literature that actin dynamics can modulate barrier function, led us to hypothesize that Rho flares serve as a tight junction repair mechanism. In order to determine whether Rho flares were important for repairing tight junctions, we needed to determine whether the barrier function was indeed compromised at the site of the flare. Popular measures of barrier function, such as TER and dye penetration assays, average barrier function across the entire population of epithelial cells. In order to spatially and temporally correlate barrier function with Rho flares, we developed a highly sensitive technique called ZnUMBA (Zinc-based Ultrasensitive Microscopic Barrier Assay), which results in high fluorescence when barrier function is compromised. In **Chapter 2**, I validate ZnUMBA as a technique by performing control experiments that compromise barrier function either globally or locally. Then, I apply ZnUMBA to the unperturbed epithelium, showing naturally-occurring transient breaches of epithelial tight junctions for the first time with live

microscopy. As we predicted, Rho flares followed these tight junction breaches and were associated with restoration of barrier function.

Because Rho flares typically occur near dividing cells or during tissue-scale morphogenetic events, we hypothesized that the transient barrier breaches that trigger Rho flares are related to changes in cell shape or tissue tension. In the developing embryo, tight junctions are frequently subjected to both cell- and tissue-scale forces that result from cell division and tissue bending, stretching, and folding (Figure 1.2). In epithelia grown in 2D culture, cells are typically grown on a filter support. These cells become less mobile and divide less frequently once the cells reach confluence, explaining why Rho flares may not have been observed in cultured cells (Priya et al., 2015). However, even in adult epithelial tissues, cells divide and extrude, and tissues are subject to changing mechanical forces due to normal tissue function. Thus, the dynamic environment of an intact embryo may better represent some aspects of epithelial mechanics than cell culture models.

Multiple studies in dynamic epithelial or endothelial tissues, such as those subject to osmotic stress (Tokuda et al., 2016), low cell density (Abu Taha et al., 2014), multicellular wound healing (Clark et al., 2009; Razzell et al., 2014), sprouting angiogenesis (Cao et al., 2017), and neural tube closure (Hashimoto et al., 2015), have reported transient accumulations of F-actin and/or myosin II. However, many of these studies focused on the adherens junctions as the cause of these transient accumulations and/or the intended target of the F-actin and myosin II accumulation (Abu Taha et al., 2014; Cao et al., 2017; Hashimoto et al., 2015; Razzell et al., 2013), probably because adherens junctions are seen as the primary tension-sensing and

generating apparatuses in epithelial tissues. In **Chapter 3**, I demonstrate that multiple tight junction proteins, as well as barrier function, are compromised prior to Rho flares and are restored afterwards. Rho flares drive barrier reinstatement through localized ROCK-mediated actomyosin contraction of the junction. While adherens junctions may be involved in driving contraction during Rho flares, only the tight junctions show any apparent defect. This highlights the need to consider how both tight junctions and adherens junctions influence the dynamics of cell-cell junctions.

Rho flares are associated with dynamic protrusions of the plasma membrane. However, the force that drives membrane protrusion as well as the function of membrane protrusions is unclear. In **Chapter 4**, I explore the mechanics of membrane protrusions that are associated with Rho flares, presenting data regarding the dynamics of F-actin, myosin II, and actin nucleation factors. Finally, in **Chapter 5**, I discuss how my findings about Rho flares fit into our existing knowledge of endothelial junction repair, speculate which GEFs, GAPs, and scaffolding proteins may contribute to Rho flare signaling, discuss how local loss of ZO-1 and occludin contribute to the leak pathway, speculate on the event that triggers Rho flares, and discuss future directions for this work. Rho flares represent an exciting new mechanism of rapid tight junction repair that is relevant during development, and probably during normal tissue homeostasis and disease as well.

References:

Abu Taha, A., Taha, M., Seebach, J., and Schnittler, H.-J. (2014). ARP2/3-mediated junction-associated lamellipodia control VE-cadherin-based cell junction dynamics and maintain monolayer integrity. Molecular Biology of the Cell *25*, 245–256.

Anderson, J.M., and Van Itallie, C.M. (2009). Physiology and function of the tight junction. Cold Spring Harb Perspect Biol *1*, a002584–a002584.

Arnold, T.R., Stephenson, R.E., and Miller, A.L. (2017). Rho GTPases and actomyosin: Partners in regulating epithelial cell-cell junction structure and function. Exp. Cell Res. *358*, 20–30.

Balda, M.S., Whitney, J.A., Flores, C., González, S., Cereijido, M., and Matter, K. (1996). Functional dissociation of paracellular permeability and transepithelial electrical resistance and disruption of the apical-basolateral intramembrane diffusion barrier by expression of a mutant tight junction membrane protein. J. Cell Biol. *134*, 1031–1049.

Bianconi, E., Piovesan, A., Facchin, F., Beraudi, A., Casadei, R., Frabetti, F., Vitale, L., Pelleri, M.C., Tassani, S., Piva, F., et al. (2013). An estimation of the number of cells in the human body. Ann. Hum. Biol. *40*, 463–471.

Breznau, E.B., Semack, A.C., Higashi, T., and Miller, A.L. (2015). MgcRacGAP restricts active RhoA at the cytokinetic furrow and both RhoA and Rac1 at cell-cell junctions in epithelial cells. Molecular Biology of the Cell *26*, 2439–2455.

Buckley, C.D., Tan, J., Anderson, K.L., Hanein, D., Volkmann, N., Weis, W.I., Nelson, W.J., and Dunn, A.R. (2014). Cell adhesion. The minimal cadherin-catenin complex binds to actin filaments under force. Science *346*, 1254211–1254211.

Buschmann, M.M., Shen, L., Rajapakse, H., Raleigh, D.R., Wang, Y., Wang, Y., Lingaraju, A., Zha, J., Abbott, E., McAuley, E.M., et al. (2013). Occludin OCEL-domain interactions are required for maintenance and regulation of the tight junction barrier to macromolecular flux. Molecular Biology of the Cell *24*, 3056–3068.

Cao, J., Ehling, M., März, S., Seebach, J., Tarbashevich, K., Sixta, T., Pitulescu, M.E., Werner, A.-C., Flach, B., Montanez, E., et al. (2017). Polarized actin and VE-cadherin dynamics regulate junctional remodelling and cell migration during sprouting angiogenesis. Nat Commun *8*, 2210.

Capaldo, C.T., and Nusrat, A. (2009). Cytokine regulation of tight junctions. Biochim. Biophys. Acta *1788*, 864–871.

Carattino, M.D., Prakasam, H.S., Ruiz, W.G., Clayton, D.R., McGuire, M., Gallo, L.I., and Apodaca, G. (2013). Bladder filling and voiding affect umbrella cell tight junction organization and function. Am. J. Physiol. Renal Physiol. *305*, F1158–F1168.

Charras, G., and Yap, A.S. (2018). Tensile Forces and Mechanotransduction at Cell-Cell Junctions. Current Biology *28*, R445–R457.

Citi, S., Guerrera, D., Spadaro, D., and Shah, J. (2014). Epithelial junctions and Rho family GTPases: the zonular signalosome. Small GTPases *5*, 1–15.

Clark, A.G., Miller, A.L., Vaughan, E., Yu, H.-Y.E., Penkert, R., and Bement, W.M. (2009). Integration of single and multicellular wound responses. Curr. Biol. *19*, 1389–1395.

Claude, P., and Goodenough, D.A. (1973). Fracture faces of zonulae occludentes from "tight" and “leaky” epithelia. J. Cell Biol. *58*, 390–400.

Duszyc, K., Gomez, G.A., Schroder, K., Sweet, M.J., and Yap, A.S. (2017). In life there is death: How epithelial tissue barriers are preserved despite the challenge of apoptosis. Tissue Barriers *5*, e1345353.

Fanning, A.S., Jameson, B.J., Jesaitis, L.A., and Anderson, J.M. (1998). The tight junction protein ZO-1 establishes a link between the transmembrane protein occludin and the actin cytoskeleton. J. Biol. Chem. *273*, 29745–29753.

Fanning, A.S., and Anderson, J.M. (2009). Zonula occludens-1 and -2 are cytosolic scaffolds that regulate the assembly of cellular junctions. Ann. N. Y. Acad. Sci. *1165*, 113–120.

Fanning, A.S., Lye, M.F., Anderson, J.M., and Lavie, A. (2007). Domain swapping within PDZ2 is responsible for dimerization of ZO proteins. J. Biol. Chem. *282*, 37710–37716.

Fanning, A.S., Van Itallie, C.M., and Anderson, J.M. (2012). Zonula occludens-1 and -2 regulate apical cell structure and the zonula adherens cytoskeleton in polarized epithelia. Molecular Biology of the Cell *23*, 577–590.

Farquhar, M.G., and Palade, G.E. (1963). Junctional complexes in various epithelia. J. Cell Biol. *17*, 375–412.

Furuse, M., Fujita, K., Hiiragi, T., Fujimoto, K., and Tsukita, S. (1998a). Claudin-1 and -2: novel integral membrane proteins localizing at tight junctions with no sequence similarity to occludin. J. Cell Biol. *141*, 1539–1550.

Furuse, M., Sasaki, H., Fujimoto, K., and Tsukita, S. (1998b). A single gene product, claudin-1 or -2, reconstitutes tight junction strands and recruits occludin in fibroblasts. J. Cell Biol. *143*, 391–401.

Günzel, D., and Yu, A.S.L. (2013). Claudins and the modulation of tight junction permeability. Physiol. Rev. *93*, 525–569.

Harris, T.J.C., and Tepass, U. (2010). Adherens junctions: from molecules to morphogenesis. Nat. Rev. Mol. Cell Biol. *11*, 502–514.

Hashimoto, H., Robin, F.B., Sherrard, K.M., and Munro, E.M. (2015). Sequential contraction and exchange of apical junctions drives zippering and neural tube closure in a simple chordate. Dev. Cell *32*, 241–255.

Higashi, T., Arnold, T.R., Stephenson, R.E., Dinshaw, K.M., and Miller, A.L. (2016). Maintenance of the Epithelial Barrier and Remodeling of Cell-Cell Junctions during Cytokinesis. Curr. Biol. *26*, 1829–1842.

Hooper, C.E.S. (1956). Cell turnover in epithelial populations. J. Histochem. Cytochem. *4*, 531–540.

Hull, B.E., and Staehelin, L.A. (1976). Functional significance of the variations in the geometrical organization of tight junction networks. J. Cell Biol. *68*, 688–704.

Itoh, M., Furuse, M., Morita, K., Kubota, K., Saitou, M., and Tsukita, S. (1999). Direct binding of three tight junction-associated MAGUKs, ZO-1, ZO-2, and ZO-3, with the COOH termini of claudins. J. Cell Biol. *147*, 1351–1363.

Khandelwal, P., Abraham, S.N., and Apodaca, G. (2009). Cell biology and physiology of the uroepithelium. Am. J. Physiol. Renal Physiol. *297*, F1477–F1501.

Libby, E., Conlin, P.L., Kerr, B., and Ratcliff, W.C. (2016). Stabilizing multicellularity through ratcheting. Philos. Trans. R. Soc. Lond., B, Biol. Sci. *371*, 20150444.

Lingaraju, A., Long, T.M., Wang, Y., Austin, J.R., and Turner, J.R. (2015). Conceptual barriers to understanding physical barriers. Semin. Cell Dev. Biol. *42*, 13–21.

López-Posadas, R., Stürzl, M., Atreya, I., Neurath, M.F., and Britzen-Laurent, N. (2017). Interplay of GTPases and Cytoskeleton in Cellular Barrier Defects during Gut Inflammation. Front Immunol *8*, 1240.

Macara, I.G., Guyer, R., Richardson, G., Huo, Y., and Ahmed, S.M. (2014). Epithelial homeostasis. Curr. Biol. *24*, R815–R825.

Marchiando, A.M., Graham, W.V., and Turner, J.R. (2010). Epithelial barriers in homeostasis and disease. Annu Rev Pathol *5*, 119–144.

Mehta, F. (2016). Report: economic implications of inflammatory bowel disease and its management. Am J Manag Care *22*, s51–s60.

Michael, M., Meiring, J.C.M., Acharya, B.R., Matthews, D.R., Verma, S., Han, S.P., Hill, M.M., Parton, R.G., Gomez, G.A., and Yap, A.S. (2016). Coronin 1B Reorganizes the Architecture of F-Actin Networks for Contractility at Steady-State and Apoptotic Adherens Junctions. Dev. Cell *37*, 58–71.

Odenwald, M.A., and Turner, J.R. (2013). Intestinal permeability defects: is it time to treat? Clin. Gastroenterol. Hepatol. *11*, 1075–1083.

Priya, R., Gomez, G.A., Budnar, S., Verma, S., Cox, H.L., Hamilton, N.A., and Yap, A.S. (2015). Feedback regulation through myosin II confers robustness on RhoA signalling at E-cadherin junctions. Nat Cell Biol *17*, 1282–1293.

Quiros, M., and Nusrat, A. (2014). RhoGTPases, actomyosin signaling and regulation of the epithelial Apical Junctional Complex. Semin. Cell Dev. Biol. *36*, 194–203.

Raleigh, D.R., Boe, D.M., Yu, D., Weber, C.R., Marchiando, A.M., Bradford, E.M., Wang, Y., Wu, L., Schneeberger, E.E., Shen, L., et al. (2011). Occludin S408 phosphorylation regulates tight junction protein interactions and barrier function. J. Cell Biol. *193*, 565–582.

Ratheesh, A., Gomez, G.A., Priya, R., Verma, S., Kovacs, E.M., Jiang, K., Brown, N.H., Akhmanova, A., Stehbens, S.J., and Yap, A.S. (2012). Centralspindlin and [alpha]-catenin regulate Rho signalling at the epithelial zonula adherens. Nat Cell Biol *14*, 818–828.

Razzell, W., Evans, I.R., Martin, P., and Wood, W. (2013). Calcium flashes orchestrate the wound inflammatory response through DUOX activation and hydrogen peroxide release. Curr. Biol. *23*, 424–429.

Razzell, W., Wood, W., and Martin, P. (2014). Recapitulation of morphogenetic cell shape changes enables wound re-epithelialisation. Development *141*, 1814–1820.

Reyes, C.C., Jin, M., Breznau, E.B., Espino, R., Delgado-Gonzalo, R., Goryachev, A.B., and Miller, A.L. (2014). Anillin Regulates Cell-Cell Junction Integrity by Organizing Junctional Accumulation of Rho-GTP and Actomyosin. Current Biology *24*, 1263–1270.

Rosenthal, R., Günzel, D., Theune, D., Czichos, C., Schulzke, J.-D., and Fromm, M. (2017). Water channels and barriers formed by claudins. Ann. N. Y. Acad. Sci. *1397*, 100–109.

Sasaki, H., Matsui, C., Furuse, K., Mimori-Kiyosue, Y., Furuse, M., and Tsukita, S. (2003). Dynamic behavior of paired claudin strands within apposing plasma membranes. Proc Natl Acad Sci USA *100*, 3971–3976.

Scott, D.W., Tolbert, C.E., and Burridge, K. (2016). Tension on JAM-A activates RhoA via GEF-H1 and p115 RhoGEF. Molecular Biology of the Cell *27*, 1420–1430.

Severs, N.J. (2007). Freeze-fracture electron microscopy. Nat Protoc *2*, 547–576.

Shen, L., Weber, C.R., and Turner, J.R. (2008). The tight junction protein complex undergoes rapid and continuous molecular remodeling at steady state. J. Cell Biol. *181*, 683–695.

Shen, L., Weber, C.R., Raleigh, D.R., Yu, D., and Turner, J.R. (2011). Tight junction pore and leak pathways: a dynamic duo. Annu. Rev. Physiol. *73*, 283–309.

Solnica-Krezel, L., and Sepich, D.S. (2012). Gastrulation: making and shaping germ layers. Annu. Rev. Cell Dev. Biol. *28*, 687–717.

Spadaro, D., Le, S., Laroche, T., Mean, I., Jond, L., Yan, J., and Citi, S. (2017). Tension-Dependent Stretching Activates ZO-1 to Control the Junctional Localization of Its Interactors. Curr. Biol. *27*, 3783–3795.e3788.

Spalding, K.L., Bhardwaj, R.D., Buchholz, B.A., Druid, H., and Frisén, J. (2005). Retrospective birth dating of cells in humans. Cell *122*, 133–143.

Stephenson, R.E., and Miller, A.L. (2017). Tools for live imaging of active Rho GTPases in Xenopus. Genesis *55*, e22998.

Takeichi, M. (2014). Dynamic contacts: rearranging adherens junctions to drive epithelial remodelling. Nat. Rev. Mol. Cell Biol. *15*, 397–410.

Terry, S.J., Zihni, C., Elbediwy, A., Vitiello, E., Leefa Chong San, I.V., Balda, M.S., and Matter, K. (2011). Spatially restricted activation of RhoA signalling at epithelial junctions by p114RhoGEF drives junction formation and morphogenesis. Nat Cell Biol *13*, 159–166.

Tokuda, S., Hirai, T., and Furuse, M. (2016). Effects of Osmolality on Paracellular Transport in MDCK II Cells. PLoS ONE *11*, e0166904.

Truschel, S.T., Wang, E., Ruiz, W.G., Leung, S.-M., Rojas, R., Lavelle, J., Zeidel, M., Stoffer, D., and Apodaca, G. (2002). Stretch-regulated exocytosis/endocytosis in bladder umbrella cells. Molecular Biology of the Cell *13*, 830–846.

Turner, J.R., Buschmann, M.M., Romero-Calvo, I., Sailer, A., and Shen, L. (2014). The role of molecular remodeling in differential regulation of tight junction permeability. Semin. Cell Dev. Biol. *36*, 204–212.

Utepbergenov, D.I., Fanning, A.S., and Anderson, J.M. (2006). Dimerization of the scaffolding protein ZO-1 through the second PDZ domain. J. Biol. Chem. *281*, 24671–24677.

Van Itallie, C.M., and Anderson, J.M. (2014). Architecture of tight junctions and principles of molecular composition. Semin. Cell Dev. Biol. *36*, 157–165.

Van Itallie, C.M., Fanning, A.S., Bridges, A., and Anderson, J.M. (2009). ZO-1 stabilizes the tight junction solute barrier through coupling to the perijunctional cytoskeleton. Molecular Biology of the Cell *20*, 3930–3940.

Van Itallie, C.M., Tietgens, A.J., and Anderson, J.M. (2017). Visualizing the dynamic coupling of claudin strands to the actin cytoskeleton through ZO-1. Molecular Biology of the Cell *28*, 524–534.

Vasquez, C.G., and Martin, A.C. (2016). Force transmission in epithelial tissues. Dev. Dyn. *245*, 361–371.

Verma, S., Shewan, A.M., Scott, J.A., Helwani, F.M., Elzen, den, N.R., Miki, H., Takenawa, T., and Yap, A.S. (2004). Arp2/3 activity is necessary for efficient formation of E-cadherin adhesive contacts. J. Biol. Chem. *279*, 34062–34070.

Wade, J.B., and Karnovsky, M.J. (1974). Fracture faces of osmotically disrupted Zonulae Occludentes. J. Cell Biol. *62*, 344–350.

Weber, C.R. (2012). Dynamic properties of the tight junction barrier. Ann. N. Y. Acad. Sci. *1257*, 77–84.

Weber, C.R., Liang, G.H., Wang, Y., Das, S., Shen, L., Yu, A.S.L., Nelson, D.J., and Turner, J.R. (2015). Claudin-2-dependent paracellular channels are dynamically gated. Elife *4*, e09906.

Williams, J.M., Duckworth, C.A., Burkitt, M.D., Watson, A.J.M., Campbell, B.J., and Pritchard, D.M. (2015). Epithelial cell shedding and barrier function: a matter of life and death at the small intestinal villus tip. Vet. Pathol. *52*, 445–455.

Yamazaki, D., Oikawa, T., and Takenawa, T. (2007). Rac-WAVE-mediated actin reorganization is required for organization and maintenance of cell-cell adhesion. J. Cell. Sci. *120*, 86–100.

Yao, M., Qiu, W., Liu, R., Efremov, A.K., Cong, P., Seddiki, R., Payre, M., Lim, C.T., Ladoux, B., Mège, R.-M., et al. (2014). Force-dependent conformational switch of α-catenin controls vinculin binding. Nat Commun *5*, 4525.

Yap, A.S., Gomez, G.A., and Parton, R.G. (2015). Adherens Junctions Revisualized: Organizing Cadherins as Nanoassemblies. Dev. Cell *35*, 12–20.

Yonemura, S., Wada, Y., Watanabe, T., Nagafuchi, A., and Shibata, M. (2010). alpha-Catenin as a tension transducer that induces adherens junction development. Nat Cell Biol *12*, 533–542.

Yu, D., Marchiando, A.M., Weber, C.R., Raleigh, D.R., Wang, Y., Shen, L., and Turner, J.R. (2010). MLCK-dependent exchange and actin binding region-dependent anchoring of ZO-1 regulate tight junction barrier function. Proc. Natl. Acad. Sci. U.S.a. *107*, 8237–8241.

Zihni, C., and Terry, S.J. (2015). RhoGTPase signalling at epithelial tight junctions: Bridging the GAP between polarity and cancer. Int. J. Biochem. Cell Biol. *64*, 120–125.

Zihni, C., Mills, C., Matter, K., and Balda, M.S. (2016). Tight junctions: from simple barriers to multifunctional molecular gates. Nat. Rev. Mol. Cell Biol. *17*, 564–580.

Notes:

Figures 1.6 and 1.7, as well as portions of the section “Methods for studying Rho GTPase activation” were originally published in “Tools for live imaging of active Rho GTPases in *Xenopus*” by Rachel E. Stephenson and Ann L. Miller, *Genesis 55* (2017) e22998.

Chapter 2

Zinc-based Ultrasensitive Microscopic Barrier Assay detects transient, localized breaches of the epithelial barrier

Abstract: Epithelial barrier function is determined by tight junctions, multiprotein complexes that form between cells and restrict the flow of materials through the paracellular space. Epithelial tissues are subject to mechanical strain through tissue bending, stretching, and folding, as well as cell shape changes like extrusion and cytokinesis. However, little is known about how tight junctions adapt to these changes in mechanical force and whether barrier function is maintained. In this chapter, I present the Zinc-based Ultrasensitive Microscopic Barrier Assay (ZnUMBA), which we used to determine that epithelial barrier function is not uniform over space and time. Instead, transient, localized leaks occur, and these correspond to sites of Rho flares. This new technique will enable us to investigate more about the events preceding and following barrier breaches in control and perturbed settings, allowing us to learn how cell and tissue mechanics relate to barrier function.

Introduction

Epithelial tissues generate specialized compartments within multicellular organisms, regulate nutrient and water transport, and create barriers to pathogens. In vertebrates, tight junction protein complexes regulate the amount and type of molecules that pass through the paracellular space (the space between cells). Large quantities of ions and water can cross the tight junction through the pore pathway, which is established by claudin-family proteins forming size- and charge-selective pores (Shen et al., 2011). Smaller quantities of macromolecules cross the tight junction through the leak pathway, which is thought to be regulated by the breaking and annealing of claudin strands (Zihni et al., 2016). Both pathways are typically evaluated with global measures of barrier function; the pore pathway with transepithelial electrical resistance (TER) and the leak pathway by tracing penetrance of macromolecules across the tissue (Figure 2.1). Because these tissue-scale measurements are frequently used, little is known about how these pathways are regulated at cellular and subcellular scales.

Epithelial tissues are intrinsically mechanosensitive: physical characteristics such as cell geometry, cell shape change, and global changes in tension or shear stress can influence adherens junctions and tight junctions, leading to structural and signaling changes in cells. The mechanosensitivity of adherens junctions is well-established, with changes in tensile force regulating intermolecular interactions, cell signaling, and tissue stiffening (Charras and Yap, 2018; Vasquez and Martin, 2016). The actin cytoskeleton plays a major role in both generating and responding to forces in epithelial tissues (Vasquez and Martin, 2016). Mechanosensitive molecules within the tight junction have also been identified (Scott et al., 2016; Spadaro et al., 2017), and crosstalk between

Figure 2.1

a transepithelial electrical resistance

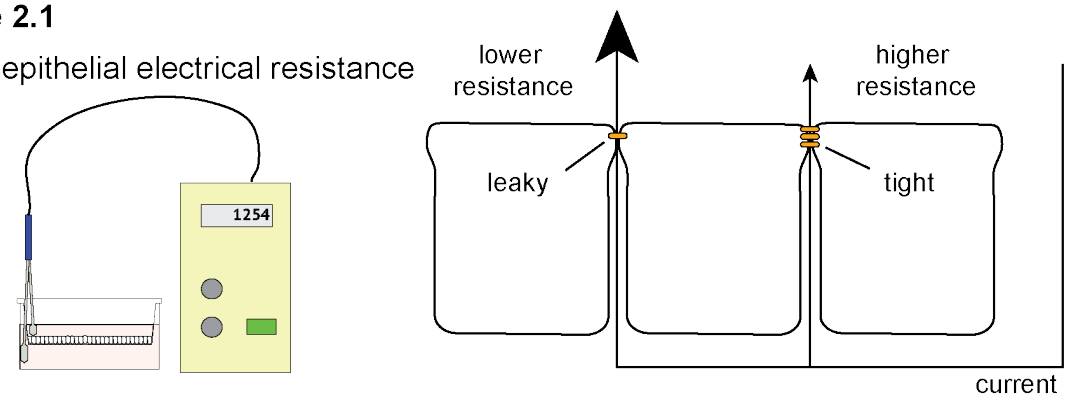

b tracer penetration assay

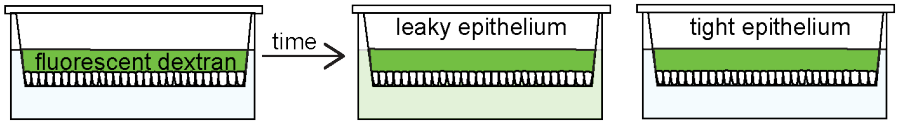

c sandwich assay

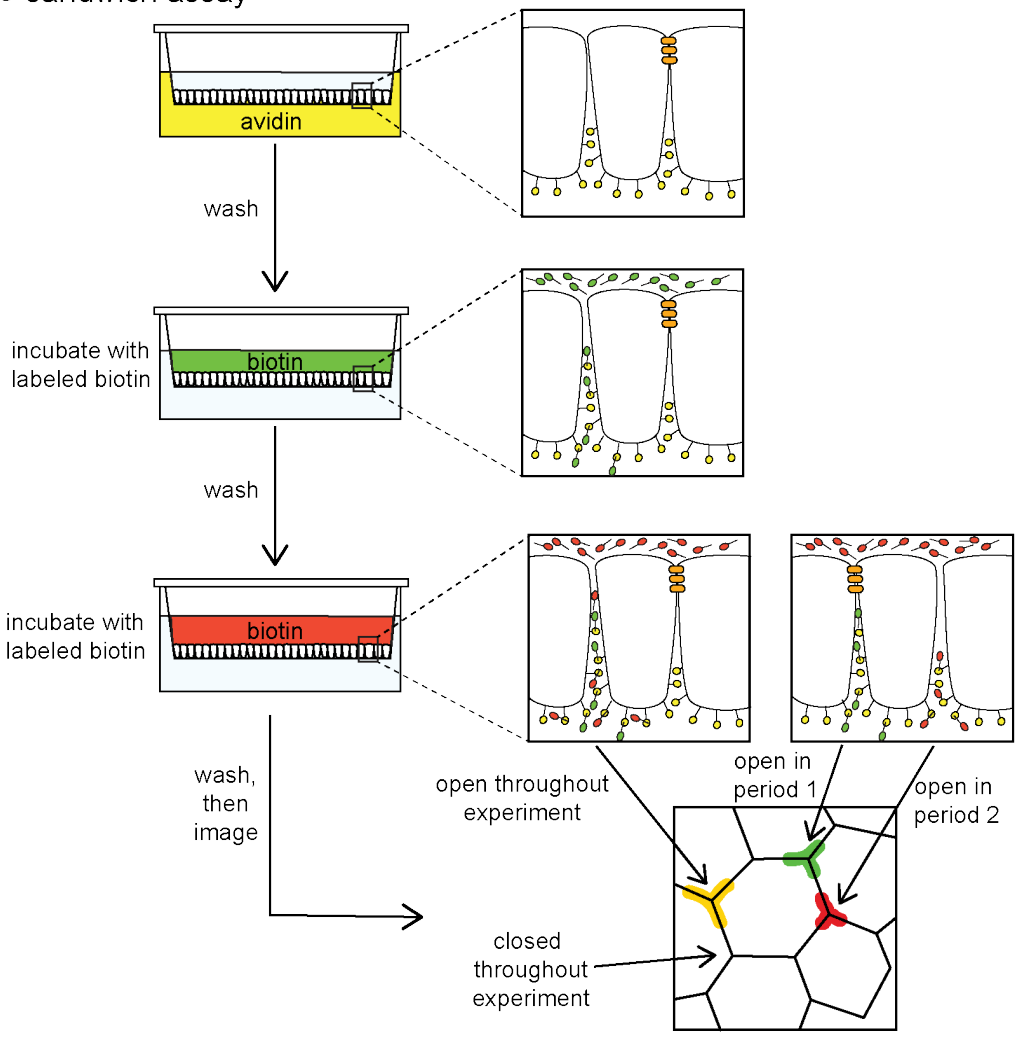

Figure 2.1: Global and local approaches to studying epithelial barrier function. (a) Transepithelial electrical resistance (TER) is a global measure of the high-capacity pore pathway. A current is applied to a tissue, and the resistance is measured. Tight junctions resist the current, so strong barrier function is associated with high TER. **(b)** Tracer penetration assays measure the penetrance of a tracer applied to one side of the epithelium to the other side. In this example, a fluorescent dextran is added to the apical compartment, then, after several hours, the medium in the basal compartment is collected and the quantity of the tracer is measured. Large amounts of tracer correspond to reduced barrier function. **(c)** Sandwich assays employ avidin and biotin to capture macromolecules as they cross the epithelium. In this example, avidin is added to the basal compartment and some of it remains adhered to the basolateral membrane after washing. During the first period, green fluorescent biotin is added to the apical compartment. Any biotin that crosses the tight junction will be immobilized by the basolateral avidin. Following washing, red fluorescent biotin is added to the apical compartment, incubated, and then both sides are washed and the epithelium visualized. Areas of the epithelium displaying single color of biotin represent leak sites that were open either during period one or period two. Areas displaying both colors of biotin represent leak sites that were open during both period one and period two. Because single colors can be detected, this indicates that the leak pathway opens and closes over time, rather than persisting at discrete sites.

adherens junctions and tight junctions has been documented (Campbell et al., 2017; Hatte et al., 2018; Shigetomi et al., 2018; Zihni et al., 2016). Changes in leak pathway regulation are associated with perturbations that result in global changes to the cytoskeleton (Fanning et al., 2012; Turner et al., 2014; Van Itallie et al., 2015). Therefore, it stands to reason that epithelial barrier function could be affected by mechanical force; however, direct evidence to this point is lacking. Furthermore, the mechanical forces within an epithelial tissue are not uniform; therefore, we predict that local mechanical forces could produce local changes in barrier function.

In contrast to the tissue-scale measures of barrier function, recently developed "sandwich assays" allow visualization of local barrier function at fixed time points. These assays employ fluorescently-labeled avidin and biotin applied to either the apical or basal side of the tissue to capture the macromolecules as they cross the tight junction barrier, which can be visualized via fluorescence microscopy at the experiment end point (Figure 2.1c). These studies have revealed that barrier function to macromolecules is not uniform across the cell and tissue level, that the leak pathway opens and closes over time, and that changes in barrier function occur in response to

fluid shear stress (Dubrovskyi et al., 2013; Ghim et al., 2017; Richter et al., 2016). Additionally, intestinal barrier function has been visualized with confocal laser endomicroscopy, which uses intravenous fluorescein injection to visualize the leakiness of healthy and diseased intestinal epithelia. This technique has shown that there are particularly leaky areas of the intestinal epithelium *in vivo*, and these correlate with disease severity (Lim et al., 2014; Rasmussen et al., 2015). However, the low temporal and/or spatial resolution of these techniques make it difficult to determine the events preceding and following leaks in barrier function.

In previous work, we tried visualizing the penetration of fluorescent molecules such as Alexa Fluor 488-Dextran (3000 Da) (Reyes et al., 2014) or fluorescein (332 Da) (Higashi et al., 2016) beyond the tight junction. Reyes et al. (2014) found that anillin knockdown results in increased depth of penetration of Alexa Fluor 488-Dextran; however, this likely reflects the disruption of junction organization rather than increased permeability because dextran did not penetrate to the basal compartment (Reyes et al., 2014). Higashi et al. (2016) examined epithelial barrier function during cytokinesis by directly imaging fluorescein applied to the apical surface of *Xenopus laevis* embryos. Under control conditions, it was not possible to detect the tracer beyond the tight junctions, even at the contractile ring, a site that undergoes a major cell shape change and represents a potential challenge to junction integrity (Hatte et al., 2018; Higashi et al., 2016). We reasoned that small volumes of a fluorescent tracer might be difficult to detect against the high background of apical fluorescein. Therefore, we sought to develop a more sensitive barrier assay with minimal background, in which a breach of tight junctions results in strongly increased fluorescence.

Figure 2.2

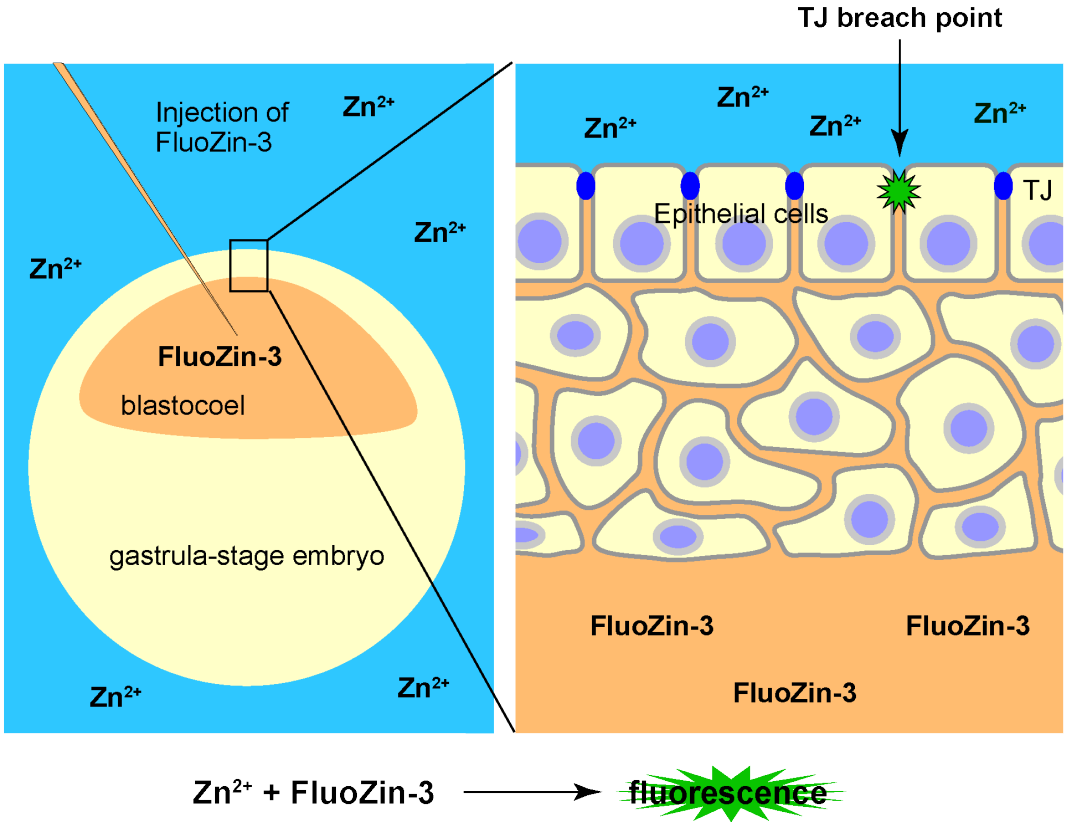

Figure 2.2: Schematic of Zinc-based Ultrasensitive Microscopic Barrier Assay for use in *X. laevis* embryos Left: the cell-impermeable zinc indicator FluoZin3 (orange) is injected into the blastocoel of a gastrula-stage *X. laevis* embryo, and the embryo is mounted in a solution containing Zn^{2+} (blue). Right: when a tight junction is locally breached, Zn^{2+} will bind to FluoZin3, and the local increase in fluorescence will be detectable with confocal fluorescence microscopy. Figure courtesy of Tomohito Higashi.

We achieved this by using the small cell-impermeable dye FluoZin3 (FZ3, 847 Da), which increases in fluorescence more than 50-fold when bound to zinc (65 Da). By applying FZ3 to the basal medium and adding media containing $ZnCl_2$ to the apical medium, localized breaches of the tight junction result in localized increases in FZ3 fluorescence that can be easily detected with conventional confocal microscopy. We call this assay ZnUMBA (Zinc-based Ultrasensitive Microscopic Barrier Assay) (Figure 2.2). ZnUMBA can detect both local and global changes in barrier function on sub-minute time scales. Using ZnUMBA in *X. laevis* embryos allowed us to visualize naturally

occurring transient leaks in the epithelium and correlate them with local loss of tight junction proteins, local Rho activation, and changes in cell shape.

Results:

Gastrula-staged *X. laevis* embryos possess a fully polarized epithelium with apical tight junctions facing the external environment, allowing tight junction dynamics to be easily viewed with confocal microscopy while leaving the embryo completely intact. To perform ZnUMBA in *X. laevis*, we microinjected FZ3 into the blastocoel of gastrula-stage embryos and mounted the embryos in media containing $ZnCl_2$ immediately before imaging.

Microinjection causes a multicellular wound in the embryo; however, the wounds heal rapidly. Allowing the embryos to heal from microinjection for 5-10 minutes was typically sufficient to avoid FZ3 leaking out of the injection site during imaging (data not shown). Once injected, FZ3 remains in the blastocoel for hours, so batches of embryos can be injected in FZ3 and kept for several hours before they are imaged.

Former Miller Lab postdoc, Tomohito Higashi, optimized the concentrations of FZ3 and $ZnCl_2$ used in the assay, as well as the image acquisition parameters. During the optimization phase, we found that higher concentrations of $ZnCl_2$ (~10 mM) led to steadily increasing FZ3 fluorescence, which made the barrier assay effective for only 20-30 minutes. However, embryo viability was not affected by the FZ3 or $ZnCl_2$ (data not shown). Decreasing the $ZnCl_2$ concentration to 2 mM, increasing image acquisition exposure time, and adding Ca^{2+}/EDTA to the FZ3 to sequester endogenous Zn^{2+} in the blastocoel improved background fluorescence and reduced noise. (Note: EDTA has a

higher affinity for Zn^{2+} than Ca^{2+}. However, because the Ca^{2+} chelation activity of EDTA has the potential to disrupt adherens junctions, equimolar Ca^{2+} was added along with EDTA to mitigate this effect.) Nevertheless, the assay is still subject to gradually increasing fluorescence over time, so a method of normalizing signal to background is required for appropriate data interpretation (see Appendix 1 for Materials and Methods).

Figure 2.3

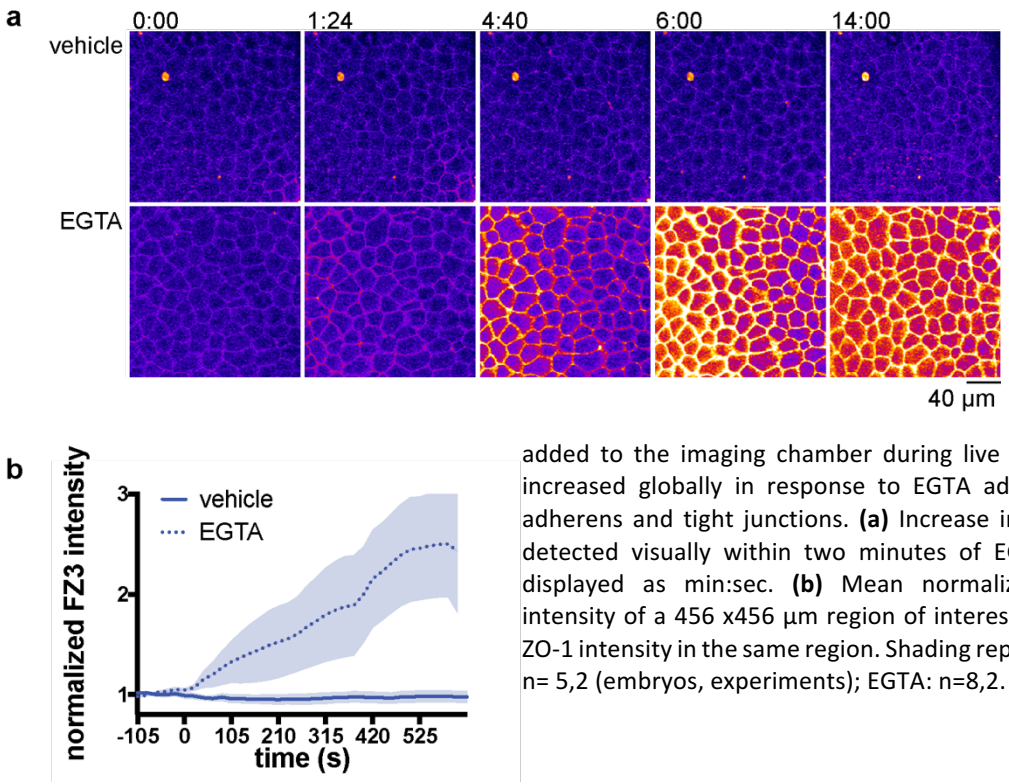

Figure 2.3: ZnUMBA detects global disruption of epithelial barrier function caused by EGTA. Embryos were injected with FluoZin3. At time 0, a solution containing 2 mM $ZnCl_2$ (vehicle) or 2 mM $ZnCl_2$ + 10 mM EGTA (EGTA) was added to the imaging chamber during live imaging. FZ3 intensity increased globally in response to EGTA addition, which disrupts adherens and tight junctions. **(a)** Increase in FZ3 intensity can be detected visually within two minutes of EGTA addition. Time is displayed as min:sec. **(b)** Mean normalized FZ3 fluorescence intensity of a 456 x456 µm region of interest normalized to mRFP-ZO-1 intensity in the same region. Shading represents S.E.M. Vehicle: n= 5,2 (embryos, experiments); EGTA: n=8,2.

Once ZnUMBA was optimized, we performed several experiments to perturb barrier function on local and global scales in order to validate the assay. Adhesion of E-cadherin molecules on neighboring cells is Ca^{2+}-dependent. Thus, Ca^{2+} depletion can be used to disrupt adherens junctions and tight junctions, which are dependent on the strong cell-cell adhesion provided by adherens junctions for their normal structure and function. EGTA, which preferentially chelates Ca^{2+}, can be used experimentally to

perturb epithelial integrity (Higashi et al., 2016; Rothen-Rutishauser et al., 2002). Indeed, FZ3 intensity began increasing globally within two minutes of adding EGTA to the *X. laevis* embryos during live imaging, indicating the high temporal sensitivity of the assay (Figure 2.3).

Exogenous ATP addition causes a tissue-wide wave-like contractile response in *X. laevis* embryos (Kim et al., 2014). We predicted that this global change in contractility would affect barrier function in *X. laevis* embryos. Indeed, following ATP addition, cell-cell junctions transitioned from taut to wavy, and FZ3 intensity increased globally, indicating that ATP addition affects barrier function across the tissue (Figure 2.4).

Figure 2.4

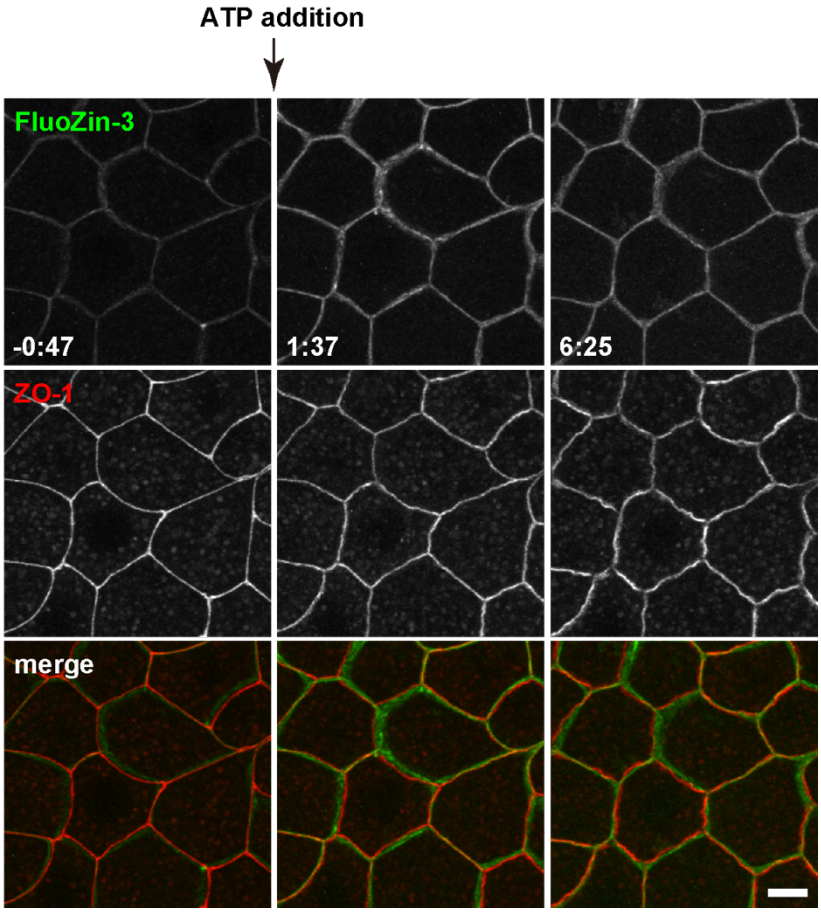

Figure 2.4: Global increase in contractility mediated by exogenous ATP affects tissue-wide barrier function. 250 µM ATP was added at time 0 (not shown). Upon ATP addition, ZO-1 signal transitions from linear to wavy, indicating a contractile response. FZ3 intensity increases across the tissue, indicating a global lapse in barrier function. Scale bar = 10 µm. Figure courtesy of Tomohito Higashi.

To locally perturb barrier function, a 405 nm laser was used to locally wound the junction. Sites of junction injury showed a rapid, highly localized increase in FZ3 that was followed by an increase in F-actin and contraction of the junction (Figure 2.5). FZ3 intensity declined during the increase in F-actin and contraction of the junction (Figure 2.5), which we interpreted as an injury response associated with barrier restoration.

Figure 2.5

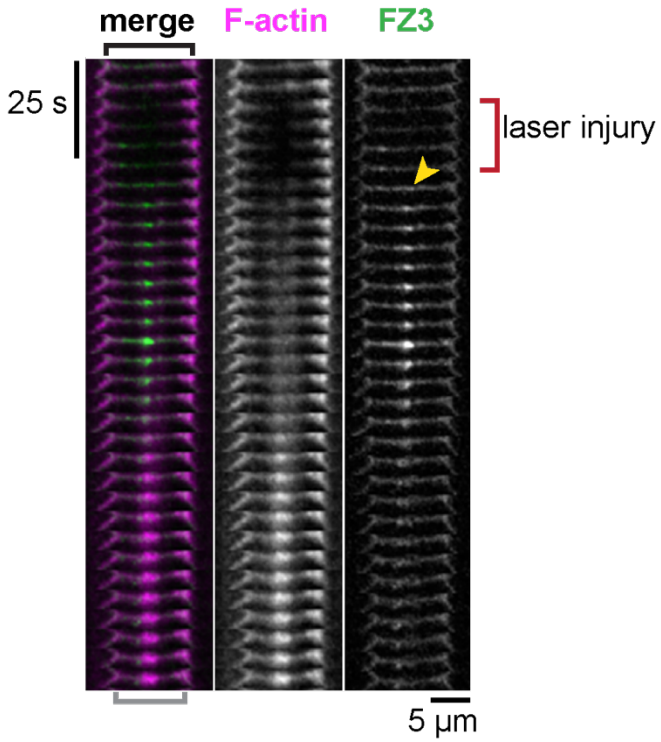

Figure 2.5: Laser injury results in rapid, local increase in FZ3 fluorescence. A 405 nm laser was used to locally induce an injury of the junction (red bracket). FluoZin3 (FZ3, green) increases in intensity (yellow arrowhead) following injury and persists for roughly 75 seconds. Note that F-actin (Lifeact-RFP, magenta) accumulates at the site of injury, and the junction contracts (black bracket vs. grey bracket).

Finally, we applied ZnUMBA to the unperturbed epithelium of *X. laevis* embryos to observe whether barrier function is dynamic under control conditions. We observed short-lived leaks that were usually localized along a single junction or confined to a small region of the junction (Figure 2.6a). Because of the contractile response that accompanied restoration of barrier function following laser injury, we hypothesized that the small GTPase RhoA, a master regulator of contractility, may accumulate at the site

of leaks. Using a probe for active, GTP-bound Rho (GFP-rGBD), I found that FZ3 increase is followed by an increase in active Rho (Figure 2.6 b,c). At the onset of Rho activation, FZ3 signal begins to decline. ZO-1 signal increases as Rho is activated, indicating that Rho activation and ZO-1 may cooperate to restore barrier function at the sites of leaks (Figure 2.6c).

Figure 2.6

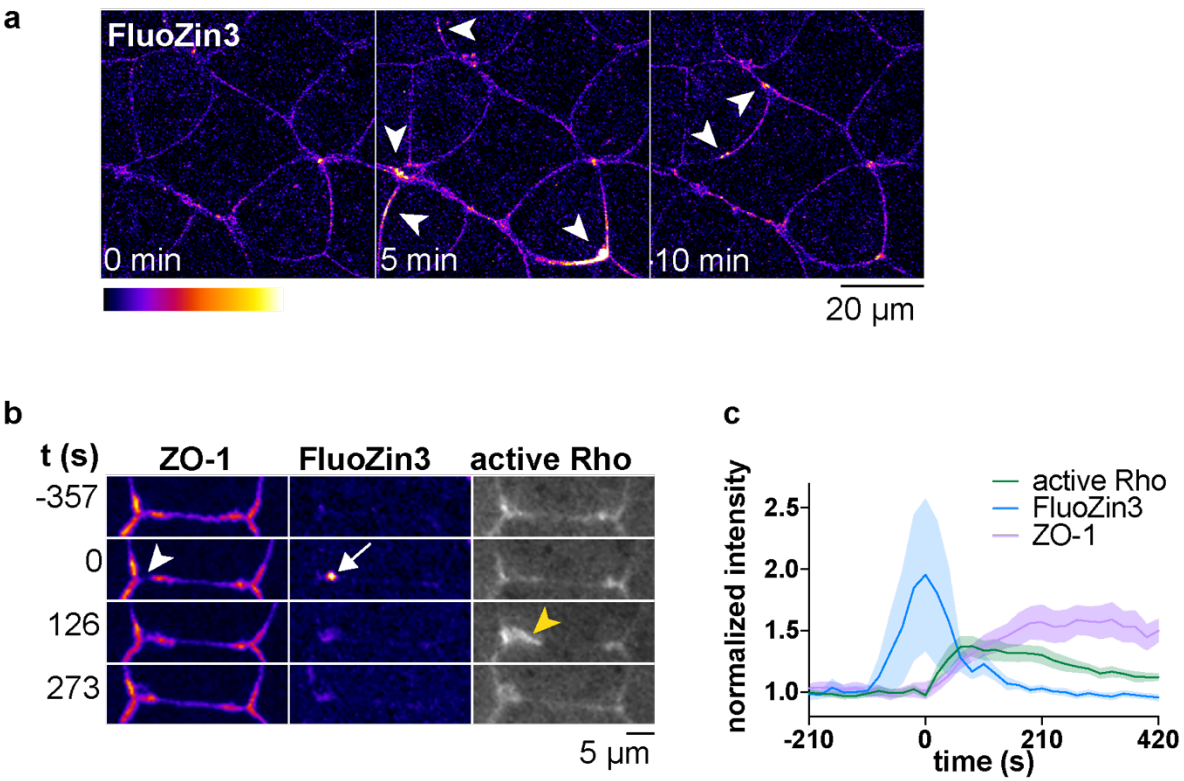

Figure 2.6: ZnUMBA detects sporadically occurring leaks in the *X. laevis* embryo. (a) FIRE Lookup Table (LUT) applied to FZ3 in the unperturbed *X. laevis* epithelium. Arrowheads indicate short-lived, localized leaks. **(b)** Leaks (FZ3, white arrow) occur at sites of local ZO-1 loss (white arrowhead), and Rho flares (yellow arrowhead) follow at these sites. FZ3 intensity decreases while ZO-1 intensity increases following Rho flares. **(c)** Mean normalized intensity for active Rho (mCherry-2xrGBD), FZ3, and ZO-1 (BFP-ZO-1) at the site of the Rho flare over time quantified from **(b)** and additional movies. Shading represents standard error of the mean (S.E.M.). n=17,7,5 (flares, embryos, experiments).

Discussion

The data presented in this chapter are proof-of-principle studies that validate ZnUMBA, a technique we developed to measure local or global changes in barrier function on short time scales with live imaging. Currently, our assay uses a commercially available dye, FZ3, and Zn^{2+} applied to the basal and apical sides of the barrier, respectively. These widely available reagents make this assay accessible to a wide array of researchers for use in diverse model systems, such as 2D cell culture, organoids, and other intact model organisms. One drawback of this approach is that some epithelial tissues are permeable to cations; that is, the tight junctions act as a sieve to allow high volumes of cations to cross the barrier, while restricting anions and other molecules. In epithelial tissues that express claudins that form cation pores, it will be difficult to distinguish between the leak pathway (i.e., breaking of claudin strands) and the opening and closing of claudin pores. There are two strains of Madin-Darby Canine Kidney (MDCK) cells that have similar tight junction morphology but differ in the profile of claudins they express (Furuse et al., 2001). MDCK I cells do not express claudin-2, while MDCK II cells do (Furuse et al., 2001; Tokuda et al., 2016). Because claudin-2 is a cation pore, comparing ZnUMBA in these cell lines would give us insight into how expression of cation pores affects the usefulness of ZnUMBA. Alternatively, finding or developing other molecule pairs analogous to FZ3/Zn^{2+} where both molecules are too large to travel through claudin pores would avoid this issue.

Fortunately, the gastrula-stage *X. laevis* embryo is relatively impermeable to cations. At stage 10, the beginning of gastrulation, the most highly expressed claudins by RNA-seq data are claudin-6.1, claudin-6.2, claudin-7, and claudin-4, each with >900

transcripts per million at stage 10 (Xenbase; (Session et al., 2016). Claudin-6 and claudin-4 are barrier forming claudins with decreased permeability to cations, whereas claudin-7 is a pore-forming claudin with increased permeability to anions (Günzel and Yu, 2013). The claudins known to act as cation pores are claudin-2, -10b, -15, and -16 (Günzel and Yu, 2013). These claudins are weakly expressed at stage 10, with all four combined totaling fewer than 10 transcripts per million (Xenbase: (Session et al., 2016). Thus, based on the available RNA-seq data, there are several orders of magnitude fewer cation pore-forming claudins than other claudins. Because of this, the most likely explanation for the increase in fluorescence we observed in the ZnUMBA experiments reported is a non-specific, short-lived opening of the tight junction barrier.

There are a number of known perturbations that increase flux of macromolecules across the tight junction, including knockdown of ZO-1 (and ZO-2), Toca-1 (a regulator of junctional actin and membrane dynamics) knock down, and myosin light chain kinase activation through TNF-α (Fanning et al., 2012; Turner et al., 2014; Van Itallie et al., 2015; 2009). However, it is not known if all of these perturbations influence the leak pathway in the same way. That is, do these perturbations increase the frequency of leaks or their duration? Increased leak frequency could indicate active disruption the tight junction barrier, while increased leak duration could indicate a defect in barrier restoration. Thus, the ability to visualize and quantify the number and duration of leaks will be a powerful tool for increasing our understanding of factors that influence the leak pathway.

The bioavailability of some drugs is limited by their ability to cross epithelial tissues such as the skin, nasal mucosa, and gastrointestinal tract (Rosenthal et al.,

2012). Chemical agents and bacterial toxins that increase paracellular permeability are sometimes co-administered with drugs in order to enhance absorption (Krug et al., 2013; 2017). ZnUMBA could be very useful in monitoring how effective these permeability enhancers are. In future work, I will use ZnUBMA to test the effect of angubindin, a modified *Clostridium perfringens* toxin that uses angulin-1, a tricellular tight junction protein, as a receptor to enter the cell. Angubindin is reported to selectively enhance permeability at tricellular junctions (Krug et al., 2017; Zeniya et al., 2018).

Here, I have introduced ZnUMBA, a novel live imaging barrier assay. Using ZnUMBA, I demonstrated that sporadic leaks occur in the unperturbed epithelium of the *X. laevis* gastrula-stage embryo. In the future, it will be important to collect statistics about the average frequency, duration, and location of leaks in this tissue in order to compare our results with those from other tissues, model systems, and upon various experimental perturbations. Developing high throughput quantitative tools to gather these statistics is a priority. This, in combination with experimental and computational approaches to measure and predict changing forces in the epithelial tissue, will allow us to understand the roles that mechanical forces and molecular perturbations have on leak pathway regulation and tight junction barrier stability.

References:

Campbell, H.K., Maiers, J.L., and DeMali, K.A. (2017). Interplay between tight junctions & adherens junctions. Exp. Cell Res. *358*, 39–44.

Charras, G., and Yap, A.S. (2018). Tensile Forces and Mechanotransduction at Cell-Cell Junctions. Current Biology *28*, R445–R457.

Dubrovskyi, O., Birukova, A.A., and Birukov, K.G. (2013). Measurement of local permeability at subcellular level in cell models of agonist- and ventilator-induced lung injury. Lab. Invest. *93*, 254–263.

Fanning, A.S., Van Itallie, C.M., and Anderson, J.M. (2012). Zonula occludens-1 and -2 regulate apical cell structure and the zonula adherens cytoskeleton in polarized epithelia. Molecular Biology of the Cell *23*, 577–590.

Furuse, M., Furuse, K., Sasaki, H., and Tsukita, S. (2001). Conversion of zonulae occludentes from tight to leaky strand type by introducing claudin-2 into Madin-Darby canine kidney I cells. J. Cell Biol. *153*, 263–272.

Ghim, M., Alpresa, P., Yang, S.-W., Braakman, S.T., Gray, S.G., Sherwin, S.J., van Reeuwijk, M., and Weinberg, P.D. (2017). Visualization of three pathways for macromolecule transport across cultured endothelium and their modification by flow. American Journal of Physiology-Heart and Circulatory Physiology *313*, H959–H973.

Günzel, D., and Yu, A.S.L. (2013). Claudins and the modulation of tight junction permeability. Physiol. Rev. *93*, 525–569.

Hatte, G., Prigent, C., and Tassan, J.-P. (2018). Tight junctions negatively regulate mechanical forces applied to adherens junctions in vertebrate epithelial tissue. J. Cell. Sci. *131*, jcs208736.

Higashi, T., Arnold, T.R., Stephenson, R.E., Dinshaw, K.M., and Miller, A.L. (2016). Maintenance of the Epithelial Barrier and Remodeling of Cell-Cell Junctions during Cytokinesis. Curr. Biol. *26*, 1829–1842.

Kim, Y., Hazar, M., Vijayraghavan, D.S., Song, J., Jackson, T.R., Joshi, S.D., Messner, W.C., Davidson, L.A., and LeDuc, P.R. (2014). Mechanochemical actuators of embryonic epithelial contractility. Proc. Natl. Acad. Sci. U.S.a. *111*, 14366–14371.

Krug, S.M., Amasheh, M., Dittmann, I., Christoffel, I., Fromm, M., and Amasheh, S. (2013). Sodium caprate as an enhancer of macromolecule permeation across tricellular tight junctions of intestinal cells. Biomaterials *34*, 275–282.

Krug, S.M., Hayaishi, T., Iguchi, D., Watari, A., Takahashi, A., Fromm, M., Nagahama, M., Takeda, H., Okada, Y., Sawasaki, T., et al. (2017). Angubindin-1, a novel paracellular absorption enhancer acting at the tricellular tight junction. J Control Release *260*, 1–11.

Lim, L.G., Neumann, J., Hansen, T., Goetz, M., Hoffman, A., Neurath, M.F., Galle, P.R., Chan, Y.H., Kiesslich, R., and Watson, A.J. (2014). Confocal endomicroscopy identifies loss of local barrier function in the duodenum of patients with Crohn's disease and ulcerative colitis. Inflamm. Bowel Dis. *20*, 892–900.

Rasmussen, D.N., Karstensen, J.G., Riis, L.B., Brynskov, J., and Vilmann, P. (2015). Confocal Laser Endomicroscopy in Inflammatory Bowel Disease--A Systematic Review. J Crohns Colitis *9*, 1152–1159.

Reyes, C.C., Jin, M., Breznau, E.B., Espino, R., Delgado-Gonzalo, R., Goryachev, A.B., and Miller, A.L. (2014). Anillin regulates cell-cell junction integrity by organizing junctional accumulation of Rho-GTP and actomyosin. Curr. Biol. *24*, 1263–1270.

Richter, J.F., Schmauder, R., Krug, S.M., Gebert, A., and Schumann, M. (2016). A novel method for imaging sites of paracellular passage of macromolecules in epithelial sheets. J Control Release *229*, 70–79.

Rosenthal, R., Heydt, M.S., Amasheh, M., Stein, C., Fromm, M., and Amasheh, S. (2012). Analysis of absorption enhancers in epithelial cell models. Ann. N. Y. Acad. Sci. *1258*, 86–92.

Rothen-Rutishauser, B., Riesen, F.K., Braun, A., Günthert, M., and Wunderli-Allenspach, H. (2002). Dynamics of tight and adherens junctions under EGTA treatment. J. Membr. Biol. *188*, 151–162.

Scott, D.W., Tolbert, C.E., and Burridge, K. (2016). Tension on JAM-A activates RhoA via GEF-H1 and p115 RhoGEF. Molecular Biology of the Cell *27*, 1420–1430.

Session, A.M., Uno, Y., Kwon, T., Chapman, J.A., Toyoda, A., Takahashi, S., Fukui, A., Hikosaka, A., Suzuki, A., Kondo, M., et al. (2016). Genome evolution in the allotetraploid frog Xenopus laevis. Nature *538*, 336–343.

Shen, L., Weber, C.R., Raleigh, D.R., Yu, D., and Turner, J.R. (2011). Tight junction pore and leak pathways: a dynamic duo. Annu. Rev. Physiol. *73*, 283–309.

Shigetomi, K., Ono, Y., Inai, T., and Ikenouchi, J. (2018). Adherens junctions influence tight junction formation via changes in membrane lipid composition. J. Cell Biol. *113*, jcb.201711042.

Spadaro, D., Le, S., Laroche, T., Mean, I., Jond, L., Yan, J., and Citi, S. (2017). Tension-Dependent Stretching Activates ZO-1 to Control the Junctional Localization of Its Interactors. Curr. Biol. *27*, 3783–3795.e3788.

Tokuda, S., Hirai, T., and Furuse, M. (2016). Effects of Osmolality on Paracellular Transport in MDCK II Cells. PLoS ONE *11*, e0166904.

Turner, J.R., Buschmann, M.M., Romero-Calvo, I., Sailer, A., and Shen, L. (2014). The role of molecular remodeling in differential regulation of tight junction permeability. Semin. Cell Dev. Biol. *36*, 204–212.

Van Itallie, C.M., Fanning, A.S., Bridges, A., and Anderson, J.M. (2009). ZO-1 stabilizes the tight junction solute barrier through coupling to the perijunctional cytoskeleton. Molecular Biology of the Cell *20*, 3930–3940.

Van Itallie, C.M., Tietgens, A.J., Krystofiak, E., Kachar, B., and Anderson, J.M. (2015). A complex of ZO-1 and the BAR-domain protein TOCA-1 regulates actin assembly at the tight junction. Molecular Biology of the Cell *26*, 2769–2787.

Vasquez, C.G., and Martin, A.C. (2016). Force transmission in epithelial tissues. Dev. Dyn. *245*, 361–371.

Zeniya, S., Kuwahara, H., Daizo, K., Watari, A., Kondoh, M., Yoshida-Tanaka, K., Kaburagi, H., Asada, K., Nagata, T., Nagahama, M., et al. (2018). Angubindin-1 opens the blood-brain barrier in vivo for delivery of antisense oligonucleotide to the central nervous system. J Control Release *283*, 126–134.

Zihni, C., Mills, C., Matter, K., and Balda, M.S. (2016). Tight junctions: from simple barriers to multifunctional molecular gates. Nat. Rev. Mol. Cell Biol. *17*, 564–580.

Notes and acknowledgements:

I would like to thank Tomohito Higashi, whose creativity and vision led to the development of ZnUMBA. Tomohito identified FluoZin3 as a potential indicator of barrier function and performed initial optimization and validation of ZnUMBA. Tomohito contributed Figures 2.2 and 2.4 to this chapter.

Materials and Methods for this chapter can be found in Appendix 1.

Chapter 3

Rho flares locally repair the tight junction barrier

Abstract: The small GTPase RhoA is an important regulator of cell-cell junction formation, homeostasis, and disassembly. While it is well appreciated that active RhoA promotes actomysosin contractility in epithelial tissues at the cell and tissue scales, little is known about how RhoA regulates junction dynamics on a subcellular scale or how junctional Rho activity changes over short time scales. Here, I describe transient, localized accumulations of active Rho ("Rho flares") at junctions in the epithelium of gastrula-stage *Xenopus laevis* embryos. In order to investigate the cause and consequence of Rho flares, I co-imaged active Rho with fluorescently-tagged tight junction and adherens junction proteins. Intriguingly, the tight junction proteins ZO-1 and occludin are locally decreased prior to the Rho flare and, along with claudin-6, are reinforced following the flare. I found that Rho flares reinforce tight junction proteins through actin polymerization and ROCK-mediated localized contraction of the cell boundary, allowing for efficient restoration of barrier function. I propose that Rho flares constitute a damage control mechanism that reinstates barrier function when tight junctions become locally compromised due to changes in cell and tissue tension.

Introduction

The small GTPase RhoA is a master regulator of contractility, stimulating formin-mediated actin polymerization and ROCK-mediated myosin II motor activity (Arnold et al., 2017; Thumkeo et al., 2013). Precise regulation of active Rho at cell-cell junctions is critical for their proper structure and function, as either too little or too much Rho activity can have negative consequences for epithelial integrity (Quiros and Nusrat, 2014). Within epithelial tissues, active Rho is important in several discrete locations in addition to cell-cell junctions, including at basal stress fibers that anchor the cells to the basal lamina, in the nucleus, and at the contractile ring of dividing cells. Biochemical approaches to measuring active Rho in a tissue, such as GST-rGBD pulldowns (Figure 1.6a), average all of these populations. Additionally, Rho activity can be dynamic both in space and in time. Therefore, visualizing Rho activity in epithelial tissues is important for understanding its true nature.

The first studies to visualize active Rho in epithelial tissues used FRET biosensors and presented only snapshots in time (Ratheesh et al., 2012; Terry et al., 2011), leading to the perception that Rho is stably activated at apical cell-cell junctions. Indeed, even time-lapse imaging of active Rho in cultured epithelial cells led to the conclusion that junctional Rho activity is “strikingly stable” (Priya et al., 2015). Here I will present data that stands in contrast to these studies. Using live imaging in the epithelium of a developing vertebrate model organism, *Xenopus laevis*, I have observed *transient, localized* accumulations of active Rho at cell-cell junctions and have uncovered their biological relevance.

To our knowledge, the first description of transient junctional accumulations of active Rho come from laser wounding experiments in *X. laevis* blastomeres (Clark et al., 2009). Laser wounding of the membrane in *X. laevis* oocytes results in influx of extracellular calcium at the wound site followed by the formation of concentric rings of active Rho, active Cdc42, F-actin, and myosin II around the wound site that constrict to rapidly repair the plasma membrane (Benink and Bement, 2005; Davenport et al., 2016). Clark et al. (2009) discovered that when wounds were made near cell-cell junctions, there was influx of calcium and transient increase in active Rho and F-actin at the nearby junctions, in addition to at the wound site. Surprisingly, Rho activation was detectable at the junctions before it could be detected at the wound site, and Rho was activated not just in the wounded cells, but also in the neighboring cells (Clark et al., 2009). Unlike naturally occurring Rho flares at gastrula-stage, these accumulations merge with the concentric ring of active Rho at the wound site (Clark et al., 2009).

In 2014, Reyes et al. coined the term “Rho flare” to describe the transient junctional accumulations of active Rho that increase in frequency when anillin is knocked down (Reyes et al., 2014). Anillin is a scaffolding protein capable of binding active Rho, F-actin, myosin-II, and many other Rho-associated proteins and cytoskeletal elements, and is important for maintaining the architecture of tight junctions and adherens junctions (Arnold et al., 2017; Reyes et al., 2014). Reyes et al. (2014) hypothesized that “the pronounced Rho-GTP flares in anillin knockdown embryos may represent sites of junction disassembly or repair”. In anillin knockdown cells, flares had increased breadth and decreased duration compared to controls, suggesting a role for anillin in contributing to flare duration and morphology (Reyes et al. 2014).

In 2015, Breznau et al. reported that perturbing MgcRacGAP's function through knockdown or knockdown and replacement with GAP-dead mutants resulted in increased frequency of "dynamic junctional accumulations of RhoA-GTP and F-actin" (Breznau et al., 2015). These mutants also exhibit severe defects in adherens junctions, but not tight junctions, as well as apical doming (Breznau et al., 2015). Qualitatively, Rho flares appear larger than average in these mutants (personal observation), which may indicate an involvement of MgcRacGAP in contributing to Rho inactivation at Rho flares. Furthermore, active Rac was not detected at these flares (Breznau et al., 2015).

Finally, in unpublished work, I found that perturbations of GEF-H1 through knockdown or overexpression of a dominant negative (GEF dead) mutant increased Rho flare frequency relative to control (not shown). GEF-H1 is a Rho GEF that localizes to tight junctions, where its GEF activity is reportedly inhibited (Aijaz et al., 2005; Benais-Pont et al., 2003; Terry et al., 2011). Thus, it is surprising that GEF-H1 perturbations increase Rho flares, both because it is largely believed to be inactive at junctions and because it is counterintuitive for GEF loss-of-function to increase Rho activation.

With so many different perturbations causing an increased number of flares, it became imperative to understand *why* flares are happening and *how* they affect cell-cell junctions. Based on the observations above, as well as the data presented in Chapter 2 that Rho flares follow local junction breaches, I examined the effect of Rho flares on tight junctions, adherens junctions, and the actin cytoskeleton. Then, I tested the mechanism of how Rho flares contribute to the restoration of barrier function I observed in Chapter 2.

Results

Rho flares reinforce tight junction proteins following local discontinuities

Because epithelial barrier function is compromised prior to Rho flares (Figure 2.6b,c), I first investigated the dynamics of tight junction proteins before, during, and after Rho flares. I found that both ZO-1 and occludin, but not claudin-6, locally decrease prior to Rho flares (Figure 3.1a-d). During Rho flares, occludin, ZO-1, and claudin-6 fluorescence levels rise rapidly, and remain elevated, or "reinforced", over baseline levels (Figure 3.1a-d). That claudin-6 signal remains unchanged at the site of Rho flares suggests that the epithelial barrier function to ions may not be compromised. Indeed, changes in the intermolecular associations between claudins, ZO-1, occludin, and the actin cytoskeleton are linked to leak pathway regulation and increased strand dynamics (Van Itallie et al., 2017; Yu et al., 2010), so localized decline in ZO-1 and occludin may indicate a molecular basis for the increase in permeability to FZ3.

In contrast to ZO-1 and occludin, the adherens junction proteins E-cadherin and α-catenin are not visibly decreased prior to Rho flares (Figure 3.1e,f). Additionally, there is no sign of separation between the neighboring cell membranes (Figure 3.2a,b), indicating that a defect in cell-cell adhesion is not a primary cause of increased permeability prior to Rho flares. However, both E-cadherin and α-catenin increase in intensity at the site of the flare (Figure 3.2e,f), indicating that the adherens junction is affected by, or perhaps participates in, the Rho flare-associated concentration of tight

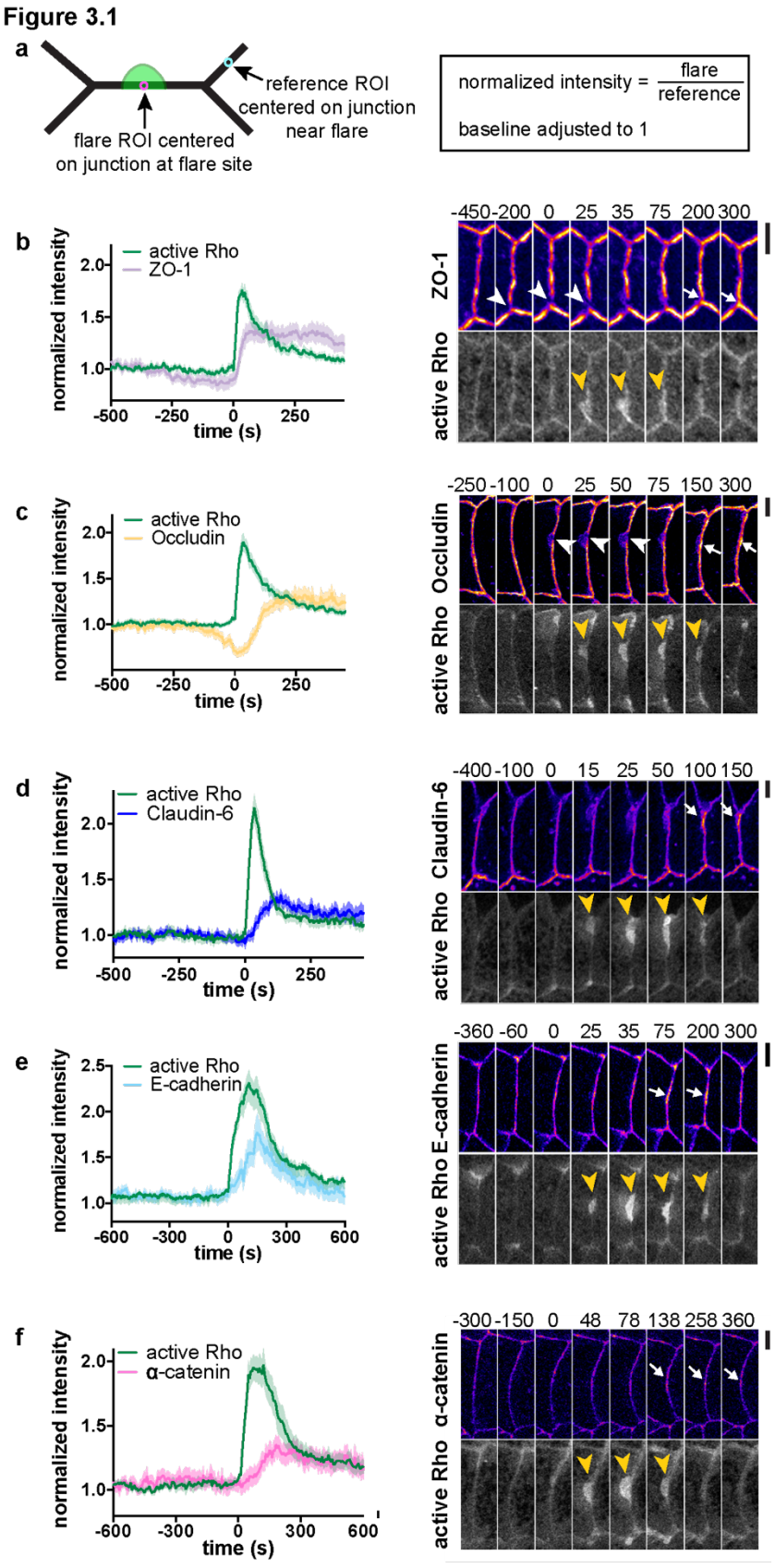

Figure 3.1: Rho flares reinforce tight junction proteins following local discontinuities.
(a) Schematic depicting the regions of interest (ROI) used for calculating normalized intensity at the junction. **(b-f) Left:** Mean of normalized intensity of a region of interest centered on the junction at the site of the flare over time (calculated as depicted in **(a)**). Shading represents S.E.M. **Right:** Co-imaging of Rho flares with junction proteins. Active Rho is shown in grey scale, all others shown with FIRE LUT. Yellow arrowheads indicate Rho flares, white arrowheads indicate local protein decrease, and white arrows indicate local protein increase. Scale bars = 5 µm. **(b)** Local decrease in ZO-1 precedes the onset of Rho flares. Following Rho flares, ZO-1 intensity is elevated over baseline. n=26,9,4 (flares, embryos, experiments); mRFP-ZO-1, GFP-rGBD. **(c)** Occludin declines sharply prior to the onset of Rho flares. Following Rho flares, occludin is locally reinforced. n=28,7,3; mCherry-occludin, GFP-rGBD. **(d)** Claudin-6 rises during Rho flares and remains reinforced following flares. n=24,8,3 mCherry-claudin-6, GFP-rGBD. **(e)** E-cadherin rises during the Rho flares, but returns to baseline levels following flares. n=22,7,3; E-cadherin-3xmCherry, GFP-rGBD. **(f)** α-catenin rises during Rho flares and remains reinforced following flares. n=24,6,3. mCherry-α-catenin, GFP-rGBD.

Figure 3.2

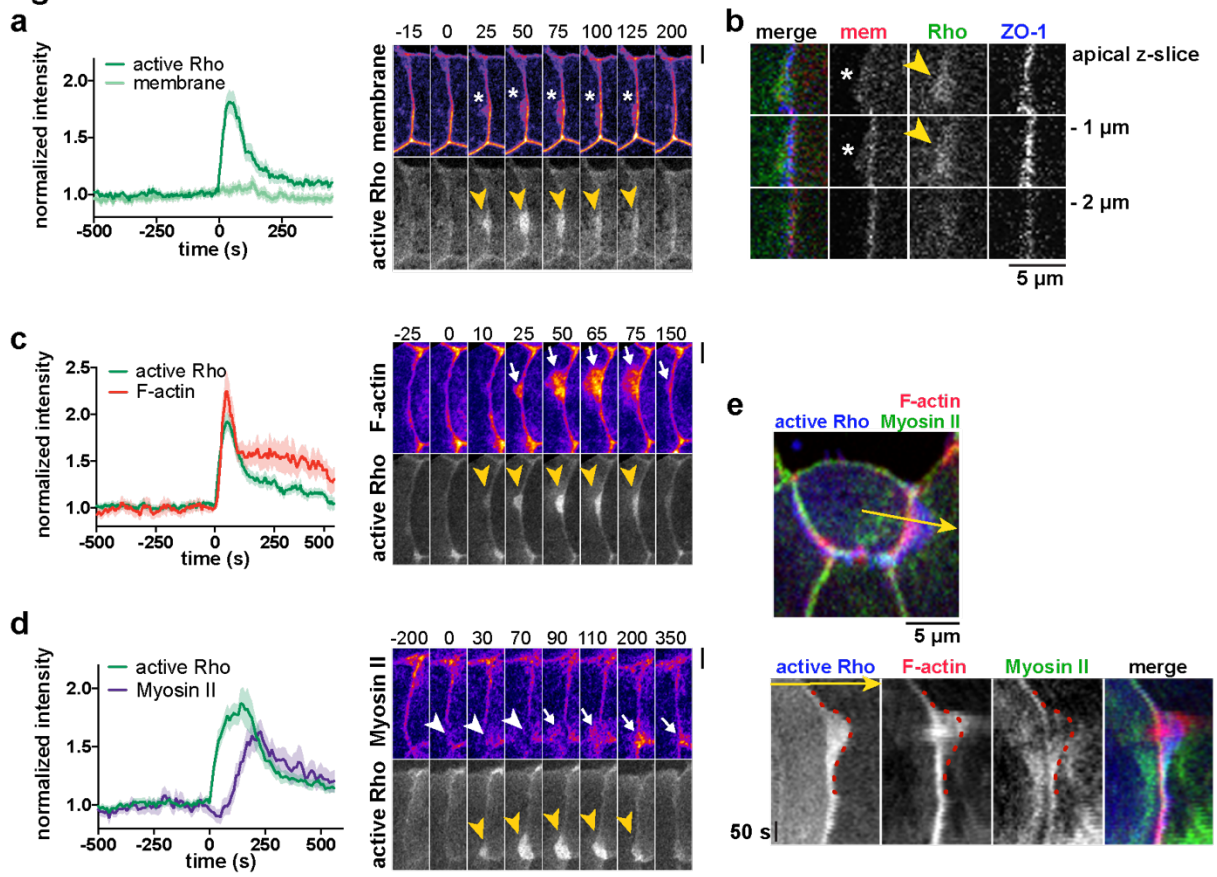

Figure 3.2: Rho flares are associated with apical plasma membrane deformations and accumulation of F-actin and myosin II. (a,c,d) Left: Mean of normalized intensity at the site of the flare over time, as calculated in Fig 3.1a. Shading represents S.E.M. **Right:** Co-imaging of Rho flares with membrane, F-actin, or Myosin II. Active Rho is shown in grey scale, all others shown with FIRE LUT. Yellow arrowheads indicate Rho flares, white arrowheads indicate local protein decrease, and white arrows indicate local protein increase. Scale bars = 5 µm **(a)** The junctional intensity of the membrane signal stays constant throughout the flare; however, plasma membrane deformations (white asterisks) are associated with Rho flares. n=25,9,5; mCherry-farnesyl, GFP-rGBD. **(b)** mCherry-farnesyl (membrane probe) was expressed mosaically, while BFP-ZO-1 and GFP-rGBD (active Rho probe) were expressed globally. Serial z-slices through the flare (yellow arrowheads) show that the plasma membrane protrudes apically (asterisks), but not basally (bottom). Note that accumulation of active Rho is also apical. **(c)** F-actin expands in the direction of Rho flares as flares expand, and retracts as flares retract. n=19,7,4; Lifeact-RFP, GFP-rGBD. **(d)** Junctional Myosin II locally decreases at the start of the flare and accumulates on the cortex as Rho flares expand and coalesces towards the junction as flares retract. n=23,7,3; SF9-mNeon, mCherry-2xrGBD. BFP-ZO-1 (not shown) was used to track the position of the junction. **(e)** Top: Triple labeling of F-actin (Lifeact-RFP), myosin II (SF9-mNeon), and active Rho (BFP-2xrGBD). Bottom: Kymograph generated from the 2-pixel wide line shown above (yellow arrow indicates orientation). Note that F-actin accumulation closely follows the timing and orientation of active Rho, whereas Myosin II accumulates at the periphery of the flare and moves towards the junction as the flare retracts. The red dotted lines trace the dense accumulation of active Rho, which corresponds to the boundary of the membrane protrusion. Note that both F-actin and myosin II can be seen beyond this boundary, indicating that they accumulate in the cell neighboring the membrane protrusion.

junction proteins. In contrast to the tight junction and adherens junction proteins I observed, the intensity of a membrane probe measured at the junction remains stable over the course of the flare (Fig 3.2a), indicating that the increases in junction protein intensity are not a flare-induced artifact.

I observed that Rho flares are typically asymmetric with respect to the junction; that is, the plasma membrane of one cell protrudes apically over its neighbor (Figure 3.2a,b). Dense, bright active Rho signal is associated with the membrane protrusion, although there is often a lighter haze of active Rho surrounding the dense signal (see Figure 3.1c-e). The protrusion grows as Rho activity increases and retracts as Rho activity declines (Figure 3.2a). F-actin emanates from the junction in the direction of the membrane protrusion, while myosin II accumulates on the periphery of the flare and flows towards the junction as the flare retracts (Figure 3.2c-e). The mechanical origin of the membrane protrusion will be explored further in Chapter 4; however, the accumulation of F-actin and myosin II on either side of the membrane protrusion (Figure 3.3e) indicate that tight junction reinforcement is a cooperative process involving adjacent cells. Notably, many of the hallmarks of Rho flares described above, including membrane protrusion, F-actin and active Rho accumulation, and ZO-1 and occludin reinforcement, can be induced by laser injury of the junction (Figure 3.3). Therefore, it seems that a Rho-mediated contractile response, similar to those observed in single- and multi-cell wound healing, could drive reinforcement of tight junction proteins (Benink and Bement, 2005; Clark et al., 2009).

Figure 3.3

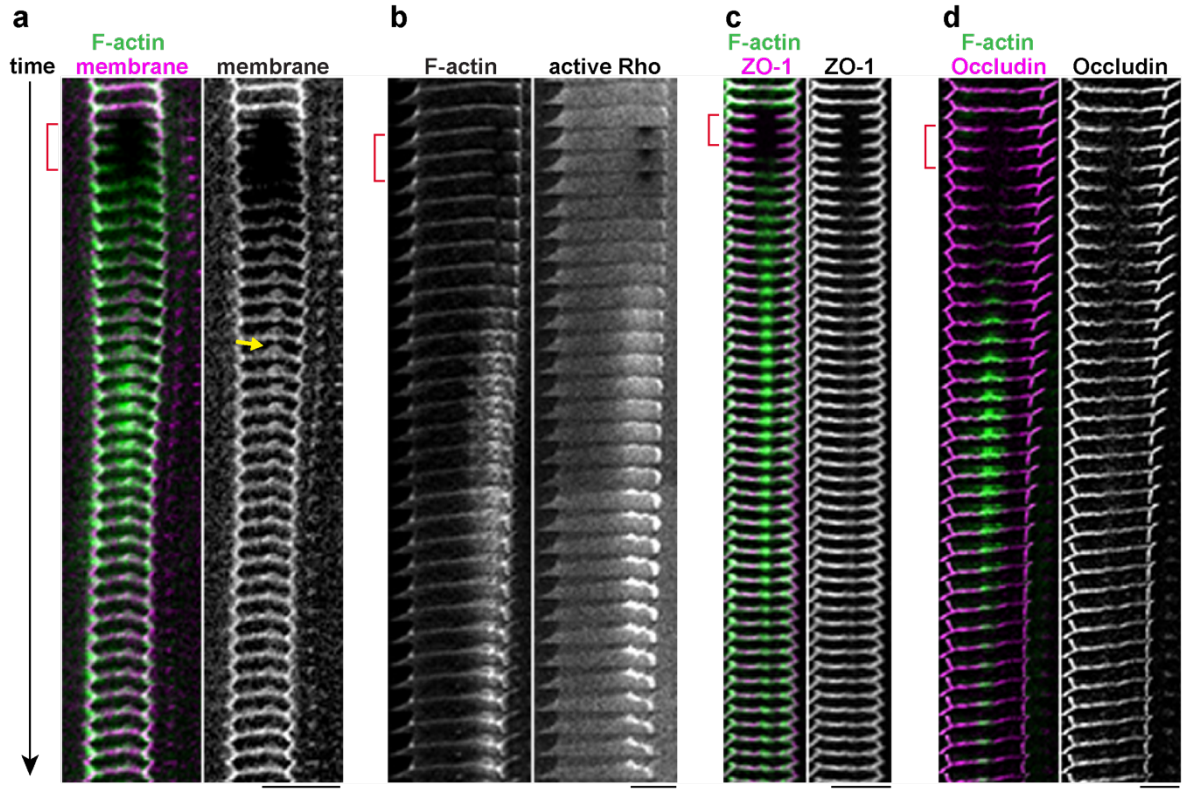

Figure 3.3: Laser injury recapitulates key aspects of Rho flare events.
A 405 nm laser was activated in a small circular region on the junction to induce an injury (as in Fig 2.5). Frames marked with red brackets indicate laser injury. Note that photobleaching accompanies injury. **(a)** Junction injury results in protrusion of the plasma membrane (yellow arrow). F-actin: Lifeact-GFP, membrane: mCherry-farnesyl. **(b)** Laser injury of the junction results in accumulation of active Rho (GFP-rGBD), which precedes F-actin (Lifeact-RFP) accumulation. **(c,d)** Laser injury results in reinforcement of mRFP-ZO-1 **(c)** and mCherry-occludin **(d)**. F-actin: Lifeact-GFP. Scale bars = 10 µm, and frames are 5 seconds apart.

Actin polymerization contributes to tight junction reinforcement

I hypothesized that actin polymerization and/or junction contraction downstream of Rho flares contribute to tight junction reinforcement. To distinguish between these possibilities, I first examined at ZO-1, an actin binding protein (Fanning et al., 2002; Itoh et al., 1997) whose recruitment and stabilization at tight junctions is dependent on actin polymerization (Yu et al., 2010). Co-imaging of active Rho, F-actin, and ZO-1 revealed

Figure 3.4

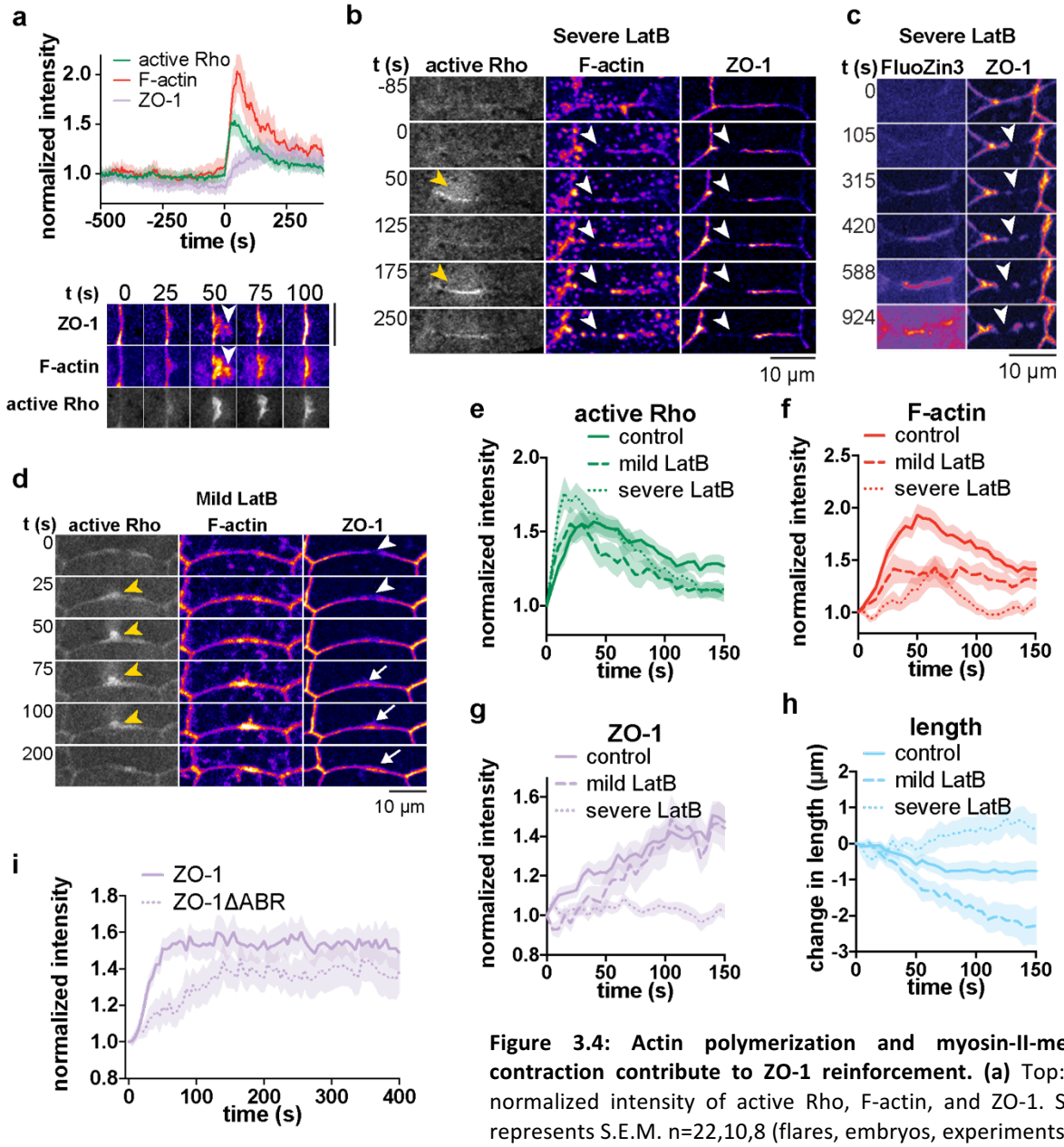

Figure 3.4: Actin polymerization and myosin-II-mediated contraction contribute to ZO-1 reinforcement. (a) Top: Mean normalized intensity of active Rho, F-actin, and ZO-1. Shading represents S.E.M. n=22,10,8 (flares, embryos, experiments). Time 0 represents the start of the flare. Bottom: ZO-1 reinforcement closely follows active Rho and F-actin accumulation in space and time. BFP-ZO-1 colocalizes with the actin structures (Lifeact-RFP) emanating from the junction at the site of Rho flares (GFP-rGBD) (white arrowheads). **(b)** Incubation with 8-10 µM LatB results in large breaks in junctional F-actin and ZO-1 (white arrowheads). Rho flares (yellow arrowheads) appear at these sites, but no actin polymerization, ZO-1 recruitment, or junction contraction follows, resulting in repeating Rho flares. **(c)** The tight junction barrier is not restored in severe LatB conditions. FluoZin3 signal continues to intensify as the discontinuity in ZO-1 (white arrowheads) expands. **(d)** Mild (1-5 µM) LatB treatment does not cause disintegration of junctional F-actin, and a subset of junctions become hypercontractile. Rho flares (yellow arrowheads) at these hypercontractile junctions result in ZO-1 reinforcement (white arrows) despite impaired actin polymerization. **(e-h)**. Quantification of active Rho (GFP-rGBD) **(e)**, F-actin (Lifeact-RFP) **(f),** ZO-1 (BFP-ZO-1) **(g)**, and junction length **(h)** in the experiments described above. Controls (untreated embryos) n=22,10,8; Severe LatB n=13,4,2; Mild LatB n=12,5,3. Time 0 represents the start of the Rho flare; data are normalized to 1 **(e-g)** or 0 **(h)** at time 0. **(i)** A mutant of ZO-1 that lacks the C-terminal actin-binding region (mRFP-ZO-1 ΔABR) is reinforced more slowly than full length ZO-1 (mRFP-ZO-1).

that ZO-1 accumulation closely follows F-actin accumulation in space and time (Fig 3.4a), indicating that actin polymerization could feasibly recruit ZO-1 to tight junctions during Rho flares.

To test how actin polymerization affects ZO-1 reinforcement, I treated embryos with Latrunculin B (LatB), which prevents actin polymerization by sequestering G-actin monomers. At 8 μM LatB and higher, I observed a severe effect, associated with large breaks in F-actin and ZO-1, as reported previously (Shen and Turner, 2005) (Fig 3.4b). Notably, these breaks colocalized with sites where repeated Rho flares occurred, mimicking endogenous Rho flares that appear at sites of decreased ZO-1. Under these circumstances, ZO-1 was not reinforced, and the barrier could not be restored (Fig 3.4b,c,e-h). Despite the lack of new actin polymerization at Rho flares, existing cortical actin becomes fragmented and forms puncta that are pulled towards the junction, where they merge with one another; in rare cases, these junctional accumulations of actin were sufficient to recruit ZO-1. However, junctions elongated during severe LatB treatment (Fig 3.4h), likely due to severe disruption of the junctional actin network, so we were not able to distinguish between the contribution of contraction and F-actin polymerization to ZO-1 reinforcement under these conditions.

To avoid completely disrupting junctional F-actin, I reduced the dose of LatB (≤5 μM). With this mild LatB treatment, I witnessed a loss of tissue integrity, resulting in some cell borders rapidly shrinking as other cells rapidly expand to compensate. Rho flares occurred on shrinking junctions, and in this scenario F-actin accumulation is strongly reduced compared to controls (Fig 3.4d,f), and ZO-1 reinforcement is slightly delayed (Fig. 3.4g), but not abolished. This indicates that increased contraction can

compensate for reduced actin accumulation to reinforce ZO-1 (Fig 3.4e-h). Furthermore, deletion of the actin binding region of ZO-1 (Fanning et al., 2002) delayed, but did not abolish, ZO-1 reinforcement (Fig 3.4i). While the actin binding region of ZO-1 has been reported to be important for its stabilization at junctions (Yu et al., 2010), the reinforcement of other tight junction proteins, such as claudins or occludin, could account for the reinforcement of ZO-1, given that ZO-1 binds to these proteins through its N-terminal domains (Fanning and Anderson, 2009). Taken together, we conclude that actin polymerization contributes to, but is not required for, ZO-1 reinforcement.

ROCK-mediated junction contraction contributes to tight junction reinforcement

We hypothesized that Myosin II-mediated contraction reinforces tight junctions by concentrating proteins within the junction. To test this hypothesis, we generated kymographs of the junction from vertex-to-vertex before, during, and after Rho flares. Kymographs highlighted a variety of Rho flare events, from simple to complex, including isolated Rho flares, repeating flares at a single location, and multiple flares along the same junction (Fig 3.6a). To simplify the interpretation of length analysis, we initially only considered only isolated flares. Quantification of these kymographs revealed that the total length of the junction is reduced during Rho flares, and the timing corresponds with the local increase in ZO-1 and occludin (Fig 3.5a,b, Fig 3.6b,c). Natural variation in junction protein intensity along the junction generates vertical lines in the kymographs that can serve as fiducial position markers. By tracing these lines, we observed that only regions of the junction associated with Rho flares contract, while other regions remain a stable length or elongate (Fig 3.5a, Fig 3.6b). This builds on previous work

Figure 3.5

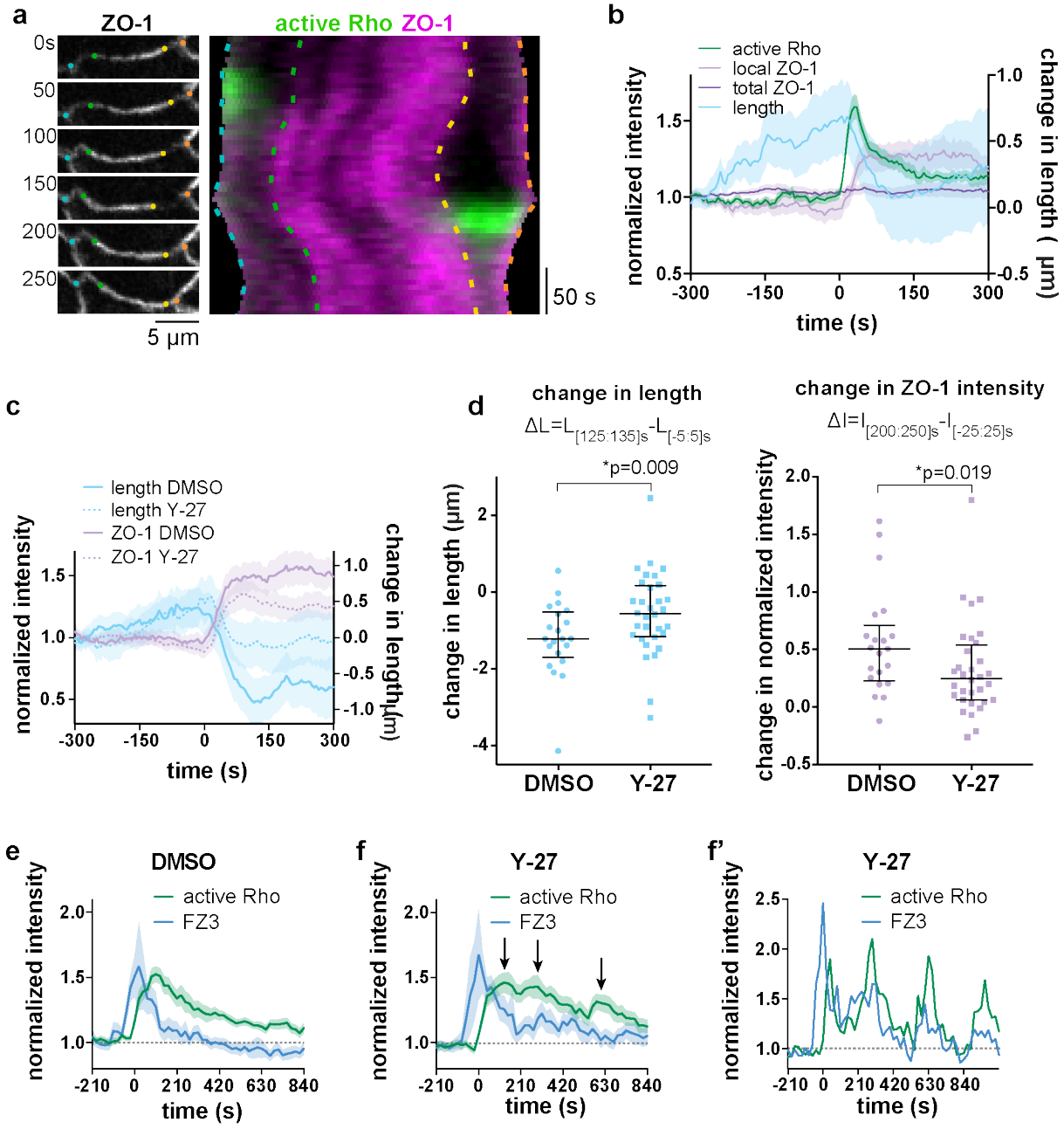

Figure 3.5: Junction contraction concentrates ZO-1 within the junction and is required for efficient reinforcement of the barrier. (a) Left: Montage of the junction shown as a kymograph on the right. Colored dots on the montage correspond to the relative position of dashed lines on the kymograph, which trace fiducial marks. Kymograph of active Rho (GFP-rGBD, green) and mRFP-ZO-1 (magenta) shows ZO-1 signal increasing as the junction contracts locally. **(b)** Quantification of junction length and protein intensity from multiple kymographs. Time 0 corresponds to the start of the Rho flare. Decrease in junction length after the Rho flare aligns with increased local ZO-1 intensity, while total ZO-1 intensity does not increase. n= 19,6,3 (flares, embryos, experiments) **(c)** Junction length vs. mRFP-ZO-1 reinforcement in embryos injected with vehicle (DMSO) or ROCK inhibitor (Y-27632). ROCK inhibitor partially inhibits junction contraction, and ZO-1 reinforcement is reduced. Vehicle: n=21,9,3; ROCK inhibitor: n=32,7,4. **(d)** Change in length and intensity were calculated from **(c)**. Significance calculated using Mann-Whitney *U* test. Bars

indicate median and interquartile range. **(e-f)** Restoration of the barrier is less efficient in embryos treated with ROCK inhibitor (Y-27632) **(f)** vs. vehicle (DMSO) **(e)**. In ROCK inhibitor-treated embryos, Rho flares (mCherry-2xrGBD) frequently repeat at the same site (arrows in f indicate multiple peaks of active Rho), and FZ3 takes longer to return to baseline (dotted horizontal line). n=19,6,3 **(e)** and 18,4,3 **(f)**. **(f')** shows an individual example of a junction with repeated flares.

demonstrating that junctions on a given cell can expand and contract independently of one another (Choi et al., 2016) by revealing that segments *within a junction* can independently expand and contract, indicating that force is not equally distributed along a junction. Notably, the analysis of junction length also revealed substantial elongation of the junction prior to flares, suggesting that junction elongation could trigger breaches in the tight junction barrier (Fig 3.5b, Fig 3.6c).

To further test whether junction contraction reinforces ZO-1, I inhibited ROCK-mediated myosin II activation with Y-27632, a ROCK inhibitor. Successful cytokinesis and normal junction architecture depend on ROCK; therefore, I used a moderate dose of ROCK inhibitor such that epithelial organization was not completely disrupted. In embryos expressing ZO-1, ROCK inhibitor partially inhibited junction contraction at isolated flares, and ZO-1 reinforcement was reduced (Fig 3.5c,d). In contrast, when embryos expressing occludin were treated with ROCK inhibitor, we did not detect a significant decrease in junction contraction or Occludin reinforcement at *isolated* flares (Fig 3.6d-f). We hypothesized that *repeating* flares might be a result of a single flare being insufficient to reinforce the barrier, and thus selecting *isolated* flares may bias the results towards control levels of contraction and reinforcement. When we included more complex flares in the analysis (*isolated, repeating,* and *multiple* flares), we observed a significant decline in both junction contraction and occludin reinforcement in ROCK inhibitor-treated embryos (Fig 3.6f). Finally, ROCK inhibitor impaired the efficient restoration of barrier function following Rho flares (Fig 3.5e,f). Similar to occludin, we

observed a high number of repeating flares when ROCK was inhibited (Fig 3.5f,f'). These repeating flares coincided with repeating increases in FZ3 intensity, indicating that repeating flares may result from incomplete restoration of barrier function (Fig 3.5f'). Taken together, these findings support a model in which Rho flares promote Myosin II-mediated contraction of a segment within the junction, thereby concentrating junction proteins locally within that region to repair the barrier.

Figure 3.6

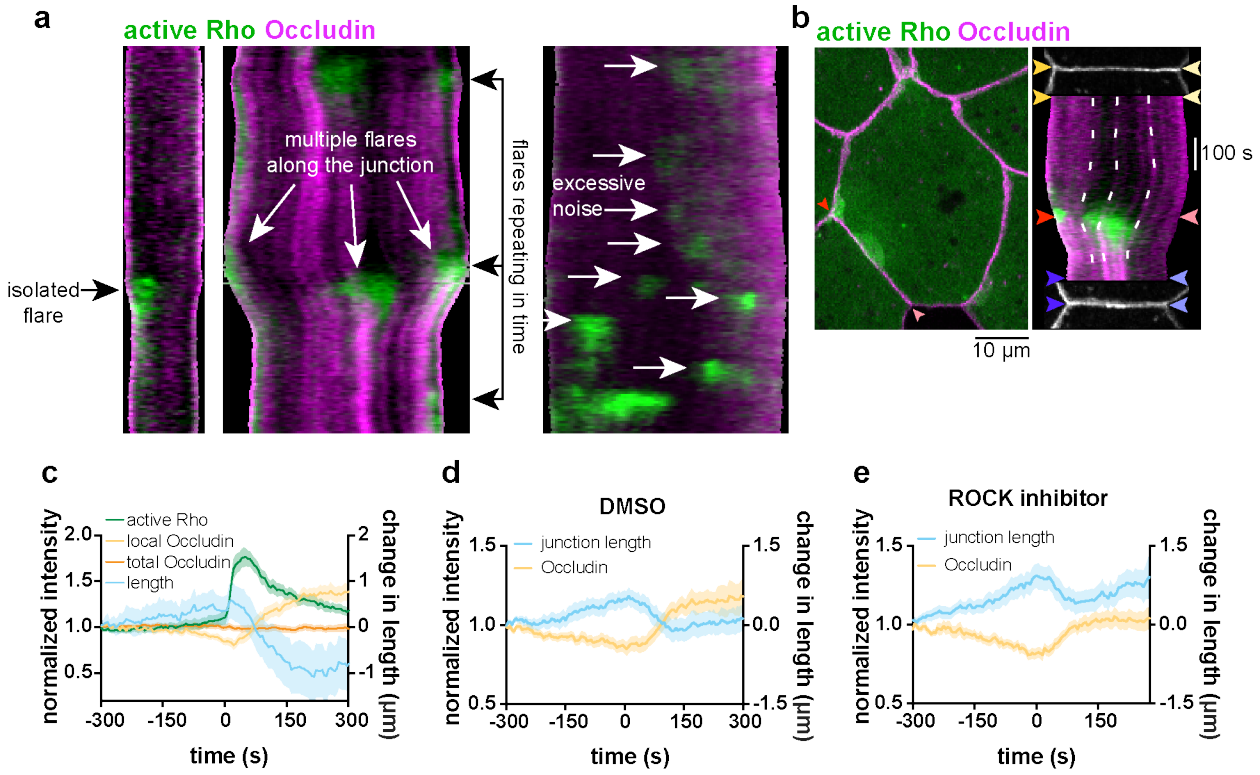

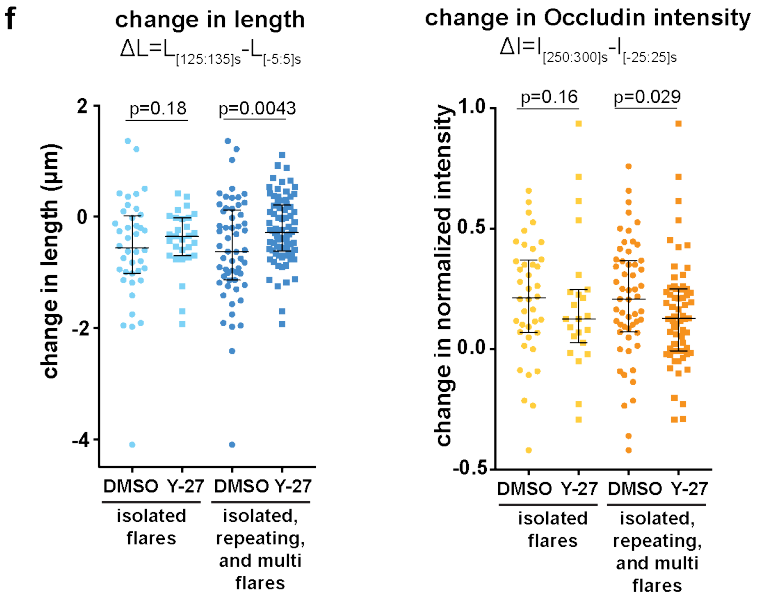

Figure 3.6: Junction contraction reinforces occludin.
(a) Kymographs of active Rho (GFP-rGBD, green) and occludin (mCherry-Occludin, magenta) showing *isolated* and complex (*repeating, multiple, excessive noise*) flares. **(b)** Occludin signal increases as the junction contracts locally. Color-coded arrowheads on the kymograph correspond to the timing of the images shown to the left, top, and bottom. Dashed white lines trace arbitrary fiducial marks in the kymograph, indicating distinct contractile units within the junction. **(c)** Quantification of data from multiple kymographs. Time 0 corresponds to the start of the Rho flare. n=22,7,3 (flares, embryos, experiments) **(d,e)** In isolated flares, ROCK inhibitor (Y-27632) did not significantly influence junction contraction relative to vehicle (DMSO), although elongation prior to the flare was increased. **(d)** n=40,8,3. **(e)** n=42,7,3 **(f)** Change in junction length and occludin intensity was calculated from **(d,e)** for isolated flares. When complex flares were considered in addition to isolated flares, both contraction and occludin reinforcement are significantly reduced. DMSO: n=58,8,3 (note: one outlier was omitted from the DMSO plot: ΔL=-0.95, ΔI=3.14); Y-27632: n=99,7,3. P-values were calculated using Mann-Whitney *U* test.

Figure 3.7

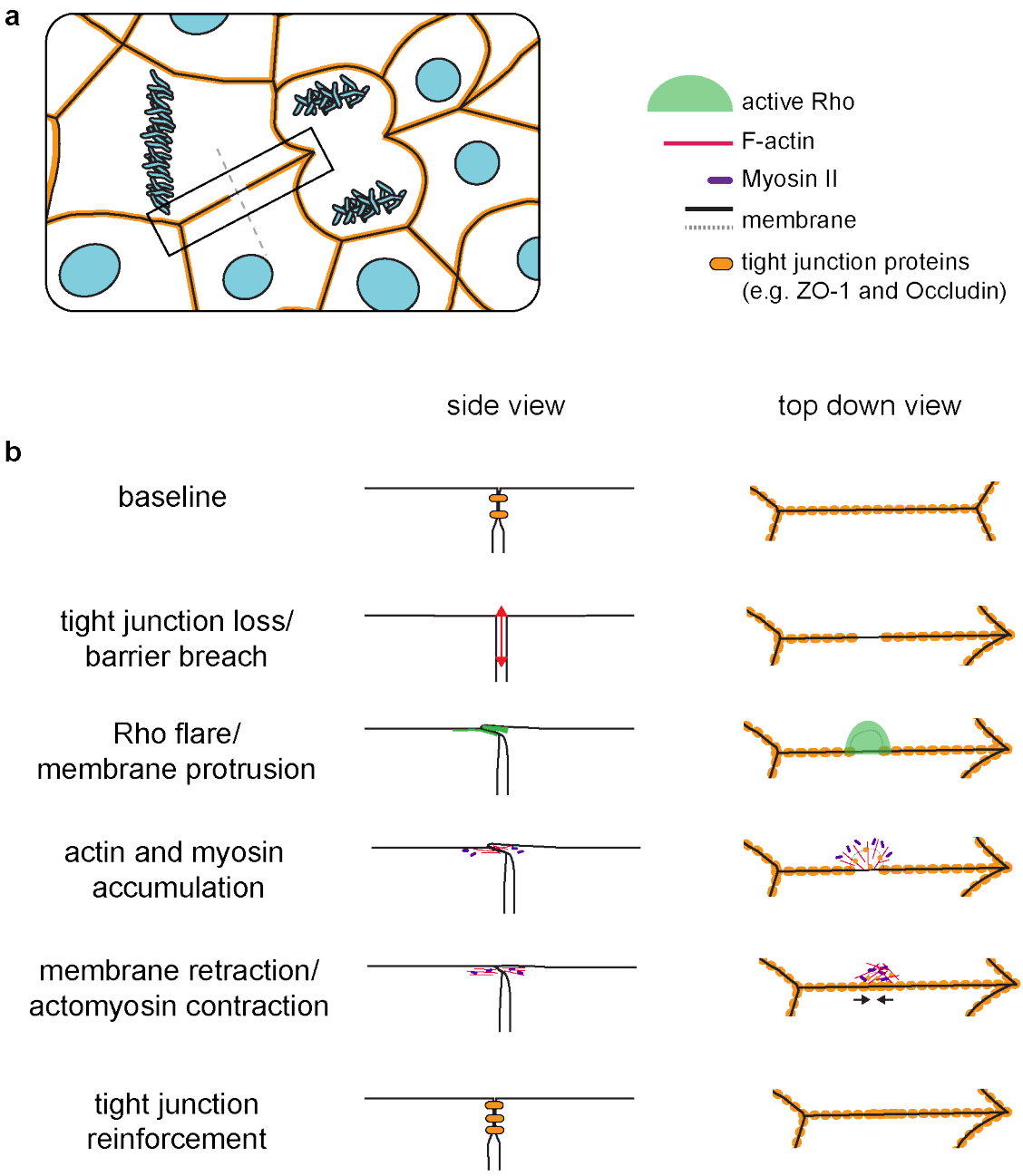

Figure 3.7: Model of how Rho flares reinforce tight junction proteins following junction breaches. A cell- and tissue-scale model of how Rho flares reinforce the epithelial barrier. **(a)** Epithelial cells undergo cell shape changes (e.g., as a result of cytokinesis), and epithelial cell-cell junctions must adapt to these cell shape changes. **(b)** Local loss of tight junction proteins following junction elongation results in a leaky barrier. Flares of active Rho appear at the site of barrier loss, and the tight junction is reinforced through actomyosin-mediated contraction of the junction. Left: cross-section of the junction corresponding to the grey dashed line in **(a)**. Right: *en face* model of the region portrayed in the black box in **(a)**.

Discussion

Steady-state Rho activation is important for proper junction structure; however, too much or too little Rho activation can have detrimental effects on barrier function (Quiros and Nusrat, 2014) and is associated with inflammatory diseases (Capaldo and Nusrat, 2009; López-Posadas et al., 2017). Our results show that dynamic, local Rho flares are important for maintaining epithelial barrier function, and thus measuring total pools of active Rho with biochemical assays, or even imaging active Rho with a snapshot in time, is insufficient to capture the whole picture of how Rho activity affects epithelial junctions.

In mature cultured epithelia, levels of active Rho have been reported to be stable over short time scales (Priya et al., 2015). However, our data indicate that active Rho dynamics are important for maintaining barrier function in a developing vertebrate epithelium, in which cells are undergoing shape changes from cell divisions as well as morphogenesis of the embryo. Epithelia in adult organisms also undergo high rates of cell division and cell extrusion, as epithelial tissues experience relatively high rates of cell turnover (Hooper, 1956). Indeed, other groups have reported short-lived, localized accumulation of F-actin and/or Myosin II at junctions in *Drosophila* and cultured mammalian epithelial and endothelial cells during junction remodeling, indicating that Rho flare-like events may be a conserved process (Abu Taha et al., 2014; Breslin et al., 2015; Cao et al., 2017; Hashimoto et al., 2015; Pope and Harris, 2008; Razzell et al., 2014; Tokuda et al., 2016). However, the majority of these studies focus on the adherens junctions as the cause or target of the F-actin and/or Myosin II accumulation. Here we showed that tight junction defects appear to drive junctional actomyosin

accumulation, highlighting the need to consider both barrier function and mechanics when considering what drives cell shape change. We propose that the Rho flare mechanism described here may be broadly important for maintaining normal barrier function in developing and adult tissues. As small molecule inhibitors that target Rho and ROCK have been developed to treat diseases that result from barrier dysfunction (Deng et al., 2011; Feng et al., 2016), it will be important to consider that Rho-mediated local junction reinforcement contributes to restoring barrier function in some contexts. Similar studies in different epithelial and endothelial tissues will need to be performed in order to understand how ubiquitous Rho flares are as a method of barrier repair in adult tissues.

Collectively, these findings advance our understanding of how epithelia maintain overall barrier function while remaining plastic enough to allow for cell shape changes. Many excellent studies have explored how cell-cell junctions are remodeled in response to tension (Choi et al., 2016; Leerberg et al., 2014; Oda et al., 2014). However, these studies tend to use global, long-term perturbations to increase or reduce tension. Here, we examined junction remodeling in response to endogenous cell- and tissue-scale forces that naturally occur within the developing frog embryo. We found that junction elongation can locally compromise the barrier properties of the epithelium; however, Rho flares restore the barrier on the order of minutes, so that small leaks do not pose a serious threat to organ homeostasis.

References

Abu Taha, A., Taha, M., Seebach, J., and Schnittler, H.-J. (2014). ARP2/3-mediated junction-associated lamellipodia control VE-cadherin-based cell junction dynamics and maintain monolayer integrity. Molecular Biology of the Cell *25*, 245–256.

Aijaz, S., D'Atri, F., Citi, S., Balda, M.S., and Matter, K. (2005). Binding of GEF-H1 to the tight junction-associated adaptor cingulin results in inhibition of Rho signaling and G1/S phase transition. Dev. Cell *8*, 777–786.

Arnold, T.R., Stephenson, R.E., and Miller, A.L. (2017). Rho GTPases and actomyosin: Partners in regulating epithelial cell-cell junction structure and function. Exp. Cell Res. *358*, 20–30.

Benais-Pont, G., Punn, A., Flores-Maldonado, C., Eckert, J., Raposo, G., Fleming, T.P., Cereijido, M., Balda, M.S., and Matter, K. (2003). Identification of a tight junction-associated guanine nucleotide exchange factor that activates Rho and regulates paracellular permeability. J. Cell Biol. *160*, 729–740.

Benink, H.A., and Bement, W.M. (2005). Concentric zones of active RhoA and Cdc42 around single cell wounds. J. Cell Biol. *168*, 429–439.

Breslin, J.W., Zhang, X.E., Worthylake, R.A., and Souza-Smith, F.M. (2015). Involvement of local lamellipodia in endothelial barrier function. PLoS ONE *10*, e0117970.

Breznau, E.B., Semack, A.C., Higashi, T., and Miller, A.L. (2015). MgcRacGAP restricts active RhoA at the cytokinetic furrow and both RhoA and Rac1 at cell-cell junctions in epithelial cells. Molecular Biology of the Cell *26*, 2439–2455.

Cao, J., Ehling, M., März, S., Seebach, J., Tarbashevich, K., Sixta, T., Pitulescu, M.E., Werner, A.-C., Flach, B., Montanez, E., et al. (2017). Polarized actin and VE-cadherin dynamics regulate junctional remodelling and cell migration during sprouting angiogenesis. Nat Commun *8*, 2210.

Capaldo, C.T., and Nusrat, A. (2009). Cytokine regulation of tight junctions. Biochim. Biophys. Acta *1788*, 864–871.

Choi, W., Acharya, B.R., Peyret, G., Fardin, M.-A., Mège, R.-M., Ladoux, B., Yap, A.S., Fanning, A.S., and Peifer, M. (2016). Remodeling the zonula adherens in response to tension and the role of afadin in this response. J. Cell Biol. *213*, 243–260.

Clark, A.G., Miller, A.L., Vaughan, E., Yu, H.-Y.E., Penkert, R., and Bement, W.M. (2009). Integration of single and multicellular wound responses. Curr. Biol. *19*, 1389–1395.

Davenport, N.R., Sonnemann, K.J., Eliceiri, K.W., and Bement, W.M. (2016). Membrane dynamics during cellular wound repair. Molecular Biology of the Cell *27*, 2272–2285.

Deng, J., Feng, E., Ma, S., Zhang, Y., Liu, X., Li, H., Huang, H., Zhu, J., Zhu, W., Shen, X., et al. (2011). Design and Synthesis of Small Molecule RhoA Inhibitors: A New Promising Therapy for Cardiovascular Diseases? J. Med. Chem. *54*, 4508–4522.

Fanning, A.S., and Anderson, J.M. (2009). Zonula occludens-1 and -2 are cytosolic scaffolds that regulate the assembly of cellular junctions. Ann. N. Y. Acad. Sci. *1165*, 113–120.

Fanning, A.S., Ma, T.Y., and Anderson, J.M. (2002). Isolation and functional characterization of the actin binding region in the tight junction protein ZO-1. Faseb J. *16*, 1835–1837.

Feng, Y., LoGrasso, P.V., Defert, O., and Li, R. (2016). Rho Kinase (ROCK) Inhibitors and Their Therapeutic Potential. J. Med. Chem. *59*, 2269–2300.

Hashimoto, H., Robin, F.B., Sherrard, K.M., and Munro, E.M. (2015). Sequential contraction and exchange of apical junctions drives zippering and neural tube closure in a simple chordate. Dev. Cell *32*, 241–255.

Hooper, C.E.S. (1956). Cell turnover in epithelial populations. J. Histochem. Cytochem. *4*, 531–540.

Itoh, M., Nagafuchi, A., Moroi, S., and Tsukita, S. (1997). Involvement of ZO-1 in cadherin-based cell adhesion through its direct binding to alpha catenin and actin filaments. J. Cell Biol. *138*, 181–192.

Leerberg, J.M., Gomez, G.A., Verma, S., Moussa, E.J., Wu, S.K., Priya, R., Hoffman, B.D., Grashoff, C., Schwartz, M.A., and Yap, A.S. (2014). Tension-sensitive actin assembly supports contractility at the epithelial zonula adherens. Curr. Biol. *24*, 1689–1699.

López-Posadas, R., Stürzl, M., Atreya, I., Neurath, M.F., and Britzen-Laurent, N. (2017). Interplay of GTPases and Cytoskeleton in Cellular Barrier Defects during Gut Inflammation. Front Immunol *8*, 1240.

Oda, Y., Otani, T., Ikenouchi, J., and Furuse, M. (2014). Tricellulin regulates junctional tension of epithelial cells at tricellular contacts through Cdc42. J. Cell. Sci. *127*, 4201–4212.

Pope, K.L., and Harris, T.J.C. (2008). Control of cell flattening and junctional remodeling during squamous epithelial morphogenesis in Drosophila. Development *135*, 2227–2238.

Priya, R., Gomez, G.A., Budnar, S., Verma, S., Cox, H.L., Hamilton, N.A., and Yap, A.S. (2015). Feedback regulation through myosin II confers robustness on RhoA signalling at E-cadherin junctions. Nat Cell Biol *17*, 1282–1293.

Quiros, M., and Nusrat, A. (2014). RhoGTPases, actomyosin signaling and regulation of the epithelial Apical Junctional Complex. Semin. Cell Dev. Biol. *36*, 194–203.

Ratheesh, A., Gomez, G.A., Priya, R., Verma, S., Kovacs, E.M., Jiang, K., Brown, N.H., Akhmanova, A., Stehbens, S.J., and Yap, A.S. (2012). Centralspindlin and [alpha]-catenin regulate Rho signalling at the epithelial zonula adherens. Nat Cell Biol *14*, 818–828.

Razzell, W., Wood, W., and Martin, P. (2014). Recapitulation of morphogenetic cell shape changes enables wound re-epithelialisation. Development *141*, 1814–1820.

Reyes, C.C., Jin, M., Breznau, E.B., Espino, R., Delgado-Gonzalo, R., Goryachev, A.B., and Miller, A.L. (2014). Anillin Regulates Cell-Cell Junction Integrity by Organizing Junctional Accumulation of Rho-GTP and Actomyosin. Current Biology *24*, 1263–1270.

Shen, L., and Turner, J.R. (2005). Actin depolymerization disrupts tight junctions via caveolae-mediated endocytosis. Molecular Biology of the Cell *16*, 3919–3936.

Terry, S.J., Zihni, C., Elbediwy, A., Vitiello, E., Leefa Chong San, I.V., Balda, M.S., and Matter, K. (2011). Spatially restricted activation of RhoA signalling at epithelial junctions by p114RhoGEF drives junction formation and morphogenesis. Nat Cell Biol *13*, 159–166.

Thumkeo, D., Watanabe, S., and Narumiya, S. (2013). Physiological roles of Rho and Rho effectors in mammals. Eur. J. Cell Biol. *92*, 303–315.

Tokuda, S., Hirai, T., and Furuse, M. (2016). Effects of Osmolality on Paracellular Transport in MDCK II Cells. PLoS ONE *11*, e0166904.

Van Itallie, C.M., Tietgens, A.J., and Anderson, J.M. (2017). Visualizing the dynamic coupling of claudin strands to the actin cytoskeleton through ZO-1. Molecular Biology of the Cell *28*, 524–534.

Yu, D., Marchiando, A.M., Weber, C.R., Raleigh, D.R., Wang, Y., Shen, L., and Turner, J.R. (2010). MLCK-dependent exchange and actin binding region-dependent anchoring of ZO-1 regulate tight junction barrier function. Proc. Natl. Acad. Sci. U.S.a. *107*, 8237–8241.

Notes and acknowledgements:

The data presented in this chapter are part of an unpublished manuscript entitled “Rho flares locally repair tight junction leaks” by Rachel E. Stephenson, Tomohito Higashi, Ivan Erofeev, Torey R. Arnold, Marcin Leda, Andrew Goryachev, and Ann L. Miller.

I would like to thank Ivan Erofeev, Andrew Goryachev, and Marcin Leda, our collaborators on this work. Collectively, they developed code to generate the kymographs and associated analysis presented in figures 3.5 and 3.6. I would also like to thank Tomohito Higashi and Torey Arnold for their intellectual contributions to this work, as well as for generating some of the DNA constructs used in this study.

The materials and methods for this chapter can be found in Appendix 1.

Chapter 4:

Mechanics and molecular mechanism of Rho flare-associated membrane protrusions

Abstract: A distinctive feature of Rho flares is the associated protrusion of the plasma membrane. The cause of the membrane protrusion and its function are thus far unclear. In this chapter, I explore possible mechanisms of membrane protrusion, including blebbing, actin-based pushing, and actomyosin-based pulling from the neighboring cell, as well as the processes that may govern membrane retraction. By carefully examining the spatial and temporal accumulation of F-actin, myosin II, and actin nucleators, I conclude that a bleb-like method of membrane protrusion is likely, while the mechanism governing membrane retraction remains unclear. I propose that the membrane protrusion functions to temporarily seal the paracellular space while the tight junction is reinforced. Understanding what causes membrane protrusion will allow us to perturb it and test this hypothesis.

Introduction:

In the previous chapters, I demonstrated that Rho flares reinforce the tight junction barrier, in part by locally concentrating tight junction proteins within the junction. However, in addition to a simple shortening of the cell edge at the site of the flare, there is an accompanying protrusion of the plasma membrane that occurs prior to the onset of junction contraction. In this chapter, I will show that Rho is activated within the protrusion, basal to the protrusion in the non-protruding cell, and, frequently, in a dimmer “haze” in the non-protruding cell surrounding the membrane protrusion (Figure 4.1a,b). Active Rho intensity increases as the membrane protrusion expands and decreases as the membrane is retracted. However, the mechanical origin of the membrane protrusion, its functionality, and its relationship to signaling and organization of the cytoskeleton remain mysterious.

In some cases, a membrane protrusion is not apparent at a Rho flare, possibly due to the small size of the protrusion or its location over a tricellular junction. However, there can still be asymmetric distribution of active Rho in these instances. In other cases, active Rho accumulates symmetrically at or on either side of the junction, with no membrane protrusion visible (Figure 4.1c), similar to Rho flares that occur in the presence of Latrunculin B (Figure 3.4). Finally, some junctions exhibit many small flares in the absence of apparent tight junction defects when the apical membrane is slack rather than taut (Figure 4.1d). Based on these observations, it appears that Rho flares are not the cause of membrane deformation. However, the observation that small Rho flares occur in the slackened membrane indicates that membrane deformation may somehow contribute to Rho activation. Possible functions of the membrane protrusion

Figure 4.1

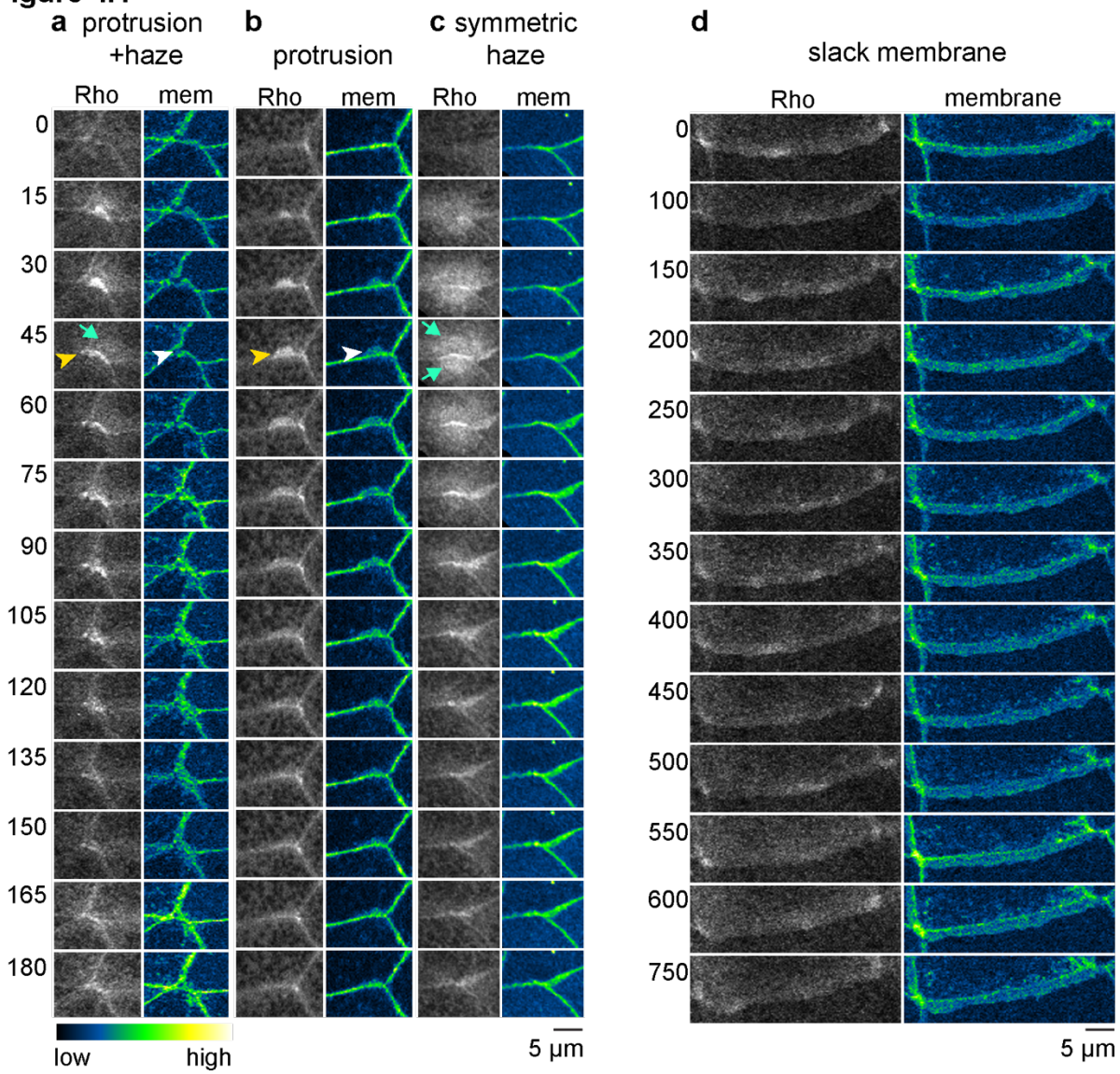

Figure 4.1: Membrane morphology and sub-populations of active Rho at Rho flares. **(a)** Rho flares are typically associated with an asymmetric protrusion of the plasma membrane (white arrowhead), and a dense accumulation of active Rho follows the morphology of the membrane protrusion (yellow arrowheads). Additionally, a haze of active Rho is often visible beyond the membrane protrusion (green arrows). **(b)** In some instances, no haze of active Rho is apparent beyond the site of the membrane protrusion. **(c)** In other cases, there is no visible membrane protrusion, and a haze of active Rho accumulates symmetrically on either side of the dense junctional accumulation of active Rho (green arrows). **(d)** Finally, in instances where the apical plasma membrane is wavy rather than taut, there are small, short-lived, irregular Rho flares that occur within the slack membrane protrusion. Greyscale: active Rho, GFP-rGBD; Green fire blue LUT: membrane, mCherry-farnesyl.

are: 1) to act as a flap that temporarily blocks the paracellular space while the tight junction is repaired, or 2) to expand the surface area of cell-cell contact between neighboring cells. Expanding the area of cell-cell contact could allow for the formation of additional trans interactions between transmembrane tight junction proteins in neighboring cells (e.g., JAMs or occludin), before condensing them into a smaller area during retraction (Cao et al., 2017). Alternatively, the membrane protrusion could be an unintended consequence of related processes with no useful function. Understanding the molecular and mechanical mechanism that causes the protrusion will allow us to perturb it and probe its possible function.

Models of membrane protrusion and retraction:

Blebbing: The plasma membrane is linked to a cortical meshwork of contractile actomyosin that generates hydrostatic pressure in the cytoplasm (Paluch and Raz, 2013). Blebs are spherical protrusions of the plasma membrane that occur when the membrane is no longer supported by the underlying cortical cytoskeleton due to local contractions or fracturing of the cortical cytoskeleton (Charras, 2008; Tinevez et al., 2009)(Figure 4.2a). When this happens, the hydrostatic pressure of the cytoplasm pushes the membrane outward, and the membrane expands until pressure is equalized or the cortex is reassembled beneath the membrane and the membrane is retracted (Charras et al., 2008). Classic blebs follow a stereotypical lifecycle: nucleation, expansion, cortex reassembly, and retraction (Figure 4.2a). Blebbing is common during cell division in isolated cells (Sedzinski et al., 2011), amoeboid migration (a type of migration used by non-adherent or weakly adherent cells) (Bergert et al., 2012; Diz-Muñoz et al., 2010), and apoptosis (Coleman et al., 2001; Cotter et al., 1992).

Figure 4.2

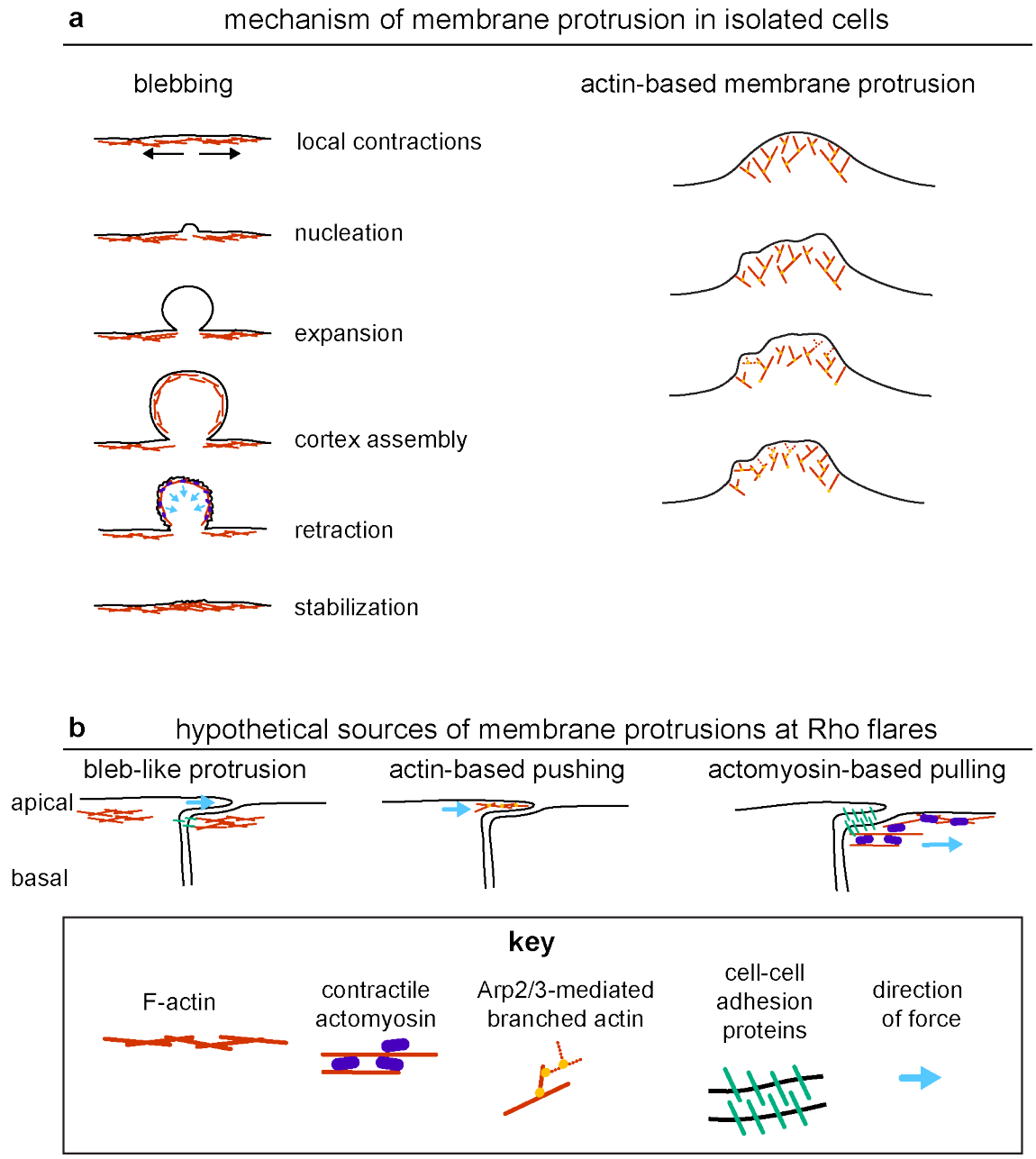

Figure 4.2: Possible sources of membrane protrusions at Rho flares. (a) In isolated cells, two common sources of membrane protrusion are blebbing and actin-based protrusion. (left) Blebs are created when the membrane-cortex connection fails, due to fracturing of the cortex or loss of membrane/cytoskeleton cross-linking. Cytoplasmic pressure causes the cortex-free membrane to expand until pressure is equalized or the cortex is reassembled beneath the bleb membrane. Recruitment of F-actin and Myosin II results in retraction of the bleb. (right) Actin-based membrane protrusions, such as lamellipodia, are formed when Arp2/3-mediated branched actin nucleation stabilizes small deformations in the plasma membrane, resulting in forward movement of the membrane. (b) The apical portions of two neighboring epithelial cells are depicted, with the protruding cell on the left, and the non-protruding cell on the right. Membrane protrusions at Rho flares could be the result of blebs (left), actin-based pushing (middle), or actomyosin-based pulling (right). Actomyosin-based pulling requires cell-cell adhesion, and the non-protruding cell performs the work, in contrast to the other two models of protrusion.

Membrane protrusions described as blebs have been reported in epithelial and endothelial cells; however, blebs are frequently reported to appear at the apical or basal surfaces of cells, rather than at cell-cell junctions. In some cases, the studies lack sufficient detail to determine whether the protrusions follow the classic bleb lifecycle (Hughes and Berger, 2018; Rothschild et al., 2017; Sugrue and Hay, 1981; Svoboda et al., 1999). However, at least one study depicts blebs at tight junctions in Madin-Darby Canine Kidney (MDCK) II epithelial cells exposed to osmotic stress (Tokuda et al., 2016). In this paper, Tokuda et al. found that inducing an osmotic gradient such that osmolality is higher on the basal side of the tissue reduces the Na^+/Cl^- selectivity of the tight junctions. Reduced selectivity is accompanied by odd changes in TJ morphology during live imaging—in particular, bulges or loops of Claudin-2, Claudin-3, ZO-1, occludin, F-actin, and myosin heavy chain were observed. When viewed with SEM and TEM (scanning electron microscopy and transmission electron microscopy, respectively), these structures appeared as spherical protrusions that extended above the apical surface, and examination of freeze fracture replicas showed TJ strands on the blebbed areas, explaining the bulging of TJ proteins they observed. These changes were reversed when osmotic balance was restored. This response also depended on claudin-2, which allows water transport across the epithelium. When osmolality is increased basally, water will move to the basal compartment, potentially inducing stretching of the junctions. Indeed, bulges were accompanied by straightening of the junctions, suggesting a change in tissue tension. Thus, there is a precedent for blebbing at the level of tight junctions in response to mechanical stress in epithelial cells (Figure 4.2b).

Actin-driven protrusion: While blebs rely on cytoplasmic pressure to drive membrane protrusions, membrane protrusions can also be driven by forces from the cytoskeleton. Lamellipodia are broad membrane protrusions that use Arp2/3-mediated branched actin assembly to drive forward progression of the leading edge of migrating cells (Figure 4.2a). In support of this model for driving membrane protrusion at Rho flares (Figure 4.2b) are a number of studies in dynamic endothelial tissues reporting that junctional lamellipodia are important for maintaining barrier function and monolayer integrity (Abu Taha et al., 2014; Breslin et al., 2015; Cao et al., 2017; Martinelli et al., 2013). These protrusions are Rac1 and Arp2/3 dependent, and F-actin and the Arp2/3 complex localize to the leading edge of the junction-associated lamellipodia, similar to the lamellipodia of migrating cells. The apparent purpose of these lamellipodia is to support cell-cell adhesion through VE-cadherin clustering.

Pulling force from neighbor: A third mechanism for membrane protrusion is somewhat passive on the part of the protruding cell. In this scenario, a pulling force from the non-protruding cell causes the protruding cell membrane to expand over its apical surface (Figure 4.2b). This scenario is dependent on adhesion between the two membranes and on actomyosin accumulation in the neighboring cell. This mechanism could work in concert with the pushing and blebbing models, especially since actomyosin appears to accumulate in adjacent cells (Figure 3.2), indicating a degree of cooperation between neighbors.

Protrusion retraction: Bleb retraction is driven by contractile cortex reassembly underneath the bleb membrane, and this retraction mechanism could work independently of the trigger for bleb protrusion. Junctional lamellipodia retract when

there is no longer protrusive actin generated by Arp2/3; the inherent contractility of the cortical cytoskeleton allows it to contract in the absence of a pushing force (Cao et al., 2017). A third mechanism for retraction could be pushing from the neighbor cell via branched actin or contractile actin flow toward the junction.

Each of the models described above is associated with distinct predictions about the nucleation factors involved in actin polymerization, and the timing and localization of F-actin and myosin II accumulation, which are summarized in Figure 4.3. In order to investigate these hypotheses, I examined the localization and timing of F-actin, myosin II, small GTPases, and their associated actin nucleation factors.

Figure 4.3

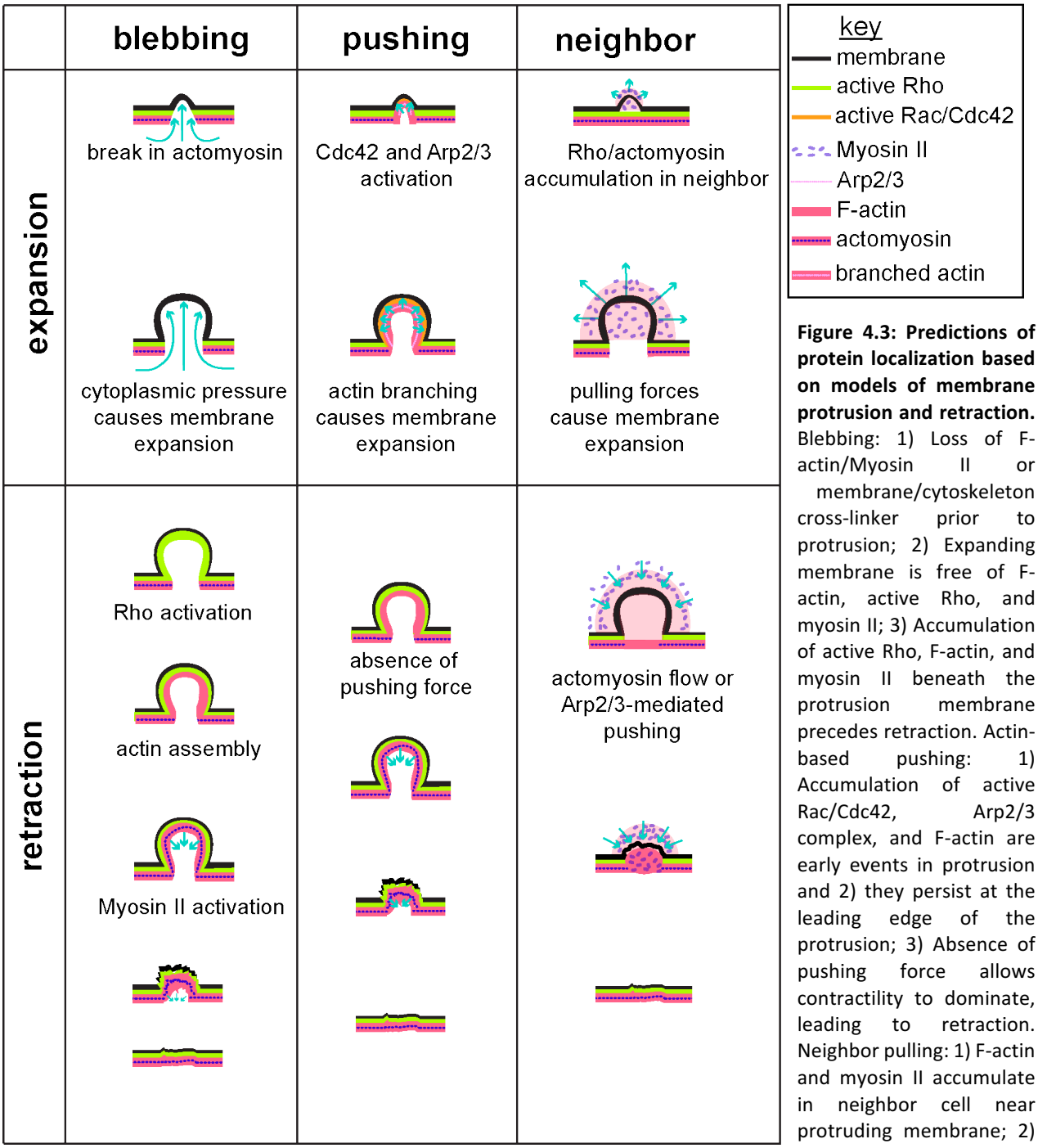

Figure 4.3: Predictions of protein localization based on models of membrane protrusion and retraction. Blebbing: 1) Loss of F-actin/Myosin II or membrane/cytoskeleton cross-linker prior to protrusion; 2) Expanding membrane is free of F-actin, active Rho, and myosin II; 3) Accumulation of active Rho, F-actin, and myosin II beneath the protrusion membrane precedes retraction. Actin-based pushing: 1) Accumulation of active Rac/Cdc42, Arp2/3 complex, and F-actin are early events in protrusion and 2) they persist at the leading edge of the protrusion; 3) Absence of pushing force allows contractility to dominate, leading to retraction. Neighbor pulling: 1) F-actin and myosin II accumulate in neighbor cell near protruding membrane; 2) This is dependent on cell-cell adhesion; 3) Flow of contractile actomyosin (or branched actin) in the non-protruding cell pushes the protruding membrane back.

Figure 4.4

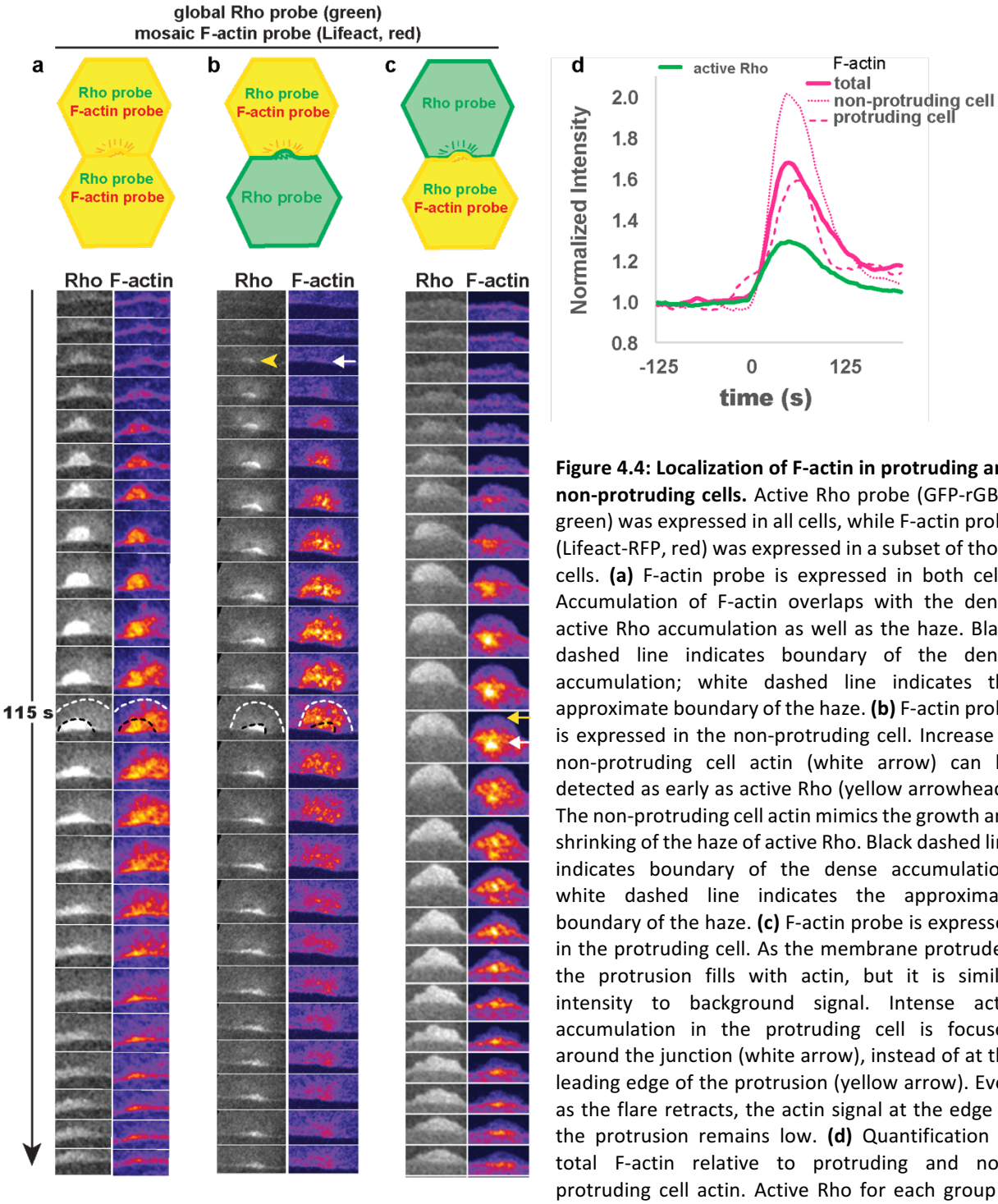

Figure 4.4: Localization of F-actin in protruding and non-protruding cells. Active Rho probe (GFP-rGBD, green) was expressed in all cells, while F-actin probe (Lifeact-RFP, red) was expressed in a subset of those cells. **(a)** F-actin probe is expressed in both cells. Accumulation of F-actin overlaps with the dense active Rho accumulation as well as the haze. Black dashed line indicates boundary of the dense accumulation; white dashed line indicates the approximate boundary of the haze. **(b)** F-actin probe is expressed in the non-protruding cell. Increase in non-protruding cell actin (white arrow) can be detected as early as active Rho (yellow arrowhead). The non-protruding cell actin mimics the growth and shrinking of the haze of active Rho. Black dashed line indicates boundary of the dense accumulation; white dashed line indicates the approximate boundary of the haze. **(c)** F-actin probe is expressed in the protruding cell. As the membrane protrudes, the protrusion fills with actin, but it is similar intensity to background signal. Intense actin accumulation in the protruding cell is focused around the junction (white arrow), instead of at the leading edge of the protrusion (yellow arrow). Even as the flare retracts, the actin signal at the edge of the protrusion remains low. **(d)** Quantification of total F-actin relative to protruding and non-protruding cell actin. Active Rho for each group is averaged together for the Rho curve. Note that non-protruding cell actin peaks slightly before total actin, while protruding cell actin peaks after total actin.

Figure 4.5: Active Rho is increased in both the protruding and non-protruding cells. GFP-rGBD (green Rho probe) was expressed in a subset of cells, and mCherry-rGBD (red Rho probe) was expressed in a different subset of cells. A flare occurring on the boundary of these cells shows that active Rho is increased in both the protruding cell and the non-protruding cell during the flare (yellow arrowheads).

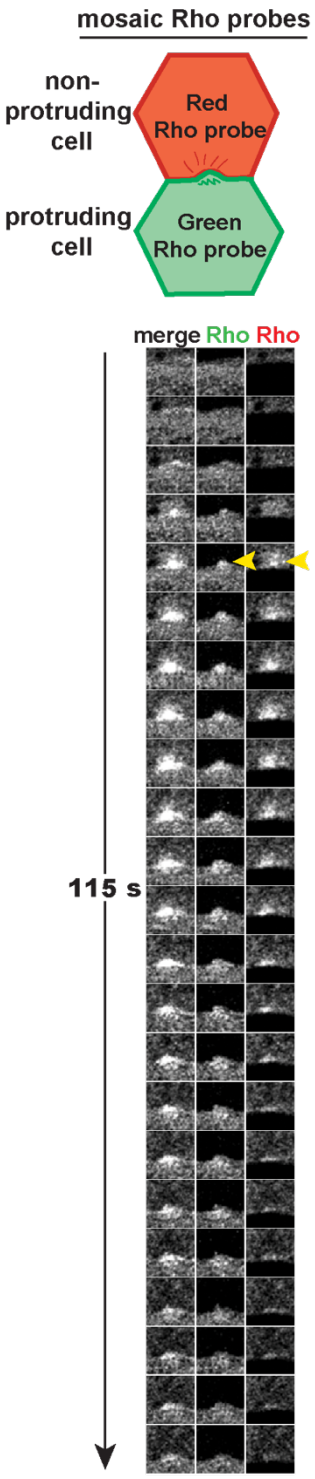

Results:

Mosaic actin accumulation: To better understand the localization of F-actin in the protruding and non-protruding cells, I mosaically expressed an F-actin probe (Lifeact-RFP) and globally expressed a probe for active Rho (GFP-rGBD). F-actin accumulates both within the protrusion in the protruding cell, and under and surrounding the protrusion in the non-protruding cell (Figure 4.4). Typically, F-actin appears first in the non-protruding cell, and is followed by F-actin accumulation in the protruding cell (Figure 4.4d). Active Rho accumulation follows a similar pattern (Figure 4.5). Interestingly, F-actin in the protrusion tends to remain close to the junction and does not extend to the edge of the protrusion, even during retraction (Figure 4.4c). This evidence supports a model of bleb-like expansion or neighbor pulling, and is inconsistent with lamellipodia-like expansion, in which we would expect to see a high concentration of F-actin that moves with the leading edge of the protrusion.

Myosin II: As described in Chapter 3, myosin II localizes to the junction until right before the start of the flare, when it disappears from the junction and reappears on the cortex at the edge of the flare (Figure 3.2). Blebs are often attributed to rupturing of the actomyosin cortex or

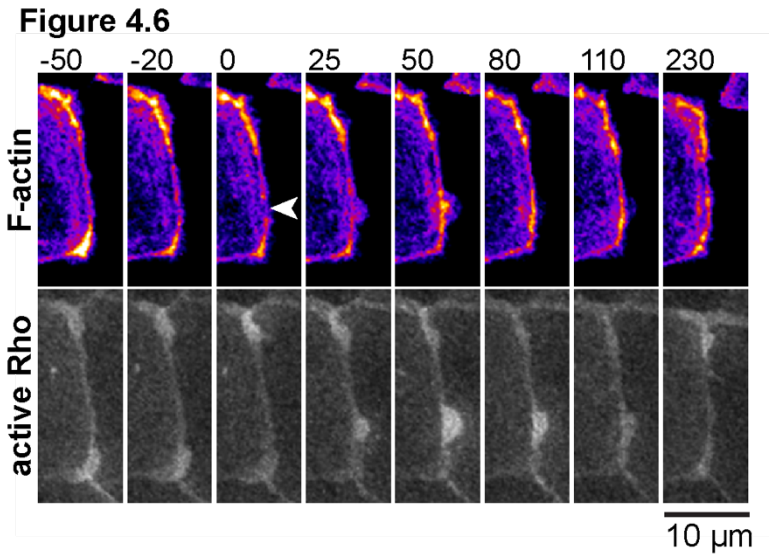

Figure 4.6: A local discontinuity in F-actin prior to onset of Rho flare. White arrowhead shows a transient break in junctional actin in the protruding cell prior to the Rho flare. F-actin (Lifeact-RFP) expressed only in the protruding cell. Active Rho probe (GFP-rGBD) expressed in both cells.

disconnection of the membrane from the cortex, so this observation is consistent with bleb-like expansion. Furthermore, there is occasionally locally reduced F-actin at the flare site, although this is not always apparent (Figure 4.6).

To better understand how the spatial and temporal patterning of F-actin and myosin II interaction governs flare expansion and retraction, I generated kymographs of F-actin, myosin II, and active Rho perpendicular to the junction (Figure 4.7a). Strikingly distinct zones of F-actin and myosin II were apparent from the kymographs generated, with a dense accumulation of F-actin overlapping with the dense active Rho accumulation along the junction, and strong myosin II accumulation just outside the F-actin (Figure 4.7b-e). 9 of the 15 kymographs had similarly intense accumulation of myosin II on either side of the flare (i.e., in both the protruding and non-protruding cells) (Figure 4.7c,e), while 6 of the 15 had myosin II accumulation predominantly on the side of the protruding cell. In instances where myosin II did accumulate in the neighboring cell (Figure 4.7c,e), it typically did so after expansion of the flare. In the neighbor pulling

model of protrusion expansion, I predicted early accumulation of myosin II in the neighbor cell, so these data do not support this model.

Figure 4.7

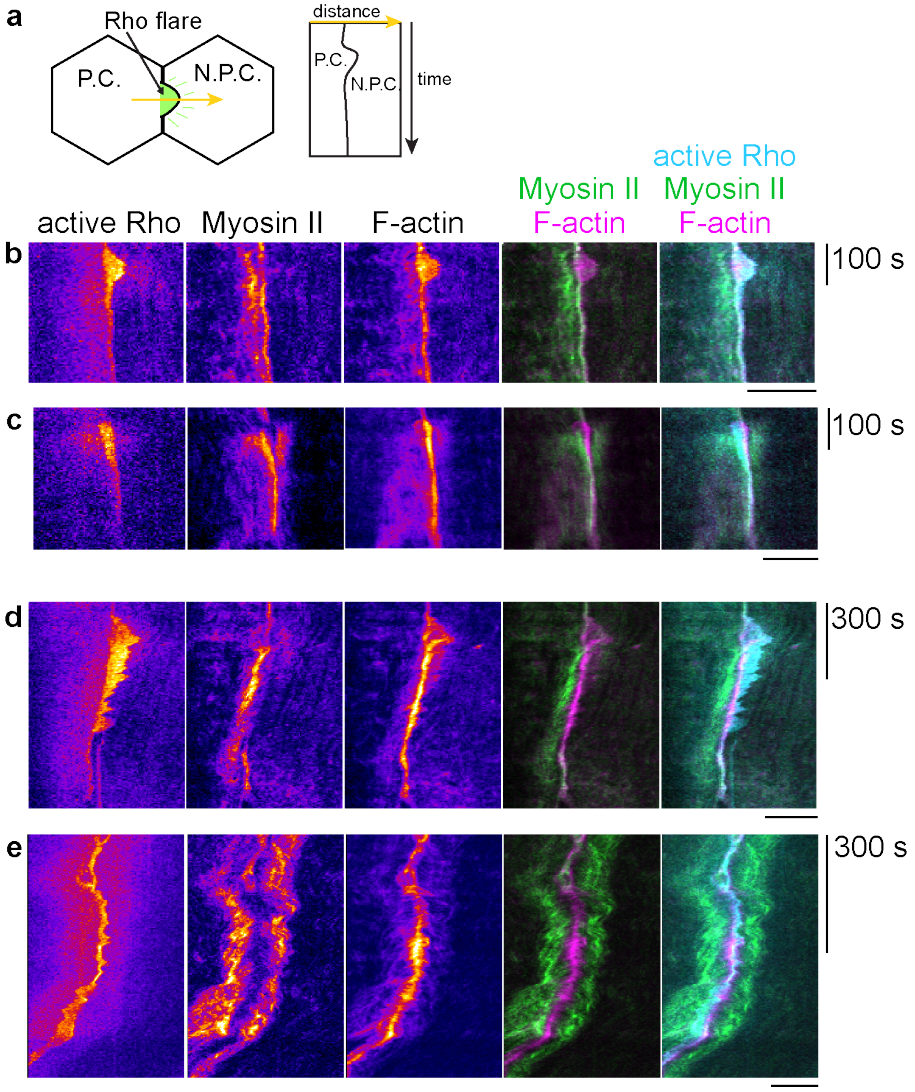

Figure 4.7: F-actin and myosin II have distinct patterns of accumulation at Rho flares. Kymographs were generated according to the diagram in **(a)**. P.C., protruding cell; N.P.C., non-protruding cell. **(b,c)** Kymographs of short flares with myosin II (SF9-mNeon) accumulation predominantly in the protruding cell **(b)** or both the protruding and non-protruding cells **(c)**. Note that there are not large areas of overlap between F-actin and myosin II, but myosin II is present at the junction as the flare ends. **(d,e)** Kymographs of repeating flares with myosin II accumulation predominantly in the protruding cell **(d)** or both the protruding and non-protruding cells **(e)**. Note that there is little overlap between F-actin and myosin II throughout the course of the repeating flares. Scale bars = 10 µm.

Next, I investigated how myosin II accumulation in the protruding vs. non-protruding cell correlates with membrane retraction. In a bleb-like retraction model, I would expect both F-actin and myosin II to accumulate at the edge of the protrusion and drive retraction. An alternate model is that actomyosin flow towards the protrusion in the

non-protruding cell pushes the membrane back towards the junction. In this model, F-actin and myosin II overlap in the non-protruding cell would correlate with retraction.

Of the kymographs generated, 8 of 15 were of short, non-repeating flares. The other 7 were of flares that were repeating or did not resolve quickly. By comparing these groups, I hoped to learn if distinct patterns of F-actin and myosin II accumulation are associated with quick resolution of the flare. For example, if flares with very little myosin II accumulation in the non-protruding cell were also repeating flares, this would suggest that myosin II accumulation in the non-protruding cell is required for efficient retraction. However, this does not appear to be the determining factor: 2 of 8 short flares and 3 of 7 long/repeating flares had myosin II accumulation predominantly on the side of the protruding cell. Additionally, myosin II and F-actin overlap at the edge of the protrusion does not appear to be required for retraction. Instead, it appears that myosin II and F-actin overlap *at the junction* marks the end of the flare (Figure 4.7). Thus, it seems that restored contractility at the junction is important for flare resolution, but may not be important for membrane retraction.

Actin nucleation: Actin polymerization and depolymerization are tightly regulated in cellular contexts to promote specific actin structures and cell behaviors. Rho GTPases coordinate actin polymerization by activating formins, which support linear actin polymerization, and nucleation promoting factors (NPFs) that aid in Arp2/3 complex activation to promote branched actin assembly.

Formins: There are fifteen formins in *Xenopus laevis,* and five of them localize to cell-cell junctions at gastrula stage: Dia1, Dia2, Dia3, Fhod1, and Fhod2 (Higashi and Miller, 2018). Of these, I have examined the localization of Dia2 and Dia3 during Rho

Figure 4.8

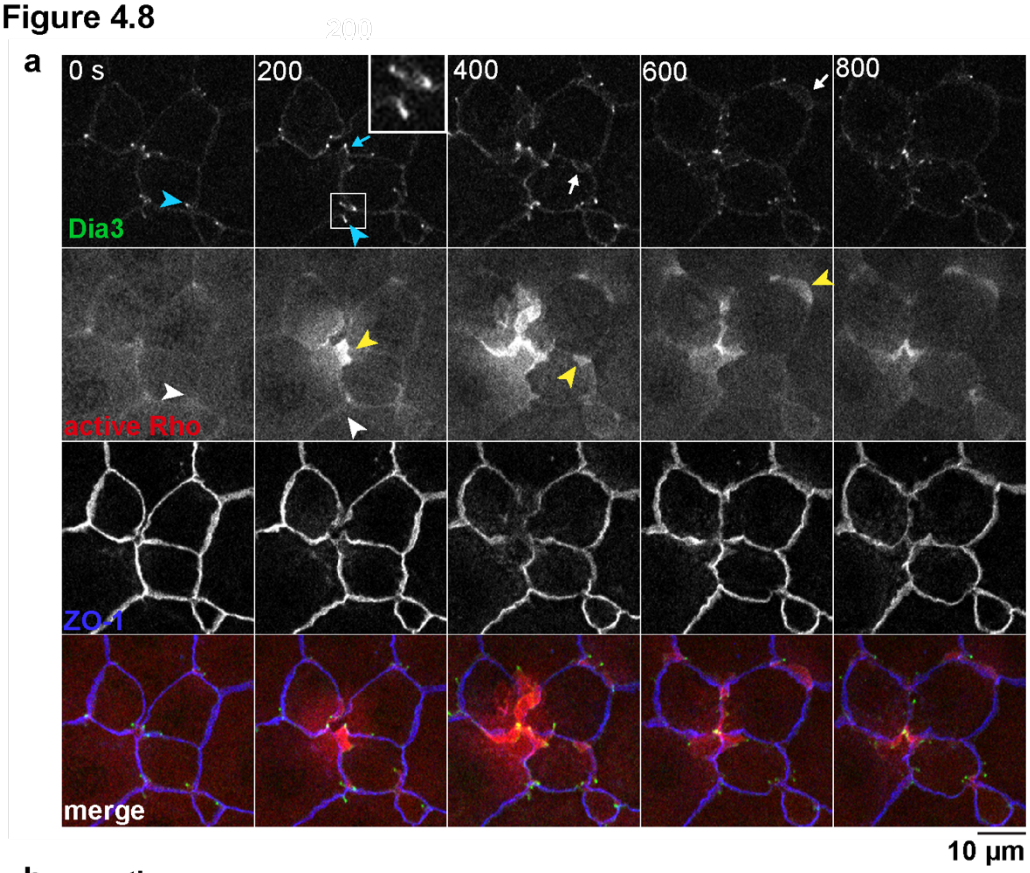

Figure 4.8: Dia3 expression induces membrane protrusions and accumulates at the edge of dense Rho activity. (a) 3xGFP-Dia3 accumulates in puncta at the tips of dynamic filopodia (blue arrowheads; enlargement shown in white box), as well as at cell-cell junctions. Filopodia were not necessarily associated with increased Rho activity (corresponding white arrowheads). However, in some cases the puncta were associated with Rho flares (blue arrow and corresponding yellow arrowhead). In other cases, Dia3 appeared at the edge of the dense Rho accumulation (white arrows and corresponding yellow arrowheads). **(b)** Montage of Dia3 during a single Rho flare. Dia3 accumulates predominately at the edge of the dense Rho accumulation (dotted white line indicates the edge position in all channels). Dia3 accumulation intensifies over the course of the flare.

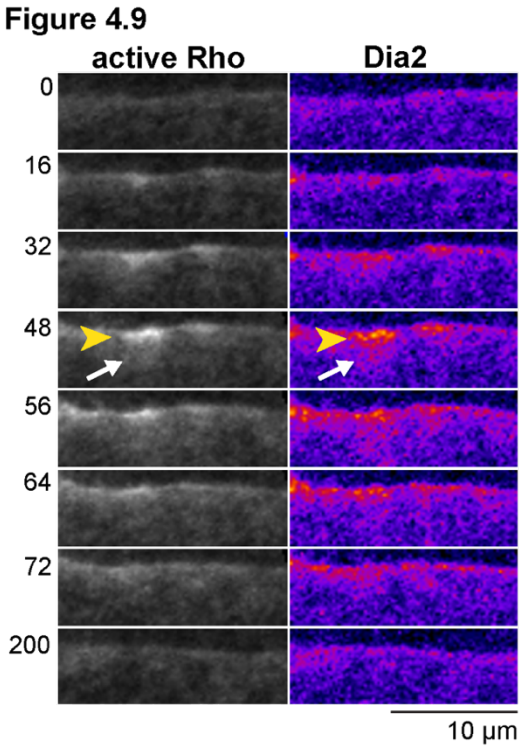

Figure 4.9: Dia2 accumulates diffusely at Rho flares. Montage of Dia2 localization at Rho flares. Dia2 accumulation overlaps with dense active Rho (yellow arrowhead) and the haze of active Rho (white arrow).

flares. Dia3 is a strong candidate because overexpression causes filopodia- and lamellipodia-like membrane protrusions similar to those seen at Rho flares (Tomohito Higashi, data not shown). When I expressed Dia3 with a probe for active Rho, I observed both filopodia- and lamellipodia-like structures. While filopodia-like structures were not usually associated with Rho flares, the broader lamellipodia-like the structures frequently were, and Dia3 could be seen accumulating at the leading edge of these protrusions over time (Figure 4.8). That is, Dia3 accumulation was not an early event, suggesting it is more likely involved in flare retraction or cortex reinstatement than protrusion. However, with the excessive protrusive activity associated with Dia3 overexpression, it is difficult to be certain that the events in these flares are similar to native Rho flares. Dia2 also appears to localize to Rho flares, but in a more diffuse pattern than Dia3 that extends beyond the dense active Rho accumulation (Figure 4.9).

Thus both Dia2 and Dia3 may be involved in nucleating actin polymerization at Rho flares, but they may contribute to generating different populations of actin.

Arp2/3 and Cdc42*:* The Arp2/3 complex can be activated by the small GTPases Rac1 and Cdc42, both of which are documented to be activated with close spatial and temporal proximity to Rho in other contexts (Benink and Bement, 2005; Machacek et al., 2009). Thus, we hypothesized that Arp2/3 could contribute to membrane protrusion if Rac1 or Cdc42 were also activated at Rho flares. Rac1 does not appear to be active at flares (Breznau et al., 2015). Thus, we examined the localization of active Cdc42 using mRFP-wGBD (WASp GTPase Binding Domain; (Benink and Bement, 2005)) and found that active Cdc42 does accumulate at Rho flares, with nearly indistinguishable temporal dynamics from Rho activation (Figure 4.10a). Spatially, active Cdc42 appears more diffuse than active Rho (Figure 4.10a). Next, we observed the Arp2/3 complex by fluorescently tagging Arp3 (Arp3-mNeon). Fluorescently tagged Arp3 can rescue Arp3 knockdown in *Drosophila*, indicating that the tag does not interfere with actin nucleation (Ingerman et al., 2013). We predicted that if membrane protrusion is driven by Arp2/3-mediated actin branching, Arp3-mNeon would be enriched at the leading edge of the membrane protrusion and would be visible early in the flare (Figure 4.3). However, Arp3-mNeon accumulates diffusely at flares and lags behind Rho accumulation, suggesting that it does not contribute to membrane protrusion but may serve another function in generating a pool of branched actin (Figure 4.10b).

Figure 4.10

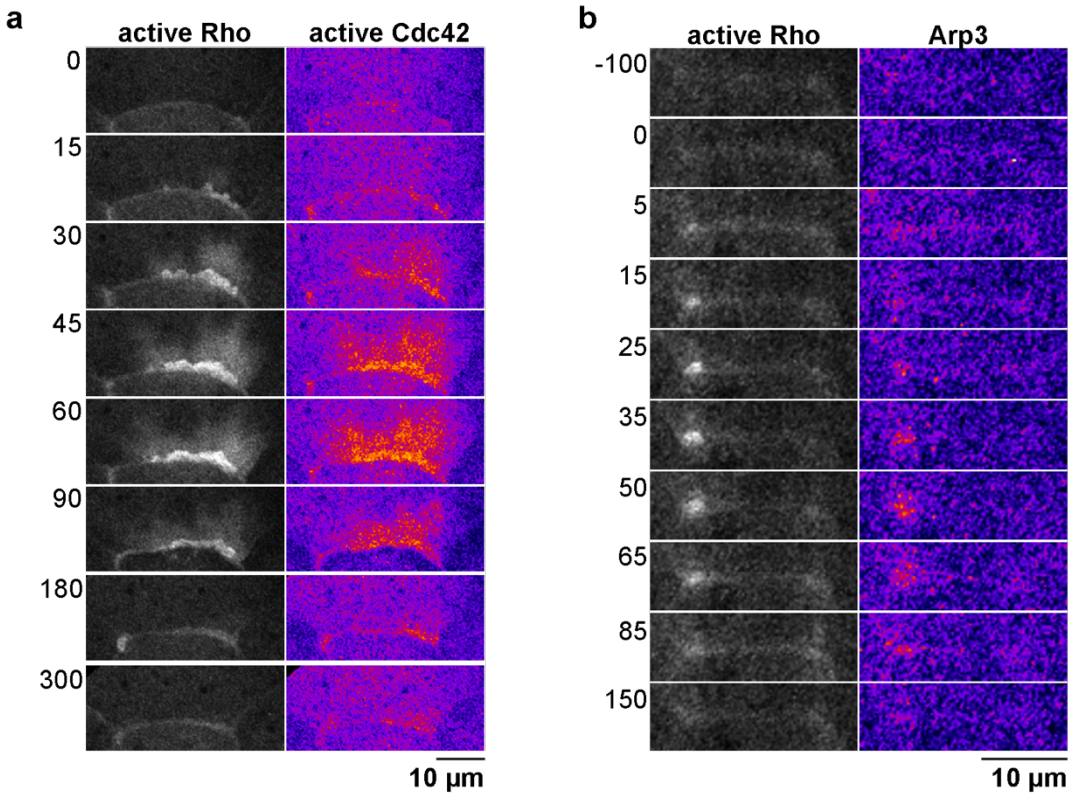

Figure 4.10: Active Cdc42 and Arp3 accumulate at Rho flares. (a) Active Cdc42 (RFP-wGBD) accumulates in a similar pattern to active Rho at flares, except that the active Cdc42 overlapping with the dense Rho accumulation appears to be approximately as intense as the active Cdc42 in the haze, indicating different patterns of Cdc42 and Rho activation. **(b)** Arp3-mNeon diffusely accumulates with dense active Rho.

Discussion

Much of the data presented in this chapter is from preliminary experiments that should be repeated and quantified. Additionally, mosaically expressing the fluorescent probes for myosin II, formins, the Arp2/3 complex, and Cdc42 (similar to Figures 4.4 and 4.5) will show with greater clarity how these proteins behave with respect to the protruding and non-protruding cells. Knowing how formin and Arp3 overexpression affect F-actin at flares will allow us to discern whether overexpression artifacts may be a concern with these proteins. Finally, future studies that examine the effects on Rho flares and F-actin using Dia3 and/or Dia2 loss-of-function approaches or an Arp2/3

inhibitor will be necessary to determine whether these proteins are functionally required for the Rho flare response.

However, based on the preliminary data presented in this chapter along with data from Chapter 3, I conclude that the blebbing model is the most likely means of membrane expansion at the site of the flare for the following reasons: 1) ZO-1 serves as a link between F-actin and the transmembrane proteins, claudins and occludin, and it is decreased prior to the flare (Figure 3.1). 2) Myosin II, and occasionally F-actin, are locally reduced at the junction prior to membrane protrusion (Figure 3.2, 4.6, 4.7). 3) Laser injury of the junction results in a plasma membrane protrusion before F-actin accumulation is apparent (Figure 3.3). Consistent with this finding, in isolated cells, laser ablation of the cortex results in blebbing (Tinevez et al., 2009). Additionally, the other models presented in Figure 4.3 are not supported for the following reasons: 1) F-actin and Arp2/3 accumulation are *not* seen in the protruding cell at the leading edge of the expanding membrane, which would be consistent with a pushing mechanism. 2) Accumulation of myosin II in the neighboring cell was not consistently observed, which would be consistent with a neighbor pulling mechanism.

So far, all the data points to decoupling of the plasma membrane from the actin cytoskeleton as the source of protrusion. However, retraction of the membrane does not appear to follow the classic bleb lifecycle for the following reasons: 1) Active Rho is present throughout the membrane protrusion during expansion of the flare, instead of just prior to retraction. 2) Myosin II and F-actin do not accumulate at the edge of the protrusion to guide retraction. The alternative model, in which the actomyosin flow towards the junction in the non-protruding cell guides retraction also does not fit the

data because myosin II does not always accumulate in the non-protruding cell (Figure 4.7). However, it does appear that myosin II restoration at the junction itself is important for flare resolution, suggesting that restoration of contractility at the junction prevents flares from reoccurring. Along these lines, inhibiting ROCK with Y-27632 resulted in an increase in repeating flares relative to control (Figure 3.6), an observation that could be explained in part by reduced myosin II accumulation at the junction.

Future directions: If the membrane protrusions truly are blebs, then one would expect them to take the path of least resistance—that is, they would expand spherically upward instead of over their neighbors. Indeed, this is how the osmolality-induced blebs appeared in the electron microscopy by Tokuda et al. (2016). Our current experimental setup involves compressing the embryo between two coverslips in order to obtain a flat imaging surface (Reyes et al., 2014). In compressing the embryo, we could be influencing the natural course of the membrane protrusion (preventing a bleb from protruding upwards, for example). To circumvent this issue, we could try fixing the embryos to observe protrusions in their uncompressed state. However, because flares are sporadic and short-lived, it would be beneficial to have embryos that have a higher than average number of flares. Fortunately, a number of perturbations, including incubating embryos in ATP (data not shown) and knocking down anillin (Reyes et al., 2014), increase the frequency of flares. Finding appropriate flare enrichment and fixation conditions would also allow us to perform more detailed microscopy, including SEM, TEM, and super resolution microscopy, to better understand the composition and organization of the actin network relative to the membrane as well as the tight junctions. Alternatively, technology like lattice light sheet microscopy allows for fast imaging of

whole organisms without compression, so it may be possible to capture the membrane dynamics with live imaging as well (Liu et al., 2018).

Of the three actin nucleators I have tested so far (Dia3, Dia2, and Arp2/3), all three localize to flares in some manner, indicating a robust system for actin polymerization. Additional formins, such as Dia1, Fhod1, or Fhod2 could also be involved in promoting actin polymerization. Characterizing roles for these proteins could be difficult, since there is probably some functional redundancy. Double and triple knockdowns may be required to see significant effects. Furthermore, having tools to perform robust statistical analysis of flare characteristics, such as measuring velocity of expansion and retraction, persistence of the protrusion, area, duration, etc. may be necessary to see an effect of perturbing only one of these proteins. We will work with our mathematical modeling collaborator, Andrew Goryachev to develop such analyses.

In addition to proteins that directly promote actin polymerization, there are many proteins that organize actin filaments by crosslinking them to other actin filaments, the membrane, adherens junctions, etc. (Arnold et al., 2017). Some of these proteins, like vinculin, anillin, zyxin, and moesin have been shown to localize to flares by other members of the lab (data not shown). These proteins are other candidates for understanding how membrane expansion and retraction occur in the context of Rho flares.

By probing the dynamics of the membrane protrusion, I hope to determine its functional significance, if it has one. One function of the membrane protrusion could be to act as a physical impedance to reduce diffusion through the paracellular space, in which case it would influence how much material leaks across the tight junction. Using

our live imaging barrier assay ZnUMBA (see Chapters 2 and 3), reduction in FZ3 roughly correlates with the onset of the Rho flare—before TJ protein reinforcement or junction contraction occurs—consistent with a role of blocking the paracellular space. Interestingly, in MDCK cells, increased flux of macromolecules is associated with a reduction of dynamic membrane protrusions (Van Itallie et al., 2015). An alternate explanation for the function of flare-associated membrane protrusions is that the membrane protrusion corrals tight junction proteins on the apical surface of the non-protruding cell membrane, as suggested by (Cao et al., 2017) for VE-cadherin in junction-associated lamellipodia in endothelial cells. If this is the case, then I would expect larger protrusions to correlate with a higher degree of reinforcement. The protrusion may also serve a role in signaling by generating unique physical properties, such as membrane curvature, that recruit BAR domain-containing proteins (Stanishneva-Konovalova et al., 2016; Van Itallie et al., 2015). Understanding the mechanical forces behind membrane protrusion and retraction, as well as organization of the actin cytoskeleton, will give us new insight into the factors that trigger flare activation and signal flare resolution.

References:

Abu Taha, A., Taha, M., Seebach, J., and Schnittler, H.-J. (2014). ARP2/3-mediated junction-associated lamellipodia control VE-cadherin-based cell junction dynamics and maintain monolayer integrity. Molecular Biology of the Cell *25*, 245–256.

Arnold, T.R., Stephenson, R.E., and Miller, A.L. (2017). Rho GTPases and actomyosin: Partners in regulating epithelial cell-cell junction structure and function. Exp. Cell Res. *358*, 20–30.

Benink, H.A., and Bement, W.M. (2005). Concentric zones of active RhoA and Cdc42 around single cell wounds. J. Cell Biol. *168*, 429–439.

Bergert, M., Chandradoss, S.D., Desai, R.A., and Paluch, E. (2012). Cell mechanics control rapid transitions between blebs and lamellipodia during migration. Proc. Natl. Acad. Sci. U.S.a. *109*, 14434–14439.

Breslin, J.W., Zhang, X.E., Worthylake, R.A., and Souza-Smith, F.M. (2015). Involvement of local lamellipodia in endothelial barrier function. PLoS ONE *10*, e0117970.

Breznau, E.B., Semack, A.C., Higashi, T., and Miller, A.L. (2015). MgcRacGAP restricts active RhoA at the cytokinetic furrow and both RhoA and Rac1 at cell-cell junctions in epithelial cells. Molecular Biology of the Cell *26*, 2439–2455.

Cao, J., Ehling, M., März, S., Seebach, J., Tarbashevich, K., Sixta, T., Pitulescu, M.E., Werner, A.-C., Flach, B., Montanez, E., et al. (2017). Polarized actin and VE-cadherin dynamics regulate junctional remodelling and cell migration during sprouting angiogenesis. Nat Commun *8*, 2210.

Charras, G.T. (2008). A short history of blebbing. J Microsc *231*, 466–478.

Charras, G.T., Coughlin, M., Mitchison, T.J., and Mahadevan, L. (2008). Life and times of a cellular bleb. Biophys. J. *94*, 1836–1853.

Coleman, M.L., Sahai, E.A., Yeo, M., Bosch, M., Dewar, A., and Olson, M.F. (2001). Membrane blebbing during apoptosis results from caspase-mediated activation of ROCK I. Nat Cell Biol *3*, 339–345.

Cotter, T.G., Lennon, S.V., Glynn, J.M., and Green, D.R. (1992). Microfilament-disrupting agents prevent the formation of apoptotic bodies in tumor cells undergoing apoptosis. Cancer Res. *52*, 997–1005.

Diz-Muñoz, A., Krieg, M., Bergert, M., Ibarlucea-Benitez, I., Muller, D.J., Paluch, E., and Heisenberg, C.-P. (2010). Control of directed cell migration in vivo by membrane-to-cortex attachment. PLoS Biol. *8*, e1000544.

Higashi, T., and Miller, A.L. (2018). Cell-cell junctions sequester Dia1 and Dia2 from the contractile ring to ensure successful epithelial cytokinesis. In revison.

Hughes, J.R., and Berger, T. (2018). Regulation of apical blebbing in the porcine epididymis. J. Anat. *232*, 515–522.

Ingerman, E., Hsiao, J.Y., and Mullins, R.D. (2013). Arp2/3 complex ATP hydrolysis promotes lamellipodial actin network disassembly but is dispensable for assembly. J. Cell Biol. *200*, 619–633.

Liu, T.-L., Upadhyayula, S., Milkie, D.E., Singh, V., Wang, K., Swinburne, I.A., Mosaliganti, K.R., Collins, Z.M., Hiscock, T.W., Shea, J., et al. (2018). Observing the cell in its native state: Imaging subcellular dynamics in multicellular organisms. Science *360*, eaaq1392–15.

Machacek, M., Hodgson, L., Welch, C., Elliott, H., Pertz, O., Nalbant, P., Abell, A., Johnson, G.L., Hahn, K.M., and Danuser, G. (2009). Coordination of Rho GTPase activities during cell protrusion. Nature *461*, 99–103.

Martinelli, R., Kamei, M., Sage, P.T., Massol, R., Varghese, L., Sciuto, T., Toporsian, M., Dvorak, A.M., Kirchhausen, T., Springer, T.A., et al. (2013). Release of cellular tension signals self-restorative ventral lamellipodia to heal barrier micro-wounds. J. Cell Biol. *201*, 449–465.

Paluch, E.K., and Raz, E. (2013). The role and regulation of blebs in cell migration. Curr. Opin. Cell Biol. *25*, 582–590.

Reyes, C.C., Jin, M., Breznau, E.B., Espino, R., Delgado-Gonzalo, R., Goryachev, A.B., and Miller, A.L. (2014). Anillin regulates cell-cell junction integrity by organizing junctional accumulation of Rho-GTP and actomyosin. Curr. Biol. *24*, 1263–1270.

Rothschild, P.-R., Salah, S., Berdugo, M., Gélizé, E., Delaunay, K., Naud, M.-C., Klein, C., Moulin, A., Savoldelli, M., Bergin, C., et al. (2017). ROCK-1 mediates diabetes-induced retinal pigment epithelial and endothelial cell blebbing: Contribution to diabetic retinopathy. Sci Rep *7*, 8834.

Sedzinski, J., Biro, M., Oswald, A., Tinevez, J.-Y., Salbreux, G., and Paluch, E. (2011). Polar actomyosin contractility destabilizes the position of the cytokinetic furrow. Nature *476*, 462–466.

Stanishneva-Konovalova, T.B., Derkacheva, N.I., Polevova, S.V., and Sokolova, O.S. (2016). The Role of BAR Domain Proteins in the Regulation of Membrane Dynamics. Acta Naturae *8*, 1–10.

Sugrue, S.P., and Hay, E.D. (1981). Response of basal epithelial cell surface and Cytoskeleton to solubilized extracellular matrix molecules. J. Cell Biol. *91*, 45–54.

Svoboda, K.K., Orlow, D.L., Ashrafzadeh, A., and Jirawuthiworavong, G. (1999). Zyxin and vinculin distribution at the cell-extracellular matrix attachment complex (CMAX) in corneal epithelial tissue are actin dependent. Anat. Rec. *254*, 336–347.

Tinevez, J.-Y., Schulze, U., Salbreux, G., Roensch, J., Joanny, J.-F., and Paluch, E. (2009). Role of cortical tension in bleb growth. Proc. Natl. Acad. Sci. U.S.a. *106*, 18581–18586.

Tokuda, S., Hirai, T., and Furuse, M. (2016). Effects of Osmolality on Paracellular Transport in MDCK II Cells. PLoS ONE *11*, e0166904.

Van Itallie, C.M., Tietgens, A.J., Krystofiak, E., Kachar, B., and Anderson, J.M. (2015). A complex of ZO-1 and the BAR-domain protein TOCA-1 regulates actin assembly at the tight junction. Molecular Biology of the Cell *26*, 2769–2787.

Notes and Acknowledgements:

The data presented in this chapter are unpublished.

I would like to thank Maria Ahmed for performing experiments contributing to Figure 4.7 and Brandon Coy for performing the experiments presented in Figure 4.10.

Materials and Methods for this chapter can be found in Appendix 1.

Chapter 5

Discussion, Conclusions, and Outlook

In this dissertation, I have shown that flares of the small GTPase Rho are capable of rapidly repairing localized breaches in the epithelial barrier of *X. laevis* embryos. I introduced a technique (ZnUMBA) that allowed us to visualize transient leaks in the tight junction barrier for the first time and correlated those events with changes in cell shape and localized loss of the tight junction proteins ZO-1 and occludin. Then, I showed that flares of active Rho mediate repair of the barrier through localized contraction of the junction. In the field of tight junction signaling, this work raises many questions, including why use Rho for tight junction repair? How will our knowledge of Rho-mediated repair influence our treatment of diseases resulting from increased paracellular permeability? What are the GEFs, GAPs, and scaffolding proteins that regulate Rho flares? How does local loss of ZO-1 and occludin, but not claudin, cause barrier breaches? In this chapter I will speculate on each of these topics and propose what I see as the most exciting future directions to follow up on this work.

Why Rho?

Both epithelial tissues and endothelial tissues act as barriers in the human body. Endothelial tissues line the blood and lymphatic vessels and consist of a single layer of thin, flat (squamous) cells attached directly to a basement membrane. Epithelial tissues,

on the other hand, are more diverse in their arrangement. Epithelial cells can vary substantially in their morphology (from squamous to cuboidal to columnar) as well as their organization (from simple monolayers to stratified layers of epithelial cells). However, both tissue types use adherens junctions and tight junctions to regulate cell-cell adhesion and paracellular permeability.

Based on what I have described in the previous chapters, it may seem counterintuitive, then, that Rho is frequently cited as “the enemy” of barrier function in endothelial tissues. Many agonists that induce leakiness of endothelial tissues, including thrombin, VEGF, histamine, and TNF-α, do so by activating the Rho/ROCK pathway, which causes the formation of radial F-actin bundles and enhanced contractility that leads to elevated permeability (van Buul and Timmerman, 2016). In contrast, Rac1 is more associated with promoting barrier function in endothelial tissues (Daneshjou et al., 2015; van Buul and Timmerman, 2016). In agreement with this, dynamic Rac1-regulated junctional lamellipodia have been associated with maintenance of endothelial barrier function (Abu Taha et al., 2014; Breslin et al., 2015; Cao et al., 2017; Martinelli et al., 2013).

Similarities between junctional lamellipodia and Rho flares

Junctional lamellipodia, sometimes called junction-associated intermittent lamellipodia, or JAIL, are protrusions of the endothelial cell plasma membrane that support endothelial barrier function (Abu Taha et al., 2014; Breslin et al., 2015; Cao et al., 2017). JAIL have often been associated with endothelial cells that are undergoing rearrangement. For example, they appear in subconfluent cultured cells, in which

endothelial cells are still establishing cell-cell contacts (Abu Taha et al., 2014), or during VEGF-mediated sprouting angiogenesis, in which cells polarize and migrate as a sheet in order to create new vasculature (Cao et al., 2017). However, one group found that junctional lamellipodia are required for maintaining barrier function in confluent cells and that decreased junctional lamellipodia formation was associated with thrombin-induced barrier defects (Breslin et al., 2015). Finally, while not specifically localized to junctions, ventral (basal) lamellipodia are transient actin structures that heal microwounds induced by leukocyte transmigration (Martinelli et al., 2013). In addition to healing holes in the membrane, ventral lamellipodia can restore cell-cell contact, promoting paracellular as well as transcellular barrier function (Martinelli et al., 2013). Regardless of the context in which they are found, these lamellipodia are dependent on Rac1 activation and Arp2/3-mediated branched actin formation (Abu Taha et al., 2014; Breslin et al., 2015; Cao et al., 2017; Martinelli et al., 2013).

There are some striking parallels between the junctional lamellipodia in endothelia and the Rho flares I have described. For example, junctional lamellipodia are likely to form along elongating junctions (Cao et al., 2017), and at “breaks” in vascular endothelial- (VE-) cadherin (Abu Taha et al., 2014; Cao et al., 2017) similar to the correlation between Rho flares, elongating junctions, and “breaks” in tight junction proteins. Furthermore, the lamellipodia create areas of membrane overlap that the authors hypothesize allow trans-interactions between VE-cadherin molecules on neighboring cells to form, and JAIL retraction drives concentration of VE-cadherin clusters at the junction (Abu Taha et al., 2014; Cao et al., 2017). Rho flares also increase the surface area of neighboring membrane overlap in an actin-based manner,

although whether membrane overlap contributes to reinforcement has not been tested. Furthermore, tension-sensing seems to be involved in triggering lamellipodia formation, as decreasing myosin II activity with Blebbistatin or the ROCK inhibitor Y-27632, changed lamellipodia frequency (Breslin et al., 2015; Cao et al., 2017; Martinelli et al., 2013). However, as of yet, there is no direct evidence that Rho-mediated actomyosin contraction plays any role in JAIL retraction or reinforcement of endothelial tight junctions or adherens junctions.

Why would endothelial cells and epithelial cells use different mechanisms of cell-cell junction repair? The answer could lie in the difference in cell shape. Because endothelial cells are relatively flat, their junctions are much closer to the integrin-based adhesions that allow them to adhere to the basal lamina. Therefore, the migratory machinery for lamellipodia-based movement is localized near the junctions so these functions are more likely to be coupled (DeMali and Burridge, 2003). In cuboidal and columnar epithelia, the basal membrane can be several tens of microns away from the apical junctions and may not be attached to the basal lamina, so it is possible that generating lamellipodia-based protrusions may not be as effective in this setting. For example, the epithelium of the animal hemisphere of gastrula-stage *X. laevis* embryos is composed of a single layer of cuboidal epithelial cells, approximately 20-40 μm in diameter and 20-30 μm in height, that is attached to a layer of deep cells rather than a basal lamina (Keller, 1980). Some migrating cells can alternate using either lamellipodia or blebs as a means of membrane protrusion depending on intrinsic and extrinsic mechanical cues (Bergert et al., 2012), so the mechanics of various tissues may dictate whether they have Rac- or Rho-based junction repair. Experimentally altering tissue

tension, as well as investigating how cell shape and cell-substrate adhesion influences the mode of junction repair may help answer these questions.

Rho activity in inflammatory diseases

The most well-studied epithelial barrier diseases are Inflammatory Bowel Diseases (IBD) like Crohn's Disease and Ulcerative Colitis. Leaky intestinal epithelium is a hallmark of these diseases (Rasmussen et al., 2015), although there is still some debate over whether leaky tight junctions are the cause of the disease or merely a consequence of inflammation (Ivanov et al., 2010; López-Posadas et al., 2017; Odenwald and Turner, 2013). Nevertheless, studies of IBD patients have found that altered RhoA signaling is associated with IBD. Two studies found that decreased Rho activation was associated with inflammation of the intestine. In the first, Rho GDI, which sequesters inactive Rho in the cytoplasm, was up-regulated, potentially lowering the pool of membrane-bound active Rho (Shkoda et al., 2007). Similarly, in a second study, down-regulation of a geranylgeranyl transferase, required for prenylation and membrane insertion of active Rho proteins, was downregulated in IBD patients (López-Posadas et al., 2016a). In contrast, a third study found that hyperactivation of Rho was associated with inflamed regions of the intestinal epithelium in Crohn's disease patients (Segain et al., 2003). Therefore, both too little and too much Rho activation have been associated with IBD, just as both inhibiting and hyper-activating Rho *in vitro* can negatively affect epithelial barrier function (Quiros and Nusrat, 2014).

Rho kinase (ROCK) is the Rho effector primarily responsible for causing hyper-contractility and barrier defects in endothelial tissues (van Buul and Timmerman, 2016).

Because of this, the ROCK inhibitor fasudil has been approved in Japan for the treatment of cerebral vasospasm, a constriction of intracranial arteries (Feng et al., 2016). Additionally, fasudil has been used in animal models to treat conditions relating to endothelial dysfunction, such as bladder dysfunction (Akaihata et al., 2018), endothelial dysfunction resulting from chronic intermittent hypoxia (Li et al., 2018), diabetic retinopathy (Rothschild et al., 2017), and epithelial inflammation, such as asthma (Xie et al., 2015), among others (Feng et al., 2016). However, fasudil has been found to worsen or have no effect on inflammation in models of IBD (Kangawa et al., 2017; Yoshikawa et al., 2017). The utility of fasudil in treating diseases of epithelial and endothelial origin will ultimately depend on the primary cause of the disease and how individual tissues respond to ROCK activation and inhibition. Because ROCK is associated with so many facets of normal cell function, including cytokinesis, cell migration, apoptosis, cell extrusion, and cell-cell junction regulation, some off-target effects of inhibiting ROCK are to be expected. Therefore, identifying molecules specific to each of these functions, such as the GEFs, GAPs, and scaffolding proteins involved, may allow for more specific targeting of the underlying defect with fewer off-target effects.

Scaffold proteins as regulators of Rho GTPase signaling specificity

Establishing the contractile actomyosin network at apical cell-cell junctions requires a stable baseline of Rho activation. I have shown that in addition to this baseline population of active Rho, there are transient, highly localized increases in Rho activity that have localized effects on the cytoskeleton and tight junctions. However, it

remains unclear how the stable and dynamic populations of active Rho are differentially regulated to carry out their distinct functions. One obvious question in this vein is: which GEFs and GAPs are involved in regulation of Rho flares, and do specific GEFs and GAPs regulate Rho flares vs. baseline Rho activity at cell-cell junctions?

It is well accepted that the placement and extent of cellular GTPase activity is the result of the net activity of GEFs and GAPs. The current list of GEFs and GAPs known to regulate Rho family GTPases at cell-cell junctions is long, and includes GEFs and GAPs important for junction assembly, maturation, homeostasis, and disassembly (for more detail see (Citi et al., 2014; Quiros and Nusrat, 2014; Zihni and Terry, 2015). It is likely that one or more of the GEFs and GAPs already established to localize to and act on cell-cell junctions is involved in regulating Rho flares. However, for the most part, the effects of these GEFs and GAPs on Rho activation over short timescales has not been studied. I have identified several GEFs and GAPs that are candidates for regulating Rho flares, which I will discuss further below.

With active Rho playing multiple essential roles related to cell-cell junctions including: junction formation, maturation, homeostasis, disassembly, multicellular wound healing, cellular dynamics during morphogenesis, as well as tight junction reinforcement, it becomes evident that there must be mechanisms in addition to GEFs and GAPs for organizing Rho signaling at cell-cell junctions so that the desired downstream effect is achieved. Scaffold proteins can fulfill this role by bringing regulators, GTPases, and effectors together to efficiently couple GTPase activation with output (Garcia-Mata and Burridge, 2007; Marinissen and Gutkind, 2005). Scaffold proteins are key components of cell signaling pathways that tether signaling

components to a discrete cellular location, promoting efficient signaling by limiting the diffusion of components and ensuring that the correct targets become activated. Furthermore, scaffold proteins may mediate the response to stimuli by participating in negative or positive feedback loops to carefully control the signaling output. Proteins that scaffold Rho signaling at apical cell-cell junctions may dictate the outcome of Rho activation in several ways including: 1) by controlling whether specific targets (e.g. ROCK, formins, or transcription factors) become activated; 2) by anchoring signaling output to specific structures (e.g. tight junctions, adherens junctions, tricellular junctions, etc.); 3) by modulating how much contractile force results from signaling (e.g. enough to generate steady-state isometric tension on the junction, cause the junction to contract, or completely disengage the junctions); and 4) by coordinating tension between neighboring cells (e.g. via mechanosensitive junctional proteins that can promote signaling in response to tension changes in neighboring cells). Therefore, I will discuss some candidate Rho scaffolding proteins and how they could mediate Rho flares through interactions with GEFs and GAPs.

Cingulin, Paracingulin, and GEF-H1

Cingulin and paracingulin have similar structures, as well as overlapping and distinct binding partners. Cingulin is localized at the tight junction in a ZO-1-dependent manner (Umeda et al., 2004), whereas paracingulin localizes to both the tight junction and adherens junction (Citi et al., 2012). Both form parallel homodimers, with a globular head domain, a long coiled-coil rod domain, and a small globular tail (Citi et al., 2012; Cordenonsi et al., 1999). Cingulin can directly bind to F-actin, myosin II, and

microtubules through its head domain (Cordenonsi et al., 1999; D'Atri and Citi, 2001; Yano et al., 2013). Paracingulin also associates with the actin and microtubule cytoskeletons, and disruption of either interferes with its junctional targeting. In contrast, only disruption of the actin cytoskeleton disrupts cingulin's junctional targeting (Paschoud et al., 2011).

Cingulin and paracingulin can both bind several Rho family GEFs and GAPs. Both proteins can bind MgcRacGAP, a RhoA GAP, and GEF-H1, a RhoA GEF that is inactivated by cingulin/paracingulin binding (Guillemot et al., 2014; Guillemot et al., 2008). A complex of cingulin, p114RhoGEF (a RhoA GEF), ROCK2, and myosin IIA is important for confining RhoA signaling to the apical junctions in Caco-2 and Human Corneal Epithelial (HCE) cells, and for normal tight junction maturation in HCE cells (Terry et al., 2011). Additionally, paracingulin can form complexes with Rac1 and the Cdc42 GEF SH3BP1 as well as recruit the Rac GEF Tiam1 to junctions (Elbediwy et al., 2012; Guillemot et al., 2008).

With so much potential for interaction with GEFs, GAPs, and cytoskeletal components, what remains unclear is how cingulin and paracingulin regulate which GEFs and GAPs are "on" at a given time. A simple interpretation is that they simply act as targeting molecules, recruiting GEFs and GAPs to the junctions where they are then activated or inactivated by other proteins (e.g. by kinases). Another possibility is that the extended rod domain functions as a molecular ruler, as was proposed for ROCK2 (Truebestein et al., 2015). Cingulin binds actin, myosin II, microtubules, and the C-terminus of ZO-1 with its head domain, whereas many GEFs and GAPs can bind to its rod domain. Perhaps the head domain anchors cingulin to the cytoskeleton while the

rod domain acts to position GEFs and GAPs near membrane-bound GTPases in certain contexts. Interestingly, Yano et al (2013) found a potential phosphorylation-dependent conformational change that enhances cingulin-microtubule binding, so it is possible that this or other modifications govern the orientation or conformation of cingulin to give GEFs and GAPs access to GTPases or couple it to the relevant cytoskeletal structures. A mechanism in which a quick conformational change induces Rho activation would be ideal for a system in which Rho activation must occur quickly and locally.

GEF-H1 was one of the first Rho GEFs identified to localize to tight junctions, making it a popular candidate for regulating junctional Rho activation (Benais-Pont et al., 2003). However, knockdown and overexpression of GEF-H1 in MDCK cells had no impact on tight junction morphology as assessed by freeze fracture electron microscopy and immunohistochemistry, although both knockdown and overexpression of GEF-H1 resulted in increased flux of macromolecules without affecting TER (Benais-Pont et al., 2003). Later studies confirmed that GEF-H1 is mostly inactive in quiescent epithelia (Aijaz et al., 2005; Guillemot et al., 2008; 2014; Terry et al., 2011; Zihni and Terry, 2015). Its inactivation is achieved by recruitment to junctions by cingulin and paracingulin, which inhibit its GEF activity (Aijaz et al., 2005; Guillemot et al., 2008).

However, more recent work in *Xenopus* embryos has shown that GEF-H1 is important for regulating the dynamic events of apical constriction and cell intercalation during development, and overexpression of GEF-H1 results in apical bleb-like protrusions in deep ectoderm cell layers (Itoh et al., 2014). GEF-H1 has also been shown to negatively regulate tension on adherens junctions in the *Xenopus* gastrula, though the molecular mechanism for this remains unclear (Hatte et al., 2018).

Nevertheless, an attractive model is that cingulin, paracingulin, or another tight junction protein, such as ZO-1, sequesters an inactive pool of GEF-H1 at tight junctions. Localized loss of the sequestering protein prior to flares may then allow GEF-H1 to locally activate Rho, and restoration of the sequestering protein could soak up the excess GEF, leading to Rho downregulation. I found that overexpression of dominant negative (GEF-dead) GEF-H1 resulted in hyperactivation of Rho at junctions, including an increased number of flares (not shown). Because we expected a dominant negative mutant of a GEF important to flares to *suppress* flares, we concluded that GEF-H1 was not likely to be required for Rho flare activation. However, an alternate interpretation is that overexpressing dominant negative GEF-H1 displaces endogenous GEF-H1 from the sequestering protein, leaving it free to hyperactivate Rho. Therefore, it may be worthwhile to revisit the role of GEF-H1 in Rho flares, as well as to determine whether changes in cingulin or paracingulin are evident at Rho flares.

p120 catenin, anillin, and cytokinesis-related GEFs and GAPs

p120 catenin is a member of the armadillo repeat (ARM) family of proteins along with β-catenin, and it binds to the juxtamembrane domain of cadherins, promoting their stability by preventing cadherin endocytosis (Kourtidis et al., 2013). p120 can influence RhoA, Rac1, and Cdc42 signaling via direct interactions and recruitment of GEFs, GAPs, and effectors to junctions (Kourtidis et al., 2013). p120 appears to coordinate RhoA/Rac1 antagonism as it can inactivate RhoA through p190RhoGAP-B recruitment and stimulate Rac1 and Cdc42 activation though the GEF Vav2 (Noren et al., 2000; Ponik et al., 2013; Valls et al., 2012; Wildenberg et al., 2006; Zebda et al., 2013).

Interestingly, downregulation of RhoA through p120 catenin requires association of p120 catenin with cadherin (Yu et al., 2016), whereas upregulation of Rac1 and Cdc42 requires unbound p120 catenin (Noren et al., 2000; Valls et al., 2012). Additionally, p120 can bind directly to RhoA-GDP *in vitro* and suppress GTP exchange, functioning similarly to Rho GDI (Anastasiadis et al., 2000). However, p120 also functions as a positive regulator of contractility by localizing ROCK1 and Shroom3 to the cadherin/catenin complex (Lang et al., 2014; Smith et al., 2012). Thus, p120 catenin can take on many roles as a regulator of GTPase signaling depending on the cell context, and these are likely controlled in part by cadherin binding, alternative splicing, and phosphorylation, all of which can change the affinity of p120 for RhoA (Castaño et al., 2007; Yanagisawa et al., 2008).

A recent study has identified a novel role for p120 catenin in regulating RhoA activation during cytokinesis. This study found that p120 catenin binds to MKLP1 and MP-GAP and constrains RhoA activity to the furrow (van de Ven et al., 2016). Anillin was also identified as a p120-interactor in this study. Interestingly, anillin and MKLP1, along with other prominent cytokinesis regulators MgcRacGAP and Ect2, also have roles in RhoA regulation at junctions (Ratheesh et al., 2012; Reyes et al., 2014), so it would be interesting to further investigate ties between these proteins and p120 catenin at junctions.

Anillin itself is a well-known scaffolding protein. It ensures successful cytokinesis by bundling F-actin, linking F-actin and myosin II to the membrane, and regulating RhoA activity at the contractile ring (Piekny and Maddox, 2010). The N-terminal domains of anillin participate in actomyosin binding/assembly, while the C-terminal domains include

C2 and PH domains, which anchor anillin to the membrane, a RhoA binding domain, which allows it to interact with active RhoA, and binding sites for interacting with the GEF Ect2 and the GAPs MgcRacGAP and p190RhoGAP-A (Frenette et al., 2012; Manukyan et al., 2015; Piekny and Maddox, 2010; Sun et al., 2015). Early in cytokinesis, anillin participates in a positive feedback loop in which its accumulation at the contractile ring is both dependent on and enhances Rho activation (Piekny and Glotzer, 2008). Later in cytokinesis, it interacts with p190RhoGAP-A in a tension-sensitive manner, inactivating RhoA in response to excessive force (Manukyan et al., 2015). Thus, in cytokinesis, anillin helps to fine-tune RhoA signaling by coupling GEFs, GAPs, and RhoA with cytoskeletal components like F-actin, myosin II, and formins.

Anillin has more recently been reported to localize to cell-cell junctions where it is important for proper accumulation of junctional actomyosin and organization of TJs and AJs in *Xenopus laevis* embryos (Reyes et al., 2014) and cultured epithelial cells (Budnar et al., 2018). Interestingly, GEFs and GAPs known to interact with anillin at the contractile ring (Ect2, MgcRacGAP, p190RhoGAP-A) are also found at cell-cell junctions (Priya et al., 2015; Ratheesh et al., 2012). In *Xenopus* gastrula-stage epithelia, anillin depletion results in an increased number, but decreased duration of Rho flares, suggesting that it may help sustain signaling, or may be required for efficient actomyosin contraction (Reyes et al., 2014). Both anillin and p190RhoGAP-A accumulate at Rho flares (Torey Arnold, unpublished), but Ect2 does not appear to localize to cell-cell junctions in the *Xenopus* embryo (Farah Huq, unpublished). MgcRacGAP loss-of-function increases the number and size of Rho flares, indicating it could be important for suppressing or down-regulating Rho activation (Breznau et al.,

2015). Future studies investigating the contributions of anillin and p120 catenin, two hubs for the regulation of Rho signaling at cell-cell junctions and the cytokinetic contractile ring, could reveal more interesting connections between cytokinesis proteins, cell-cell junction regulation, and tight junction repair.

Scaffolds for regulating distinct Rho populations

As discussed in Chapter 4, there appear to be multiple populations of active Rho within Rho flares: the dense, bright membrane protrusion-associated signal, and the dimmer haze surrounding the protrusion. During flare expansion, F-actin overlaps primarily with the protrusion-associated Rho, while myosin II associates primarily with the haze. This indicates that ROCK and formins are either differentially localized, or differentially activated, which could be regulated by scaffold proteins. Indeed, some potential scaffolds seem to prefer localizing to the haze (Anillin, p190RhoGAP-B; Torey Arnold, unpublished) or the membrane protrusion (zyxin, moesin; Brandon Coy and Sara Varadarajan, unpublished), indicating that some spatial organization at the signaling level is at play. Further investigating how the presence of these scaffolds dictates Rho signaling, actomyosin organization, and contractile output will allow us to better understand how both signaling and mechanical forces are coordinated between neighboring cells to drive tight junction reinforcement.

Tight junction dynamics and the leak pathway

The leak pathway is the route through which larger macromolecules can cross the tight junction barrier. The leak pathway has been experimentally observed for

decades by applying macromolecules to one side of the epithelium and then detecting their presence on the other side of the tissue (Hulbert et al., 1989; Milks et al., 1983; Propst et al., 1978). TNF-α, a cytokine that modulates Crohn's Disease, promotes increased leak pathway flux, and the level of leak pathway flux is associated with the severity of inflammation (Turner, 2009). Many hypothesize that increased leak pathway flux is a cause of disease, potentially allowing antigens to cross the epithelium and initiate or worsen an inflammatory response, while others argue that increased permeability is secondary to an inappropriate immune response (López-Posadas et al., 2016b; Odenwald and Turner, 2013). Increased intestinal permeability is seen in patients before IBD relapse and in close relatives without disease, suggesting that permeability is at least a contributing factor to disease (Hedin et al., 2012; López-Posadas et al., 2017). However, there is little direct evidence to suggest that it is the primary cause. Additionally, to my knowledge, there is no evidence that the leak pathway is intentionally used to traffic material across the epithelium under normal conditions. One puzzling question, then, is why does the leak pathway exist? Is it biologically useful, or just a sign of defective tight junctions?

One possibility is that the leak pathway is a consequence of the need for tight junctions to be dynamically reorganized as cells move with respect to one another. In order for tight junction rearrangement to occur quickly, as it must if the tissue is suddenly stretched or compressed, it is logical to have tight junctions that can be easily repositioned without prolonged breaks in barrier function. Based on reconstitution of claudin strands in fibroblasts, occludin tends to localize to the ends and branch points of claudin strands, and breaks are more likely to occur at these branch points (Van Itallie

et al., 2017). In fibroblasts, ZO-1, which can interact directly with both occludin and claudin, aligns claudin strands with actin filaments (Van Itallie et al., 2017). It is tempting to speculate that a complex of ZO-1, F-actin, occludin, and claudin makes a somewhat stable, but easily breakable branch point between intersecting claudin strands. This could explain how ZO-1 and occludin limit leak pathway flux (Buschmann et al., 2013; Van Itallie et al., 2009) —by stabilizing these branch points.

One puzzling aspect of occludin is that occludin knockout mice have phenotypically normal tight junctions (Saitou et al., 2000), though it is possible that the occludin-related proteins tricellulin or MarvelD3 could compensate for occludin function. Indeed, tricellulin relocalizes from tricellular junctions to bicellular junctions when occludin is knocked down in cultured cells (Buschmann et al., 2013; Ikenouchi et al., 2008). TNF-α-induced intestinal permeability is dependent on caveolin-mediated endocytosis of occludin (Marchiando et al., 2010). If occludin mediates the branching of claudin strands, then sudden loss of occludin could result in an increased number of strand breaks. Similarly, if ZO-1 serves to stabilize occludin/claudin interactions at branch points, ZO-1 loss might favor an increase in strand dynamics. In agreement with this hypothesis, disrupting ZO-1/claudin interaction in fibroblasts increased claudin strand dynamics (Van Itallie et al., 2017).

While there are still many unexplained pieces to the puzzle, this speculative model that occludin mediates the branching of claudin strands, and ZO-1 helps stabilize occludin/claudin interactions at branch points, could help us understand the localized phenomena I observed relative to Rho flares. For example, loss of ZO-1 can be seen in advance of occludin loss at flares sites. If ZO-1 acts to stabilize an occludin/claudin

interaction, then loss of ZO-1 might favor the subsequent diffusion of occludin. Once occludin and ZO-1 are lost, this could destabilize claudin strand branch points, allowing breaks large enough to permit macromolecules to pass the tight junctions. ZO-1 loss has been shown to increase junctional actin accumulation and contractility when perturbed genetically (Choi et al., 2016; Fanning et al., 2012; Tokuda et al., 2014; Van Itallie et al., 2009). While these studies used long-term, global perturbations of ZO-1, it is possible that a sudden, local loss of ZO-1 could induce the local actin accumulation and actomyosin contraction seen at Rho flares.

One important caveat of the studies mentioned above that used genetic manipulation or stimulation with inflammatory cytokines is that they require timescales much longer than the local break and repair events I have described (hours vs minutes). Thus, it remains to be seen whether tight junction remodeling over long timescales follows similar patterns to tight junction remodeling during Rho flares.

What event initiates Rho flares?

I have characterized several events that precede the onset of Rho flares, including junction elongation, barrier loss, and local loss of ZO-1 and occludin. This raises several possibilities for the events that initiate Rho flares. Junction elongation, coupled with bleb-like deformation of the plasma membrane, indicates that a mechanical trigger could initiate flares. Fellow graduate student Sara Varadarajan is currently testing whether Piezo1, a stretch-activated calcium channel, is required for Rho flare activation. In support of this hypothesis, Sara has found that intracellular calcium increases before Rho flares and that chelation of intracellular calcium results in

reduced Rho activation and prolonged ZO-1 breaks. Currently, fellow graduate student Shahana Chumki is implementing a method for optogenetically activating Rho in *Xenopus* (Strickland et al., 2012). With this system, she hopes to be able to elongate junctions and increase tension on demand, allowing her to test whether junction elongation can induce Rho flares.

Other possible triggers for Rho flares involve the loss of barrier function or tight junction components. Former post-doc Tomohito Higashi proposed a mechanism in which epithelial tissues could sense loss of barrier function using secretion targeted specifically to the apical or basal domain. For example, an apically secreted ligand would not be able to bind to a receptor on the basolateral membrane when tight junctions are intact. However, breach of the barrier would allow the ligand to bind the receptor, locally initiating a signaling cascade that results in Rho activation. Finally, the local loss of a suppressor of Rho signaling (e.g., a GAP or a factor that inhibits a GEF) could result in increased Rho activation. JAIL can be suppressed by over expressing VE-cadherin, which is normally locally decreased prior to the flare, though the molecular mechanism that suppresses this signaling has not been determined (Cao et al., 2017). These possibilities are not mutually exclusive; there could be multiple mechanisms that trigger Rho flares in order to ensure a robust system for maintaining barrier function.

Future directions

Xenopus laevis embryos provide a fantastic model epithelial tissue; it is from a vertebrate organism, represents an *in vivo* environment, can be easily imaged completely intact, and expressing fluorescent proteins of interest is simple. However, its

use does have some drawbacks, including a relative lack of good genetic tools. All the work in this dissertation was done by mildly overexpressing fluorescently tagged proteins of interest. A cleaner experimental set up would be to fluorescently tag the endogenous protein of interest at its native locus. Being able to replace endogenous genes with truncated and/or tagged versions will be especially important for determining how F-actin, ZO-1, occludin, and claudin interactions contribute to tight junction reinforcement. For this, it might be wise to move to the slightly more genetically tractable relative of *X. laevis, Xenopus tropicalis* (Tandon et al., 2017).

Alternatively, establishing a model in cell culture could go a long way in complementing the studies done in *X. laevis*, in particular because much of the tight junction literature is focused on these systems, and a wide range of reagents and assays have already been developed. For example, using pharmacological inhibitors in *X. laevis* embryos can be difficult because the embryos are surrounded by a vitelline envelope, which limits the permeability of some drugs. Of course, a significant drawback of cell culture is that Rho flares have not been reported in any cell lines, so identifying cell lines, Rho reporters, and flare-inducing conditions may be a substantial hurdle. However, this type of comparative biology may give us greater insight into the cause of tight junction leaks and their mechanism of repair. Along these lines, comparing Rho flares in different tissues within the *X. laevis* embryo and tadpole could reveal interesting information about how rates of cytokinesis, cell rearrangement, and intrinsic tissue tension influence transient tight junction breaches as well as Rho flares.

Concluding remarks

Tight junctions are complex and mysterious structures. The last three decades saw the discovery of a vast array of tight junction associated proteins and the uncovering of a staggering number of intermolecular interactions, indicating a high degree of organization and functional regulation (Anderson and Cereijido, 2009). Ten years ago, the first FRAP studies on tight junctions overturned the notion that tight junctions were static, heavily cross-linked structures, showing instead that individual proteins within the junction turn over rapidly and that these dynamics correlate with tight junction function (Buschmann et al., 2013; Raleigh et al., 2011; Shen et al., 2008; Yu et al., 2010). With the exception of a few studies (Carattino et al., 2013; Van Itallie et al., 2015), there has been relatively little emphasis on how dynamic cell shape changes relate to epithelial barrier function, no doubt in part because of the lack of available tools to study barrier function in a meaningful way at the cell scale.

In this dissertation, I have shown that the development of ZnUMBA and its adaptation to a variety of model systems have the potential to advance this field. Using ZnUMBA, I found that local loss of barrier function is associated with junction elongation and local loss of tight junction proteins. Additionally, I demonstrated that the GTPase RhoA rapidly accumulates at these tight junction breaks and restores barrier function through contraction of the junction. Furthermore, I showed that the membrane protrusion that accompanies Rho flares is likely driven by a bleb-like mechanism, further suggesting that altered cell mechanics contribute to signaling and repair of these breaches. Rho flares represent an elegant system that allow tight junctions to be rapidly repaired, allowing epithelial cells to change shape dynamically without compromising

their essential role of forming a barrier. This work highlights the important role that cell shape change has on regulating barrier function in epithelial tissue and the need to monitor cell dynamics, in addition to protein expression and localization, in order to fully understand the dynamic regulation of epithelial barrier function.

References:

Abu Taha, A., Taha, M., Seebach, J., and Schnittler, H.-J. (2014). ARP2/3-mediated junction-associated lamellipodia control VE-cadherin-based cell junction dynamics and maintain monolayer integrity. Molecular Biology of the Cell *25*, 245–256.

Aijaz, S., D'Atri, F., Citi, S., Balda, M.S., and Matter, K. (2005). Binding of GEF-H1 to the tight junction-associated adaptor cingulin results in inhibition of Rho signaling and G1/S phase transition. Dev. Cell *8*, 777–786.

Akaihata, H., Nomiya, M., Matsuoka, K., Koguchi, T., Hata, J., Haga, N., Kushida, N., Ishibashi, K., Aikawa, K., and Kojima, Y. (2018). Protective Effect of a Rho-kinase Inhibitor on Bladder Dysfunction in a Rat Model of Chronic Bladder Ischemia. Urology *111*, 238.e7–238.e12.

Anastasiadis, P.Z., Moon, S.Y., Thoreson, M.A., Mariner, D.J., Crawford, H.C., Zheng, Y., and Reynolds, A.B. (2000). Inhibition of RhoA by p120 catenin. Nat Cell Biol *2*, 637–644.

Anderson, M., and Cereijido, M. (2009). Introduction. In Tight Junctions, (CRC Press).

Benais-Pont, G., Punn, A., Flores-Maldonado, C., Eckert, J., Raposo, G., Fleming, T.P., Cereijido, M., Balda, M.S., and Matter, K. (2003). Identification of a tight junction-associated guanine nucleotide exchange factor that activates Rho and regulates paracellular permeability. J. Cell Biol. *160*, 729–740.

Bergert, M., Chandradoss, S.D., Desai, R.A., and Paluch, E. (2012). Cell mechanics control rapid transitions between blebs and lamellipodia during migration. Proc. Natl. Acad. Sci. U.S.a. *109*, 14434–14439.

Breslin, J.W., Zhang, X.E., Worthylake, R.A., and Souza-Smith, F.M. (2015). Involvement of local lamellipodia in endothelial barrier function. PLoS ONE *10*, e0117970.

Breznau, E.B., Semack, A.C., Higashi, T., and Miller, A.L. (2015). MgcRacGAP restricts active RhoA at the cytokinetic furrow and both RhoA and Rac1 at cell-cell junctions in epithelial cells. Molecular Biology of the Cell *26*, 2439–2455.

Budnar, S., Husain, K.B., Gomez, G.A., Naghibosidat, M., Verma, S., Hamilton, N.A., Morris, R.G., and Yap, A.S. (2018). Scaffolding of RhoA contractile signaling by anillin: a regulatory analogue of kinetic proofreading. BioRxiv 1–28.

Buschmann, M.M., Shen, L., Rajapakse, H., Raleigh, D.R., Wang, Y., Wang, Y., Lingaraju, A., Zha, J., Abbott, E., McAuley, E.M., et al. (2013). Occludin OCEL-domain interactions are required for maintenance and regulation of the tight junction barrier to macromolecular flux. Molecular Biology of the Cell *24*, 3056–3068.

Cao, J., Ehling, M., März, S., Seebach, J., Tarbashevich, K., Sixta, T., Pitulescu, M.E., Werner, A.-C., Flach, B., Montanez, E., et al. (2017). Polarized actin and VE-cadherin dynamics regulate junctional remodelling and cell migration during sprouting angiogenesis. Nat Commun *8*, 2210.

Carattino, M.D., Prakasam, H.S., Ruiz, W.G., Clayton, D.R., McGuire, M., Gallo, L.I., and Apodaca, G. (2013). Bladder filling and voiding affect umbrella cell tight junction organization and function. Am. J. Physiol. Renal Physiol. *305*, F1158–F1168.

Castaño, J., Solanas, G., Casagolda, D., Raurell, I., Villagrasa, P., Bustelo, X.R., García de Herreros, A., and Duñach, M. (2007). Specific phosphorylation of p120-catenin regulatory domain differently modulates its binding to RhoA. Mol. Cell. Biol. *27*, 1745–1757.

Choi, W., Acharya, B.R., Peyret, G., Fardin, M.-A., Mège, R.-M., Ladoux, B., Yap, A.S., Fanning, A.S., and Peifer, M. (2016). Remodeling the zonula adherens in response to tension and the role of afadin in this response. J. Cell Biol. *213*, 243–260.

Citi, S., Guerrera, D., Spadaro, D., and Shah, J. (2014). Epithelial junctions and Rho family GTPases: the zonular signalosome. Small GTPases *5*, 1–15.

Citi, S., Pulimeno, P., and Paschoud, S. (2012). Cingulin, paracingulin, and PLEKHA7: signaling and cytoskeletal adaptors at the apical junctional complex. Ann. N. Y. Acad. Sci. *1257*, 125–132.

Cordenonsi, M., D'Atri, F., Hammar, E., Parry, D.A., Kendrick-Jones, J., Shore, D., and Citi, S. (1999). Cingulin contains globular and coiled-coil domains and interacts with ZO-1, ZO-2, ZO-3, and myosin. J. Cell Biol. *147*, 1569–1582.

D'Atri, F., and Citi, S. (2001). Cingulin interacts with F-actin in vitro. FEBS Lett. *507*, 21–24.

Daneshjou, N., Sieracki, N., van Nieuw Amerongen, G.P., Conway, D.E., Schwartz, M.A., Komarova, Y.A., and Malik, A.B. (2015). Rac1 functions as a reversible tension modulator to stabilize VE-cadherin trans-interaction. J. Cell Biol. *208*, 23–32.

DeMali, K.A., and Burridge, K. (2003). Coupling membrane protrusion and cell adhesion. J. Cell. Sci. *116*, 2389–2397.

Elbediwy, A., Zihni, C., Terry, S.J., Clark, P., Matter, K., and Balda, M.S. (2012). Epithelial junction formation requires confinement of Cdc42 activity by a novel SH3BP1 complex. J. Cell Biol. *198*, 677–693.

Fanning, A.S., Van Itallie, C.M., and Anderson, J.M. (2012). Zonula occludens-1 and -2 regulate apical cell structure and the zonula adherens cytoskeleton in polarized epithelia. Molecular Biology of the Cell *23*, 577–590.

Feng, Y., LoGrasso, P.V., Defert, O., and Li, R. (2016). Rho Kinase (ROCK) Inhibitors and Their Therapeutic Potential. J. Med. Chem. *59*, 2269–2300.

Frenette, P., Haines, E., Loloyan, M., Kinal, M., Pakarian, P., and Piekny, A. (2012). An anillin-Ect2 complex stabilizes central spindle microtubules at the cortex during cytokinesis. PLoS ONE *7*, e34888.

Garcia-Mata, R., and Burridge, K. (2007). Catching a GEF by its tail. Trends Cell Biol. *17*, 36–43.

Guillemot, L., Guerrera, D., Spadaro, D., Tapia, R., Jond, L., and Citi, S. (2014). MgcRacGAP interacts with cingulin and paracingulin to regulate Rac1 activation and development of the tight junction barrier during epithelial junction assembly. Molecular Biology of the Cell *25*, 1995–2005.

Guillemot, L., Paschoud, S., Jond, L., Foglia, A., and Citi, S. (2008). Paracingulin regulates the activity of Rac1 and RhoA GTPases by recruiting Tiam1 and GEF-H1 to epithelial junctions. Molecular Biology of the Cell *19*, 4442–4453.

Hatte, G., Prigent, C., and Tassan, J.-P. (2018). Tight junctions negatively regulate mechanical forces applied to adherens junctions in vertebrate epithelial tissue. J. Cell. Sci. *131*, jcs208736.

Hedin, C.R., Stagg, A.J., Whelan, K., and Lindsay, J.O. (2012). Family studies in Crohn's disease: new horizons in understanding disease pathogenesis, risk and prevention. Gut *61*, 311–318.

Hulbert, W.C., Forster, B.B., Mehta, J.G., Man, S.F., Molday, R.S., Walker, B.A., Walker, D.C., and Hogg, J.C. (1989). Study of airway epithelial permeability with dextran. J Electron Microsc Tech *11*, 137–142.

Ikenouchi, J., Sasaki, H., Tsukita, S., Furuse, M., and Tsukita, S. (2008). Loss of occludin affects tricellular localization of tricellulin. Molecular Biology of the Cell *19*, 4687–4693.

Itoh, K., Ossipova, O., and Sokol, S.Y. (2014). GEF-H1 functions in apical constriction and cell intercalations and is essential for vertebrate neural tube closure. J. Cell. Sci. *127*, 2542–2553.

Ivanov, A.I., Parkos, C.A., and Nusrat, A. (2010). Cytoskeletal regulation of epithelial barrier function during inflammation. Am. J. Pathol. *177*, 512–524.

Kangawa, Y., Yoshida, T., Yonezawa, Y., Maruyama, K., Hayashi, S.-M., and Shibutani, M. (2017). Suppression of epithelial restitution using an inhibitor against Rho-associated coiled-coil containing protein kinase aggravates colitis through reduced epithelial expression of A-kinase anchor protein 13. Exp. Toxicol. Pathol. *69*, 557–563.

Keller, R.E. (1980). The cellular basis of epiboly: an SEM study of deep-cell rearrangement during gastrulation in Xenopus laevis. J Embryol Exp Morphol *60*, 201–234.

Lang, R.A., Herman, K., Reynolds, A.B., Hildebrand, J.D., and Plageman, T.F. (2014). p120-catenin-dependent junctional recruitment of Shroom3 is required for apical constriction during lens pit morphogenesis. Development *141*, 3177–3187.

Li, J.-R., Zhao, Y.-S., Chang, Y., Yang, S.-C., Guo, Y.-J., and Ji, E.-S. (2018). Fasudil improves endothelial dysfunction in rats exposed to chronic intermittent hypoxia through RhoA/ROCK/NFATc3 pathway. PLoS ONE *13*, e0195604.

López-Posadas, R., Becker, C., Günther, C., Tenzer, S., Amann, K., Billmeier, U., Atreya, R., Fiorino, G., Vetrano, S., Danese, S., et al. (2016a). Rho-A prenylation and signaling link epithelial homeostasis to intestinal inflammation. J. Clin. Invest. *126*, 611–626.

López-Posadas, R., Becker, C., Günther, C., Tenzer, S., Amann, K., Billmeier, U., Atreya, R., Fiorino, G., Vetrano, S., Danese, S., et al. (2016b). Rho-A prenylation and signaling link epithelial homeostasis to intestinal inflammation. J. Clin. Invest. *126*, 611–626.

López-Posadas, R., Stürzl, M., Atreya, I., Neurath, M.F., and Britzen-Laurent, N. (2017). Interplay of GTPases and Cytoskeleton in Cellular Barrier Defects during Gut Inflammation. Front Immunol *8*, 1240.

Manukyan, A., Ludwig, K., Sanchez-Manchinelly, S., Parsons, S.J., and Stukenberg, P.T. (2015). A complex of p190RhoGAP-A and anillin modulates RhoA-GTP and the cytokinetic furrow in human cells. J. Cell. Sci. *128*, 50–60.

Marchiando, A.M., Shen, L., Graham, W.V., Weber, C.R., Schwarz, B.T., Austin, J.R., Raleigh, D.R., Guan, Y., Watson, A.J.M., Montrose, M.H., et al. (2010). Caveolin-1-dependent occludin endocytosis is required for TNF-induced tight junction regulation in vivo. J. Cell Biol. *189*, 111–126.

Marinissen, M.J., and Gutkind, J.S. (2005). Scaffold proteins dictate Rho GTPase-signaling specificity. Trends Biochem. Sci. *30*, 423–426.

Martinelli, R., Kamei, M., Sage, P.T., Massol, R., Varghese, L., Sciuto, T., Toporsian, M., Dvorak, A.M., Kirchhausen, T., Springer, T.A., et al. (2013). Release of cellular tension signals self-restorative ventral lamellipodia to heal barrier micro-wounds. J. Cell Biol. *201*, 449–465.

Milks, L.C., Brontoli, M.J., and Cramer, E.B. (1983). Epithelial permeability and the transepithelial migration of human neutrophils. J. Cell Biol. *96*, 1241–1247.

Noren, N.K., Liu, B.P., Burridge, K., and Kreft, B. (2000). p120 catenin regulates the actin cytoskeleton via Rho family GTPases. J. Cell Biol. *150*, 567–580.

Odenwald, M.A., and Turner, J.R. (2013). Intestinal permeability defects: is it time to treat? Clin. Gastroenterol. Hepatol. *11*, 1075–1083.

Paschoud, S., Yu, D., Pulimeno, P., Jond, L., Turner, J.R., and Citi, S. (2011). Cingulin and paracingulin show similar dynamic behaviour, but are recruited independently to junctions. Mol. Membr. Biol. *28*, 123–135.

Piekny, A.J., and Glotzer, M. (2008). Anillin is a scaffold protein that links RhoA, actin, and myosin during cytokinesis. Current Biology *18*, 30–36.

Piekny, A.J., and Maddox, A.S. (2010). The myriad roles of Anillin during cytokinesis. Semin. Cell Dev. Biol. *21*, 881–891.

Ponik, S.M., Trier, S.M., Wozniak, M.A., Eliceiri, K.W., and Keely, P.J. (2013). RhoA is down-regulated at cell-cell contacts via p190RhoGAP-B in response to tensional homeostasis. Molecular Biology of the Cell *24*, 1688–99–S1–3.

Priya, R., Gomez, G.A., Budnar, S., Verma, S., Cox, H.L., Hamilton, N.A., and Yap, A.S. (2015). Feedback regulation through myosin II confers robustness on RhoA signalling at E-cadherin junctions. Nat Cell Biol *17*, 1282–1293.

Propst, K., Millen, J.E., and Glauser, F.L. (1978). The effects of endogenous and exogenous histamine on pulmonary alveolar membrane permeability. Am. Rev. Respir. Dis. *117*, 1063–1068.

Quiros, M., and Nusrat, A. (2014). RhoGTPases, actomyosin signaling and regulation of the epithelial Apical Junctional Complex. Semin. Cell Dev. Biol. *36*, 194–203.

Raleigh, D.R., Boe, D.M., Yu, D., Weber, C.R., Marchiando, A.M., Bradford, E.M., Wang, Y., Wu, L., Schneeberger, E.E., Shen, L., et al. (2011). Occludin S408 phosphorylation regulates tight junction protein interactions and barrier function. J. Cell Biol. *193*, 565–582.

Rasmussen, D.N., Karstensen, J.G., Riis, L.B., Brynskov, J., and Vilmann, P. (2015). Confocal Laser Endomicroscopy in Inflammatory Bowel Disease--A Systematic Review. J Crohns Colitis *9*, 1152–1159.

Ratheesh, A., Gomez, G.A., Priya, R., Verma, S., Kovacs, E.M., Jiang, K., Brown, N.H., Akhmanova, A., Stehbens, S.J., and Yap, A.S. (2012). Centralspindlin and [alpha]-catenin regulate Rho signalling at the epithelial zonula adherens. Nat Cell Biol *14*, 818–828.

Reyes, C.C., Jin, M., Breznau, E.B., Espino, R., Delgado-Gonzalo, R., Goryachev, A.B., and Miller, A.L. (2014). Anillin regulates cell-cell junction integrity by organizing junctional accumulation of Rho-GTP and actomyosin. Curr. Biol. *24*, 1263–1270.

Rothschild, P.-R., Salah, S., Berdugo, M., Gélizé, E., Delaunay, K., Naud, M.-C., Klein, C., Moulin, A., Savoldelli, M., Bergin, C., et al. (2017). ROCK-1 mediates diabetes-induced retinal pigment epithelial and endothelial cell blebbing: Contribution to diabetic retinopathy. Sci Rep *7*, 8834.

Saitou, M., Furuse, M., Sasaki, H., Schulzke, J.D., Fromm, M., Takano, H., Noda, T., and Tsukita, S. (2000). Complex phenotype of mice lacking occludin, a component of tight junction strands. Molecular Biology of the Cell *11*, 4131–4142.

Segain, J.-P., Raingeard de la Blétière, D., Sauzeau, V., Bourreille, A., Hilaret, G., Cario-Toumaniantz, C., Pacaud, P., Galmiche, J.-P., and Loirand, G. (2003). Rho kinase blockade prevents inflammation via nuclear factor kappa B inhibition: evidence in Crohn's disease and experimental colitis. Gastroenterology *124*, 1180–1187.

Shen, L., Weber, C.R., and Turner, J.R. (2008). The tight junction protein complex undergoes rapid and continuous molecular remodeling at steady state. J. Cell Biol. *181*, 683–695.

Shkoda, A., Werner, T., Daniel, H., Gunckel, M., Rogler, G., and Haller, D. (2007). Differential protein expression profile in the intestinal epithelium from patients with inflammatory bowel disease. J. Proteome Res. *6*, 1114–1125.

Smith, A.L., Dohn, M.R., Brown, M.V., and Reynolds, A.B. (2012). Association of Rho-associated protein kinase 1 with E-cadherin complexes is mediated by p120-catenin. Molecular Biology of the Cell *23*, 99–110.

Strickland, D., Lin, Y., Wagner, E., Hope, C.M., Zayner, J., Antoniou, C., Sosnick, T.R., Weiss, E.L., and Glotzer, M. (2012). TULIPs: tunable, light-controlled interacting protein tags for cell biology. Nat Meth *9*, 379–384.

Sun, L., Guan, R., Lee, I.-J., Liu, Y., Chen, M., Wang, J., Wu, J.-Q., and Chen, Z. (2015). Mechanistic insights into the anchorage of the contractile ring by anillin and Mid1. Dev. Cell *33*, 413–426.

Szabó, A., Cobo, I., Omara, S., McLachlan, S., Keller, R., and Mayor, R. (2016). The Molecular Basis of Radial Intercalation during Tissue Spreading in Early Development. Dev. Cell *37*, 213–225.

Tandon, P., Conlon, F., Furlow, J.D., and Horb, M.E. (2017). Expanding the genetic toolkit in Xenopus: Approaches and opportunities for human disease modeling. Dev. Biol. *426*, 325–335.

Terry, S.J., Zihni, C., Elbediwy, A., Vitiello, E., Leefa Chong San, I.V., Balda, M.S., and Matter, K. (2011). Spatially restricted activation of RhoA signalling at epithelial junctions by p114RhoGEF drives junction formation and morphogenesis. Nat Cell Biol *13*, 159–166.

Tokuda, S., Higashi, T., and Furuse, M. (2014). ZO-1 knockout by TALEN-mediated gene targeting in MDCK cells: involvement of ZO-1 in the regulation of cytoskeleton and cell shape. PLoS ONE *9*, e104994.

Truebestein, L., Elsner, D.J., Fuchs, E., and Leonard, T.A. (2015). A molecular ruler regulates cytoskeletal remodelling by the Rho kinases. Nat Commun *6*, 10029.

Turner, J.R. (2009). Intestinal mucosal barrier function in health and disease. Nature Reviews Immunology *9*, 799–809.

Umeda, K., Matsui, T., Nakayama, M., Furuse, K., Sasaki, H., Furuse, M., and Tsukita, S. (2004). Establishment and characterization of cultured epithelial cells lacking expression of ZO-1. J. Biol. Chem. *279*, 44785–44794.

Valls, G., Codina, M., Miller, R.K., Del Valle-Pérez, B., Vinyoles, M., Caelles, C., McCrea, P.D., García de Herreros, A., and Duñach, M. (2012). Upon Wnt stimulation, Rac1 activation requires Rac1 and Vav2 binding to p120-catenin. J. Cell. Sci. *125*, 5288–5301.

van Buul, J.D., and Timmerman, I. (2016). Small Rho GTPase-mediated actin dynamics at endothelial adherens junctions. Small GTPases *7*, 21–31.

van de Ven, R.A.H., de Groot, J.S., Park, D., van Domselaar, R., de Jong, D., Szuhai, K., van der Wall, E., Rueda, O.M., Ali, H.R., Caldas, C., et al. (2016). p120-catenin prevents multinucleation through control of MKLP1-dependent RhoA activity during cytokinesis. Nat Commun *7*, 13874.

Van Itallie, C.M., Fanning, A.S., Bridges, A., and Anderson, J.M. (2009). ZO-1 stabilizes the tight junction solute barrier through coupling to the perijunctional cytoskeleton. Molecular Biology of the Cell *20*, 3930–3940.

Van Itallie, C.M., Tietgens, A.J., and Anderson, J.M. (2017). Visualizing the dynamic coupling of claudin strands to the actin cytoskeleton through ZO-1. Molecular Biology of the Cell *28*, 524–534.

Van Itallie, C.M., Tietgens, A.J., Krystofiak, E., Kachar, B., and Anderson, J.M. (2015). A complex of ZO-1 and the BAR-domain protein TOCA-1 regulates actin assembly at the tight junction. Molecular Biology of the Cell *26*, 2769–2787.

Wildenberg, G.A., Dohn, M.R., Carnahan, R.H., Davis, M.A., Lobdell, N.A., Settleman, J., and Reynolds, A.B. (2006). p120-catenin and p190RhoGAP regulate cell-cell adhesion by coordinating antagonism between Rac and Rho. Cell *127*, 1027–1039.

Xie, T., Luo, G., Zhang, Y., Wang, X., Wang, X., Wu, M., and Li, G. (2015). Rho-kinase inhibitor fasudil reduces allergic airway inflammation and mucus hypersecretion by regulating STAT6 and NFκB. Clin. Exp. Allergy *45*, 1812–1822.

Yanagisawa, M., Huveldt, D., Kreinest, P., Lohse, C.M., Cheville, J.C., Parker, A.S., Copland, J.A., and Anastasiadis, P.Z. (2008). A p120 catenin isoform switch affects Rho activity, induces tumor cell invasion, and predicts metastatic disease. J. Biol. Chem. *283*, 18344–18354.

Yano, T., Matsui, T., Tamura, A., Uji, M., and Tsukita, S. (2013). The association of microtubules with tight junctions is promoted by cingulin phosphorylation by AMPK. J. Cell Biol. *203*, 605–614.

Yoshikawa, T., Wu, J., Otsuka, M., Kishikawa, T., Suzuki, N., Takata, A., Ohno, M., Ishibashi, R., Yamagami, M., Nakagawa, R., et al. (2017). Repression of MicroRNA Function Mediates Inflammation-associated Colon Tumorigenesis. Gastroenterology *152*, 631–643.

Yu, D., Marchiando, A.M., Weber, C.R., Raleigh, D.R., Wang, Y., Shen, L., and Turner, J.R. (2010). MLCK-dependent exchange and actin binding region-dependent anchoring of ZO-1 regulate tight junction barrier function. Proc. Natl. Acad. Sci. U.S.a. *107*, 8237–8241.

Yu, H.H., Dohn, M.R., Markham, N.O., Coffey, R.J., and Reynolds, A.B. (2016). p120-catenin controls contractility along the vertical axis of epithelial lateral membranes. J. Cell. Sci. *129*, 80–94.

Zebda, N., Tian, Y., Tian, X., Gawlak, G., Higginbotham, K., Reynolds, A.B., Birukova, A.A., and Birukov, K.G. (2013). Interaction of p190RhoGAP with C-terminal domain of p120-catenin modulates endothelial cytoskeleton and permeability. J. Biol. Chem. *288*, 18290–18299.

Zihni, C., and Terry, S.J. (2015). RhoGTPase signalling at epithelial tight junctions: Bridging the GAP between polarity and cancer. Int. J. Biochem. Cell Biol. *64*, 120–125.

Notes and acknowledgements:

The section of this chapter describing junctional GEFs, GAPs, and scaffolding proteins was slightly modified from “Rho GTPases and Actomyosin: Partners in regulating epithelial cell-cell junction structure and function” by Torey R. Arnold, Rachel E. Stephenson, and Ann L. Miller, originally published in *Experimental Cell Research* 358 (2017) 20-30.

I would like to acknowledge all the members of the Miller lab for stimulating discussions about Rho flares, particularly Tomohito Higashi, Torey Arnold, Saranya Varadarajan, Shahana Chumki, and Ann Miller.

Appendix 1

Materials and Methods

DNA constructs

The following constructs in pCS2+ vectors were previously published: GFP-rGBD (Benink and Bement, 2005), RFP-wGBD {Benink:2005fn}, mRFP-ZO-1 (Higashi et al., 2016), mCherry-Claudin-6 (Higashi et al., 2016), mCherry-farnesyl (Reyes et al., 2014), Lifeact-RFP (Higashi et al., 2016), BFP-membrane (Higashi et al., 2016), E-cadherin-3xmCherry (Higashi et al., 2016), and mCherry-α-catenin (Higashi et al., 2016). mCherry-2xrGBD (Davenport et al., 2016) and BFP-2xrGBD (Davenport et al., 2016) were gifts from W.M. Bement (University of Wisconsin, Madison).

pCS2+/BFP-ZO-1 was generated by PCR amplification of human ZO-1 from pCS2+/mRFP-ZO-1(Higashi et al., 2016) and cloned into pCS2+/N-BFP. pCS2+/mRFP-ZO-1ΔABR was made by deleting base pairs 3456-4116 (corresponding to amino acids 1152-1371) from human ZO-1. The N- and C-terminal fragments of ZO-1 needed to make this deletion mutant were amplified with PCR, stitched together using splicing by overlap extension (SOEing) PCR, and cloned into pCS2+/N-mRFP. pCS2+/mCherry-Occludin was generated by amplifying *X. laevis* Occludin from a cDNA clone purchased from Thermo Fisher (Clone ID: 7009477) and cloned into pCS2+/N-mCherry. pCS2+/SF9-mNeon was made by PCR-amplifying SF9 (Myosin II intrabody) from TOPO-SF9-YFP (gift from E.M. Munro, University of Chicago) and subcloning it into pCS2+/C-mNeonGreen.

Arp3-mNeon, 3xGFP-Dia2, and 3xGFP-Dia3 were PCR-amplified from a *X. laevis* cDNA library and cloned into pCS2+/C-mNeonGreen or pCS2+/N-3xGFP as indicated. The cDNA library was generated from mRNA extracted from late tailbud-stage *X. laevis* embryos using TRIzol (Thermo Fisher Scientific) and reverse transcription was performed using Superscript III First-Strand Synthesis System (Thermo Fisher Scientific). All DNA constructs were verified by sequencing (GENEWIZ, South Plainfield, NJ).

mRNA preparation, microinjection, and mRNA concentrations

mRNAs were transcribed *in vitro* from pCS2+ vectors using the mMessage mMachine SP6 kit (Ambion) and purified using the RNeasy kit (Qiagen). Prior to *in vitro* transcription, plasmid DNA was linearized with NotI (except for constructs containing ZO-1, which were linearized using KpnI). mRNAs were mixed together and microinjected into 2- to 4-cell stage embryos at 4 distinct locations in the animal hemisphere. In the case of mosaic injections, global probes were injected 4 times at the two cell stage, and then injected with the mosaic probes once or twice at the four cell stage. Each 5 nl injection contained the following amount of the appropriate mRNAs: GFP-rGBD: 80 pg, mCherry-2xrGBD: 40 pg, BFP-2xrGBD: 33 pg, BFP-ZO-1: 70 pg, mRFP-ZO-1: 220 pg, mRFP-ZO-1ΔABR: 210 pg, mCherry-Claudin-6: 14 pg, mCherry-Occludin: 6 pg, mCherry-farnesyl: 50 pg, Lifeact-RFP: 12.5 pg, SF9-mNeon: 20-40 pg, BFP-membrane: 12.5 pg, E-cadherin-3xmCherry: 40 pg, mCherry-α-catenin: 40 pg, 3xGFP-Dia2: 25 pg, 3xGFP-Dia3: 10 pg.

Xenopus embryos

All studies conducted using *Xenopus* embryos strictly adhered to the compliance standards of the US Department of Health and Human Services Guide for the Care and Use of Laboratory Animals and were approved by the University of Michigan's Institutional Animal Care and Use Committee. Embryos were collected, fertilized *in vitro*, dejellied in 2% cysteine, pH 7.8 (Sigma), and cultured in 0.1xMMR (10 mM NaCl, 200 μM KCl, 200 μM $CaCl_2$, 100 μM $MgCl_2$, 500 μM HEPES, pH 7.4). At the 2- or 4-cell stage, embryos were microinjected with mRNA and were allowed to develop to gastrula stage (Nieuwkoop and Faber stage 10-12 (Nieuwkoop, 1994)).

Live imaging

Live confocal laser scanning microscopy of gastrula-stage *Xenopus laevis* embryos was performed with an inverted Olympus Fluoview 1000 with FV10-ASW software and a 20X or 60X objective as described previously (Reyes et al., 2014).

Generally, imaging of Rho flares was performed by collecting the 3 most apical *z*-planes with a 60X objective and 2X digital zoom, a scan speed of 2 μs/pixel, and a step size of 0.5 μm for tight junction proteins (ZO-1, Occludin, and Claudin-6), membrane (farnesyl), F-actin (Lifeact), and Myosin II (SF9) (time interval: 5 seconds), or 0.75 μm for E-cadherin and α-catenin (time interval: 6 seconds). Generally, for imaging ZnUMBA, the 6-8 most apical *z*-planes were collected with a 60X objective and a 1.5X digital zoom, a step size of 0.5 μm and a scan speed of 8 μs/pixel (time interval: 15-21 seconds). The ZnUMBA/EGTA experiments were imaged with a 20X objective, a scan speed of 8

μs/pixel, and a step size of 1.55 μm for 5 z-planes (time interval: 28 seconds). In each case, channels were acquired sequentially by line to minimize bleedthrough.

Figure preparation

Images were processed in Fiji. First, z-planes were summed and the channels were independently adjusted to highlight relevant features in the image using linear adjustments that cover the full range of data. LUTs were applied as described in the figure legends. With the exception of the kymographs in Fig 4a and Extended Data Fig 5a, images were enlarged in Photoshop CS6 using bicubic interpolation.

Manual quantification of Rho flares, junction proteins, and ZnUMBA

Flare selection: We defined flares as transient increases in active Rho that arise from cell-cell junctions. Thus, we only included accumulations of active Rho that increased, peaked, and decreased within 1-4 minutes. Static or sustained increases in active Rho were not considered in the analysis. To simplify the analysis, we only included flares that were isolated in space and time from other flares over the time span to be analyzed (i.e., no other flares at the same location for 500 seconds before or after the flare). An exception is when drug treatments resulted in a limited number of non-repeating flares (Fig 3f).

Flare measurements: Flare measurements were performed in Fiji on summed z-projections of unprocessed images. The intensity of a small circular region of interest (ROI) with a diameter of 0.75 μm (with the exceptions of ZnUMBA: 1.3 μm diameter,

and F-actin quantification in Figure 4.4d: 5.5 μm diameter) was used to measure fluorescence intensity of active Rho and accompanying channels. The ROI was placed on the junction at the approximate site of the flare and was moved manually each frame to account for cell and embryo movement. A custom macro was used to measure each channel and advance the frame. To account for photobleaching and focal drift, each measurement was normalized to a reference ROI (measured as described above) on a nearby junction. Each flare was measured in triplicate with three distinct reference ROIs. The baseline was normalized to 1 by dividing the value for each frame by the average intensity of the first ten frames. Flares were aligned on the x-axis so that the frame immediately before the rapid increase in Rho activity corresponds to time 0. Rapid increase in intensity was defined by consecutive increases in Rho intensity of at least 5% of baseline for at least three of four frames. Graphs are the mean of the normalized intensity of the number of flares indicated in the figure legend; error bars represent standard error of the mean.

Kymograph generation and quantification from kymographs

Relevant to Figures 3.4-3.6:

Image and data analysis were performed with the help of Fiji and custom Python scripts using NumPy, SciPy, OpenCV, Matplotlib, pandas and other open source libraries.

Kymograph construction: Cell-cell junction positions were digitized from ZO-1 or Occludin images with the use of watershed and active vector graph algorithms(Genovesio, 2009). The intensity of circular regions of interest ROI (diameter 0.75 μm) centered at points on cell-cell junctions was used to measure fluorescence of

active Rho and accompanying channels along the cell-cell junctions forming one horizontal line of the kymograph. The stacking of center-aligned lines of successive frames resulted in the kymograph of the cell-cell junction.

Flare analysis: Flare candidates were detected using thresholding of the normalized Rho channel. Candidates were then filtered out using the following criteria: 1) minimal size of 5 pixels; 2) flare located mostly on one cell-cell junction; 3) there are at least 8.3 minutes of recording before and after the flare; 4) no other flares on the same junction within 5 minutes; 5) flare is not located on a junction associated with the cleavage furrow of a dividing cell within 8 minutes. The selected flare was identified on a corresponding junction kymograph, and a vertical path corresponding to the location of the flare on a junction was specified with the help of kymograph fiducial marks. The path points were translated back to the original frames and signal intensity of active Rho and accompanying channels was collected at these points as the averaged intensity of the circular ROI (diameter 0.75 μm). Reference values were calculated as the median of the intensity distribution on the junctions.

Normalized intensity was calculated as $I_{\mathrm{norm}} = I_{\mathrm{signal}}/I_{\mathrm{reference}}$ and normalized to a baseline of ~1 by dividing the value for each frame by the median intensity of the first 6.5 minutes. Flares were aligned on the x-axis (time) so that the moment before the rapid increase in Rho activity corresponds to time 0 (that was achieved by fitting ramp function $\square = c + k\,R(t - t_0)$ on the interval near the maximum slope of active RhoA

signal). Graphs are the mean of the normalized intensity of the number of flares indicated in the figure legend; error bars represent standard error of the mean.

Relevant to Figures 3.2 and 4.7

Kymographs were generated in Fiji by drawing a line (for Figure 3.2: 2 pixels wide; for Figure 4.7: 1 pixel wide) through the flare perpendicular to the junction of origin. The line was converted to a kymograph using the "straighten" and "make montage" functions in Fiji.

Zinc-based Ultrasensitive Microscopic Barrier Assay (ZnUMBA)

5-10 nl of 1 mM FluoZin3 (Thermo Fisher Scientific), 100 μM $CaCl_2$, and 100 μM EDTA was microinjected into the blastocoel of stage 10-11 (Nieuwkoop and Faber) *X. laevis* embryos. EDTA was used to reduce baseline levels of FluoZin3 fluorescence from endogenous Zn^{++}. Albino embryos were used to better visualize the blastocoel during microinjection. Embryos were allowed to heal from the microinjection wound for a minimum of 5 minutes before being mounted in a slide containing 1-2 mM $ZnCl_2$ in 0.1xMMR. Embryos were imaged with confocal microscopy immediately after mounting. Relative increases in FluoZin3 fluorescence were interpreted as breaches in the barrier.

Drug treatments

Latrunculin B (Sigma) was resuspended in DMSO to a concentration of 1 mM and stored in aliquots at -20° C. Just prior to imaging, embryos were mounted in 0.1xMMR

containing Latrunculin B, a range of 8-10 μM was used to achieve a severe effect, and 1-5 μM was used to produce a mild effect.

Y-27632 (Calbiochem) was resuspended in DMSO to a concentration of 30 mg/ml and stored in aliquots at -20° C. Y-27632 or an equivalent amount of DMSO was mixed with probe mRNA and microinjected into embryos at the 2- or 4-cell stage. A total of 1.5 ng Y-27632 was injected into each embryo.

Junction injury

Junction injury was performed on albino embryos using a 405 nm laser and SIM scanner on the microscope described above. A small circular ROI was placed at the junction, and the 405 nm laser was pulsed in the ROI for 15 seconds at 70% power. These settings were sufficient to induce an injury response roughly half the time and photobleaching in the other cases. Substantial recoil was not observed with these settings.

Statistics

Standard error of the mean was calculated in Microsoft Excel or GraphPad Prism 7. One-sided Mann–Whitney U tests were performed with the help of open source SciPy.stats package (function mannwhitneyu).